A STUDY OF THE PROPERTIES OF TRANSIENT CHANGES IN THE COSMIC RAY INTENSITY

by

K. G. McCRACKEN, B.Sc. (Hons.)

submitted in fulfilment of the requirements for the degree of

DOCTOR OF PHILOSOPHY

UNIVERSITY OF TASMANIA

HOBART

December, 1958.

CONTENTS

		Page
Preface		i
Summary		vi
CHAPTER 1	DESCRIPTION OF THE NEUTRON MONITORS	1
1.1	The nucleonic component of cosmic radiation	1
1.2	Detection of neutrons	1
1.3	The plateaux of a BF_3 counter	2
1.4	Detection of the cosmic ray nucleonic component	3
1.5	The design of the neutron monitors	4
1.6	Electronic circuits	6
1.7	Recording apparatus	10
1.8	Timing	12
1.9	Housing of the equipment	12
1.10	Testing procedures	13
1.11	Equipment reliability	14
CHAPTER 2	ROUTINE ANALYSIS OF NEUTRON DATA	16
2.1	Statistical fluctuations in the neutron counting rate	16
2.2	The ratio of the counting rates of two sections of a monitor	18
2.3	The dependence of neutron counting rate upon atmospheric pressure	20
2.4	Practical correction procedures	24
2.5	Errors in the corrected counting rate	26
2.6	The accuracy of the tabulated data	29
2.7	Experimental determination of the standard deviations of the daily mean intensities	30
2.8	Determination of the absorption m.f.p.	30

		Page
CHAPTER 3	THE MESON DETECTORS	33
3.1	The ionization chamber	33
3.2	Balance current and residual ionization	34
3.3	The meson telescopes	36
3.4	Correction of the meson data for atmospheric effects	36
CHAPTER 4	VARIATIONS IN THE COSMIC RAY SPECTRUM (METHODS OF ANALYSIS)	38
4.1	Comparison of data	38
4.2	Summary of the types of cosmic ray variations	38
4.3	Comparison of the amplitudes of variations	40
4.4	Functional dependence of counting rate upon primary change	44
CHAPTER 5	THE LONG TERM VARIATION	49
CHAPTER 6	SHORT TERM VARIATIONS	52
6.1	Introduction	52
6.2	Dependence of event amplitude upon altitude	54
6.3	The latitude dependence of event amplitude	55
6.4	The variability of the neutron-meson relative amplitude	59
6.5	Short term variations observed underground	61
6.6	Comparison with the literature	63
CHAPTER 7	THE ENERGY DEPENDENCE OF VARIATIONS AND COMPARISON WITH THEORY	70
7.1	Calculation of the energy dependence	70
7.2	Geocentric disordered magnetic fields	73
7.3	Geocentric electric fields	75
7.4	Ordered fields associated with streams of solar matter	77
CHAPTER 8	TIME VARIATIONS OF THE COSMIC RAY INTENSITY	81
8.1	The investigation of time variations	81

Page

8.2 Classification of short term events 82

8.3 The recurrence of symmetrical events and the duration of Forbush decreases 84

8.4 Magnetic disturbance accompanying symmetrical decreases 85

8.5 The duration of the increasing intensity phase of a symmetrical decrease 88

8.6 The two types of magnetic activity 88

8.7 Discussion of the Forbush decrease mechanism 89

8.8 The mechanism responsible for symmetrical cosmic ray decreases 90

CHAPTER 9 THE COMMENCEMENT OF FORBUSH DECREASES 94

9.1 Comparison of Forbush decreases at Mawson and Mt. Wellington 94

9.2 The time and directional dependence of the Forbush mechanism 96

9.3 Correlation with magnetic disturbance 102

9.4 Comparison with the quiet day diurnal variation 102

9.5 Review of the literature 103

9.6 Discussion 104

CHAPTER 10 THE COUNTING RATES OF NEUTRON MONITORS AND MESON TELESCOPES AS FUNCTIONS OF ASYMPTOTIC LONGITUDE 107

10.1 The zenith angle dependence due to atmospheric absorption 107

10.2 The effect of the geomagnetic field 109

References 115

PREFACE

Three decades of research have shown that the cosmic ray intensity varies with time. Some of the variations have been shown to be due to atmospheric changes, while others are apparently produced by extra-terrestrial mechanisms. It is now known that most of the variations are small, of the order of a few percent, and that they do not correlate simply with other geophysical phenomena. In order to study them satisfactorily, recorders must be constructed such that the statistical fluctuations in the observations are considerably smaller than the cosmic ray variations themselves. It has become clear that the only worthwhile observational programme is a long term one, lasting for at least a number of years.

A number of different types of cosmic ray detector have been developed, among these being the ionization chamber, the geiger counter telescope and the neutron monitor. It has been shown that comparison of neutron monitor data with those from either of the other instruments yields information on the manner in which the cosmic ray spectrum varies with time. Similar information is provided by the comparison of results obtained at high and low geomagnetic latitudes. Furthermore, observatories at different longitudes enable the directional dependence of the variations to be determined.

Late in 1953 the University of Tasmania commenced observations of the vertical meson intensity at Hobart using a large geiger counter telescope. During 1954 and early 1955 the candidate, in partial fulfilment of the requirements of the Degree of Bachelor of Science with Honours, investigated and eliminated faults which had previously prevented an ionization chamber from being operated successfully. Thus by the end of 1955, the cosmic ray intensity at Hobart was being measured by two different types of recorder.

In the latter half of 1955, I undertook to design and construct a neutron monitor. Boron Trifluoride counters were purchased from a

commercial firm, and by June, 1956, a prototype monitor was in operation at Hobart. In order to achieve a higher counting rate, it was decided to site the monitor on the slopes of Mt. Wellington, the mountain at whose foot Hobart is situated. A hut was built and by the middle of July, 1956, the monitor had been transferred from Hobart and was in fully automatic operation.

Early in 1955, Mr. N. R. Parsons established a cosmic ray observatory at the Australian National Antarctic Research Expeditions (A.N.A.R.E.) base at Mawson in Mac-Robertson Land. The meson telescopes he installed were identical to those at Hobart. While the prototype monitor was being built at Hobart, it was suggested to A.N.A.R.E. that a neutron monitor be installed at Mawson. This plan was approved in July, 1956, and the necessary finance made available. It was intended that the instrument should be installed at Mawson in the summer of 1956/57, so the whole instrument had to be designed, constructed, tested and packed for shipment by the end of November. The experience gained in the construction of the prototype monitor enabled rapid finalization of the electronic, recording and structural details, and at the same time, it enabled me to determine satisfactory testing and data handling procedures. The recording equipment was constructed by Mr. P. W. Ford, and the electronic circuits by Mr.D.E. Millwood and myself. With the assistance of Dr. J. R. Storey, I co-ordinated the various phases of the project, and assembled and tested the instrument. I wrote a handbook for the guidance of the physicist at Mawson, detailing the construction, operation, data handling and test procedures. The instrument was installed at Mawson by Mr. D. H. Johns, and his training in the operation of the instrument, and that of subsequent physicists, was my responsibility.

During 1956, Dr. A. G. Fenton, the leader of the Hobart cosmic ray research group, had suggested to the Australian Academy of Sciences that a cosmic ray observatory be installed in New Guinea for the duration of the International Geophysical Year. The Academy approved this plan and provided the necessary finance.

It was decided to install a neutron monitor and two vertical meson telescopes at Lae in the Territory of New Guinea. Thus at the same time as the Mawson instrument was being constructed, the plans were prepared for the Lae monitor. As soon as the Mawson instrument was finished, work on the Lae monitor commenced, and at the same time, the prototype Mt. Wellington monitor was replaced by a larger instrument using circuits identical to those used in the Mawson monitor. The electronic circuits for the Lae monitor were once again built by Mr. D. E. Millwood and myself, while the construction of the two meson telescopes was supervised by Dr. Fenton. I designed and assembled the timing, recording and testing apparatus for the whole station. By the end of March 1957 all the equipment had been built, tested and dispatched to New Guinea, and at the beginning of May I flew to Lae and set about the assembly of the station in a room provided by the Australian Department of Civil Aviation.

Working by myself, the whole station was in operation by the end of May. Three more months were spent at Lae in order to eliminate equipment faults peculiar to the tropics, and, during this time, the Department of Civil Aviation's senior radio technician, Mr. C. Ozorio, was trained in the operation and maintenance of the equipment, and a handbook was written.

Returning to Hobart in September, 1957, I commenced detailed analysis of the neutron and meson data obtained at the various observatories. In broad terms, my work may be summarised thus:-

(A) the initiation of a long term neutron recording programme,

(B) a study of the manner in which the cosmic ray spectrum varies during short term and long term intensity variations, and

(C) a study of the manner in which the intensity varies with time during 27 day variations and Forbush decreases.

This thesis presents the results of some of my investigations. Considerable attention has been given to the discussion and system-

atization of the variations observed during 1956/57, as I believe that a systematic description of the properties of the various types of cosmic ray event is urgently needed. Once we have such a description, we are in a much better position to theorise as to the mechanisms producing the variations.

The investigations into the time variations (Chapters 8 and 9) have been carried out in collaboration with other members of the Hobart cosmic ray group. Mr. N. R. Parsons and I shared equally in the initial work on the differences in onset time of Forbush decreases, and it was later found that Dr. Fenton, who was in Canada for a year during 1957/58, had been working along similar lines. I was responsible for the more recent work on this problem (in particular, the "surveys" of the events). Dr. Fenton and I collaborated by mail on the superposition of the various types of cosmic ray variation.

It will be clear that the successful completion of this programme depended largely upon the co-operation and enthusiasm of many people. Professor A. L. McAulay, Professor of Physics, encouraged and guided me throughout the whole project, particularly during the difficult period during which the Lae equipment was being built and established. Assistance was given by Professor E. J. G. Pitman and Mr. P. Sprent in the statistical problems associated with the analysis of data. Without the assistance of Dr. J. R. Storey, Mr. P. W. Ford, Mr. D. E. Millwood, Mr. G. G. Harman, Mr. D. H. Johns and the Physics Department workshop staff the constructional programme could never have been completed in such a short period as one year. Valuable computational assistance was given by Mrs. P. S. James, Mrs. D. M. Chappell, Miss B. E. Harrop and Mr. P. J. Edwards. The University photographic department, under Mr. T. S. McMahon, has been of very great assistance to me. I am greatly indebted to Miss M. J. Lloyd for typing this thesis, and for secretarial assistance during the last two years.

Thanks are especially due to the Australian Department of Civil Aviation for assistance during the assembly of the Lae observatory. I am indebted to the many members of the D.C.A. staff at Lae, and in particular Mr. C. Ozorio, for help of many kinds.

The majority of my work was performed during tenure of an Australian Atomic Energy Commission research scholarship. A substantial monetary grant by the Commission aided in the establishment of the Mt. Wellington neutron monitor. During recent months, I have been the holder of a General Motors Holden research fellowship.

There is a regular interchange of data between the Hobart and overseas research groups. I wish to express my gratitude to the following for data received in this way:- Dr. D. C. Rose (Ottawa, Resolute and Banff data), Professor J. A. Simpson (Climax data), Dr. A. E. Sandström (Uppsala data), Dr. Y. Miyazaki (Tokyo and Mt. Norikura data) and Mr. D. R. Palmer (Herstmonceux data).

I have had many helpful discussions with Dr. J. R. Storey, Mr. N. R. Parsons, and Mr. R. M. Jacklyn, members of the Hobart cosmic ray group. Further, these gentlemen maintained my Hobart equipment while I was in Lae. Finally, I must thank Dr. A. G. Fenton, leader of the cosmic ray group, for his assistance and interest in every phase of my work.

K.G.M.C. Cracken

Hobart; December, 1958.

SUMMARY

The following are brief summaries of the more important results reported in this thesis.

Section 2.8 A number of experimental determinations yield a weighted mean value of 138.1 ± 0.8 gm cm^{-2} for the absorption mean free path of the high energy nucleonic radiation.

Chapter 5 There was a long term decrease in the cosmic ray intensity during 1956 and 1957. In the case of the neutron component, the percentage decrease at $\lambda = 73^{\circ}S$ was equal to that at $\lambda = 52^{\circ}S$, and four times that at $\lambda = 16^{\circ}S$ (λ = geomagnetic latitude). This indicates that the long term variation was most pronounced at low rigidities, and further, that the percentage change in intensity was approximately the same for all directions in space.

Section 6.2 Comparison of the data from a number of different observatories indicates that the amplitude of a short term change in the neutron counting rate is a function of altitude, increasing by about 12 percent/1000 metres.

Section 6.3 Comparison of neutron monitor data from a number of observatories shows that the amplitude of a short term change is almost independent of latitude for $\lambda > 58^{\circ}$. This is interpreted as evidence that the mechanism producing the variations affects the radiation arriving at the earth from all directions to approximately the same extent.

Section 6.5 It is reported that three Forbush decreases were observed 40 m.w.e. underground, and that the time variations observed underground were similar to those observed by the Mt. Wellington neutron monitor. This is interpreted as evidence that the Forbush

mechanism affects the intensity of the primary radiation of energy greater than 150 Bev.

Section 6.6 Critical examination of the data reported in the literature indicates that short and long term events are more energy sensitive than has been previously thought. A similar conclusion is reached from a study of the data obtained at the observatories maintained by the University of Tasmania.

Section 7.1 From an examination of the data obtained from a number of different recorders, the average change in energy spectrum during short term variations is determined. Writing the differential energy spectrum as $j(E)$, and measuring energy in Bev, the change is shown to approximate to the law

$$\partial j(E) = \text{const.}\ j(E).(1 + E)^{-\beta}$$

where $\beta = 0.6$ or 0.8. In the case of the long term variation, $\beta = 1.2$. The difference in energy dependence of the two types of event is taken as evidence that they are produced by two different mechanisms.

Chapter 8 By averaging over a number of well defined events, the average manner in which geomagnetic disturbance varies during twenty-seven day variations in the cosmic ray intensity is determined. Considering the cosmic ray variations to be of the nature of recurrent depressions of the intensity, the commencement of a decrease is found to be accompanied, on the average, by a marked enhancement of geomagnetic disturbance. Minimum intensity is found to occur a day or two before a marked decrease in geomagnetic disturbance. It is shown that the amplitude of a Forbush decrease is a function of the duration of the event, and that there is some evidence that the duration of the increasing phase, and the amplitude of 27 day variations show this

same functional relationship. It is proposed that the mechanisms responsible for 27 day variations and Forbush decreases are similar.

Section 9.1 It is shown that the times of onset of a Forbush decrease at different longitudes sometimes differ by several hours, and that the intensity variations during the first day of the event are sometimes markedly different. On a number of occasions, transient decreases of a few hours duration were observed during the day prior to the commencement of a Forbush decrease.

Section 9.2 The time variations during fourteen Forbush decreases are studied, and a consistent behaviour is evident during all of them. The intensity in the directions between about 30° and 120° West of the earth-sun line is found to be the first to be depressed, and it suffers the greatest depression during the event. The intensity of the radiation reaching the earth from directions between 0° and 90° East of the earth-sun line is the last to be affected by the Forbush mechanism, and it suffers the least depression.

Section 10.1 The dependence of counting rate upon zenith angle is calculated for a sea level neutron monitor. It is found that over 95 percent of the counting rate is due to neutrons arriving at an angle of less than 45° to the zenith.

Section 10.2 The contribution made to the total counting rate of a cosmic ray detector by the primary radiation arriving from different asymptotic geographic longitudes is calculated for selected observatories. Both neutron monitors and geiger counter telescopes are considered. Assuming that the intensity of the cosmic radiation arriving outside the geomagnetic field is not isotropic, and that, for simplicity, it is a discontinuous function of geographic longitude, the time variations introduced into the data from these selected observatories by the rotation of the earth are calculated. The calculated variations show the same general features as are observed.

CHAPTER 1

DESCRIPTION OF THE NEUTRON MONITORS

1.1 The nucleonic component of cosmic radiation

A primary cosmic ray in collision with an atom near the top of the atmosphere disrupts the nucleus, producing high energy π mesons, nucleons and other nuclear fragments (SIMPSON et al, 1953). The nucleons produce further nucleons in similar collision processes, and in this manner a nucleonic cascade develops. The energy of the nucleons decreases as the cascade develops, until below the 200 gm. $cm.^{-2}$ level the nucleons produced in a nuclear disintegration have insufficient energy to produce further explosions, or "stars" as they are often called. These low energy nucleons then lose their energy in elastic collisions with atmospheric atoms until they attain thermal energies. Hence below the 200 gm. $cm.^{-2}$ level, the flux of high energy, star producing nucleons falls off with increasing atmospheric depth.

Almost the whole of the neutron component of the lower atmosphere is produced in such a cascade process (SIMPSON et al, 1953), and consequently the neutron intensity can be used as a measure of the primary cosmic ray intensity, provided adequate account is taken of variations of meteorological origin.

1.2 Detection of neutrons

Neutrons, being uncharged particles, cannot be detected using conventional particle counting techniques since these all depend on the production of ions by the incident particle. However, indirect methods, employing intermediate mechanisms in which the neutron produces a charged particle, which is then detected using conventional techniques, are available.

An intermediate mechanism which exhibits a cross section inversely proportional to neutron velocity, and which is consequently suitable for counting thermal neutrons is shown below

$$_5B^{10} + {}_0n^1 \longrightarrow {}_3Li^7 + {}_2He^4 + 2.5 \text{ M.e.v.}$$

A proportional counter containing a gaseous compound of Boron will detect electrons and mesons as well as neutrons. However, by virtue of the proportional nature of the counter, the pulses due to $B^{10}(n,\alpha)Li^7$ events can be distinguished from those produced by either of the other types of particles.

The efficiency of a neutron counter is largely determined by the concentration of B^{10} in the gas. Naturally occurring Boron contains roughly 20 percent of B^{10} and 80 percent of B^{11}, and since the latter isotope does not participate in the α producing reaction, it is advantageous to use Boron enriched in the B^{10} isotope. The counters used by the Hobart group contain Boron Trifluoride enriched to 96 percent in the B^{10} isotope.

1.3 The plateaux of a BF_3 counter

An idealised pulse amplitude spectrum of a BF_3 proportional counter is given in Fig. 1A. Electrons and mesons, owing to their low specific ionizations, produce small pulses, resulting in the peak at the low amplitude end of the spectrum. The amplitude of the pulse produced by a $B^{10}(n,\alpha)Li^7$ event is determined by the distance travelled within the counter by the He and Li nuclei, and as this varies from event to event, the spectral peak corresponding to the detection of neutrons is quite broad.

It is possible to count only those pulses produced by neutrons by using an amplitude sensitive counting circuit. Referring to Fig. 1A, it will be seen that the counting rate with the

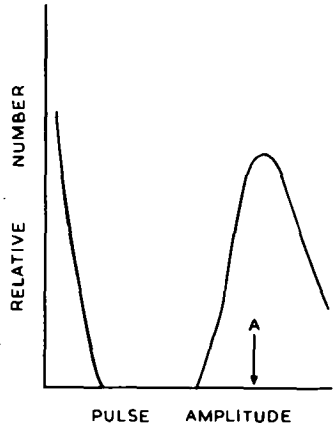
RELATIVE NUMBER
A
PULSE AMPLITUDE

1A

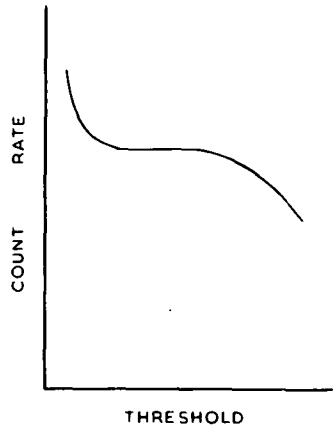
COUNT RATE
THRESHOLD

1B

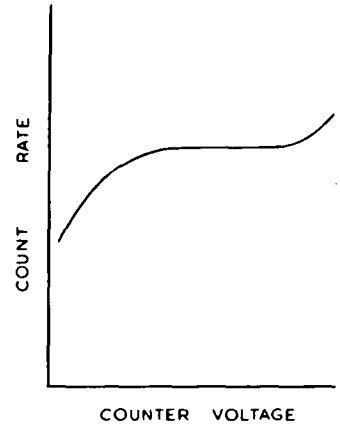
COUNT RATE
COUNTER VOLTAGE

1C

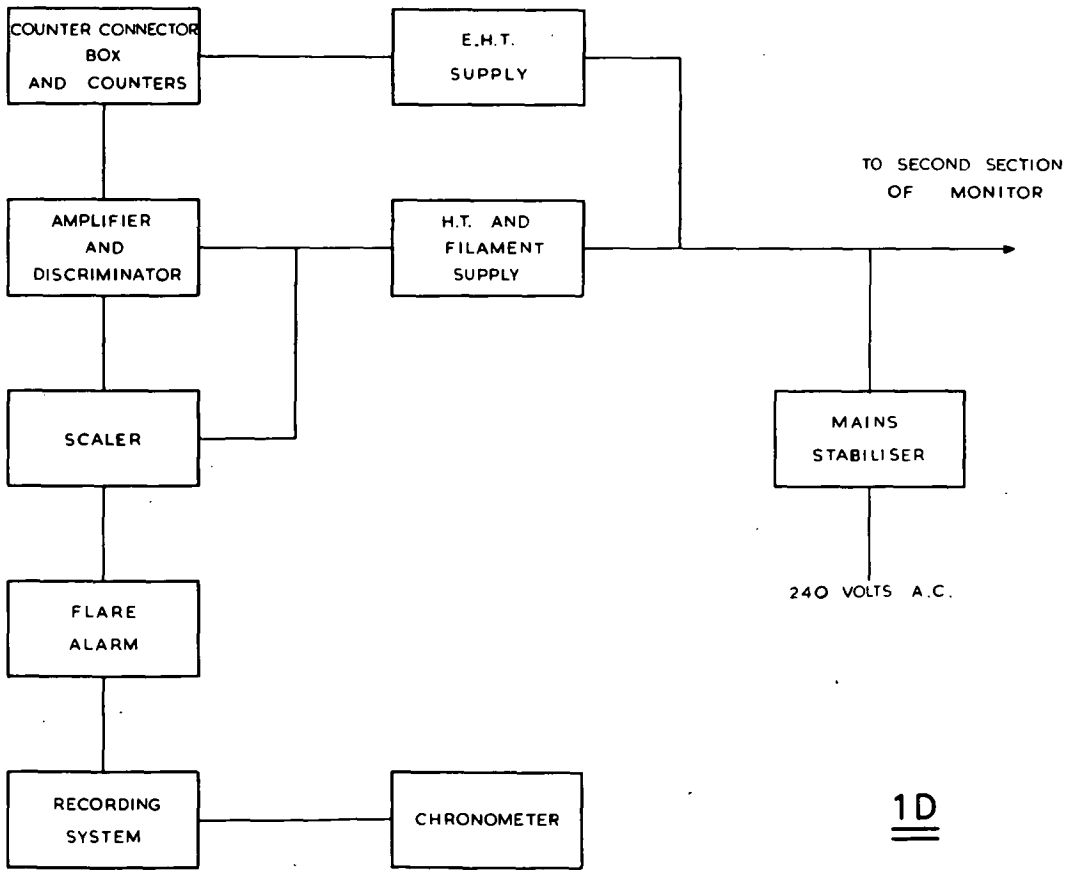
COUNTER CONNECTOR BOX AND COUNTERS
E.H.T. SUPPLY
TO SECOND SECTION OF MONITOR
AMPLIFIER AND DISCRIMINATOR
H.T. AND FILAMENT SUPPLY
SCALER
MAINS STABILISER
240 VOLTS A.C.
FLARE ALARM
RECORDING SYSTEM
CHRONOMETER

1D

threshold set at "A" is proportional to the area under the curve between A and infinity. Keeping the counter voltage constant and varying the threshold yields the curve plotted in Fig. 1B. This curve is called the bias curve of the counter, and it can be seen that the rate of change of counting rate with threshold is zero over a considerable range of threshold values. The bias curve is said to exhibit a "plateau".

Increasing the counter voltage increases the gas multiplication of the counter, and all pulse amplitudes increase. Let the threshold of a counting circuit be set at A, and let the gas multiplication change by a factor α. Whereas the portion of the counter spectrum in the amplitude range $\frac{A}{\alpha}$ to A was not recorded prior to the change, it now produces pulses of amplitude A to αA which are accepted by the counting circuit. That is, an increase in counter voltage is equivalent to a decrease in threshold level. Hence the curve of counting rate against counter voltage will exhibit a plateau (Fig. 1C), and it is clear that if for a given threshold the counter voltage is adjusted to a value on the counting rate against counter voltage plateau, then the threshold will be on the plateau in the bias curve. Consequently the detection of neutrons can be made insensitive to equipment change.

In practice, the counter spectrum does not fall to zero in between the two spectral peaks. Thus both plateaux have a slight slope.

1.4 Detection of the cosmic ray nucleonic component

At any point in the lower atmosphere there are (1) thermal neutrons, (2) low energy neutrons produced in "stars" in nearby matter, and (3) high energy nucleons capable of producing "stars". A measurement of any of these components is feasible. When the measurement is made in order to estimate the behaviour of the primary cosmic radiation it is desirable that the component least

affected by meteorological changes be chosen.

Measurement of the thermal neutron component suffers from the disadvantage that the atmosphere is being used as a moderator, so that rain, snow, fog etc. will introduce spurious variations.

A more satisfactory method is to count the low energy evaporation neutrons produced nearby, a condensed moderator such as paraffin wax being used to thermalise the neutrons. This method suffers from the disadvantage that movement of condensed material (lead, snow) in the vicinity results in changes in the flux of low energy neutrons through the detector.

The most satisfactory solution is to record the evaporation neutrons produced in a mass of condensed material, and shield the detector from evaporation neutrons produced elsewhere. It has been shown that the mass of air above such an instrument is the only meteorological parameter affecting the counting rate. (LOCKWOOD and YINGST, 1956; LOCKWOOD and CALAWA, 1957). Snow on the roof above a detector will depress the counting rate, and precautions have to be taken to avoid this. It has been shown that movement of condensed matter in the vicinity of such an instrument has no significant effect on the counting rate*.

1.5 The design of the neutron monitors

All the neutron monitors built at Hobart follow closely the design developed by Professor J. A. Simpson of the University of Chicago (SIMPSON et al, 1953; SIMPSON, 1956). The counters were purchased from the N. Wood Counter Laboratory, Chicago, U.S.A.

The Mawson, Hobart and Lae monitors employ twelve, eight

---

* The ratios of the counting rates of the two sections were compared with and without a wall of 2 tons of lead along one side of a monitor. The wall was in position for two days. No significant change in ratio occurred, indicating that any contribution by the lead was less than 1 percent of the counting rate of a single section.

and six counters respectively. The configuration of the Mawson monitor, which is similar to that of the other monitors, is shown in Fig. 2A and Fig. 2B.

The BF_3 proportional counters sit inside tubes running the full length of 4" x 4" x 40" moderator boxes which are filled with paraffin wax. The local star producing medium, lead, is stacked around these boxes. The whole assembly is supported by a steel and wood platform. A thick shield of paraffin wax around the lead minimises the response to evaporation neutrons produced outside the instrument.

The moderator boxes, and the large boxes comprising the outside shield were filled with molten paraffin wax. Since the wax shrank by about 20 percent during cooling, it was necessary to fill the boxes in stages, allowing the wax to cool completely between fillings. Otherwise contraction of the wax either (1) pulled in the sides of the boxes, or (2) created a cavity in the centre of the block of wax.

In order to achieve a higher counting rate, the four counter prototype monitor deviated from the standard design in that considerably more lead was used, resulting in a counting rate comparable with that of a standard six counter monitor.

In each monitor, provision was made for checking the counting rate efficiency with a Ra-Be neutron source. The 1 m.c. neutron sources are housed in cylindrical brass containers, which slide into tubes embedded in the monitors' wax shield. A projection near the bottom of each locating tube fits into a groove cut in the side of the neutron source container ensuring reproducible source positions. The counting rate when the source is present is contributed largely by the two or three counters nearest to the source. Thus if too few source positions are used, the deterioration of a counter situated far away from a source position may go unnoticed

Figure 2A - A twelve counter neutron monitor with portion of the outside shield and the lead removed.

Figure 2B - The electronic circuits appropriate to one section of a monitor. The amplifier is the strip circuit on the right, the scaler the one on the left. The small circuit on top of the monitor is an output circuit. The end of the counter connector box and the E.H.T. power pack can be seen in the foreground. The H.T. power supplies sit on the ledge at the rear of the monitor.

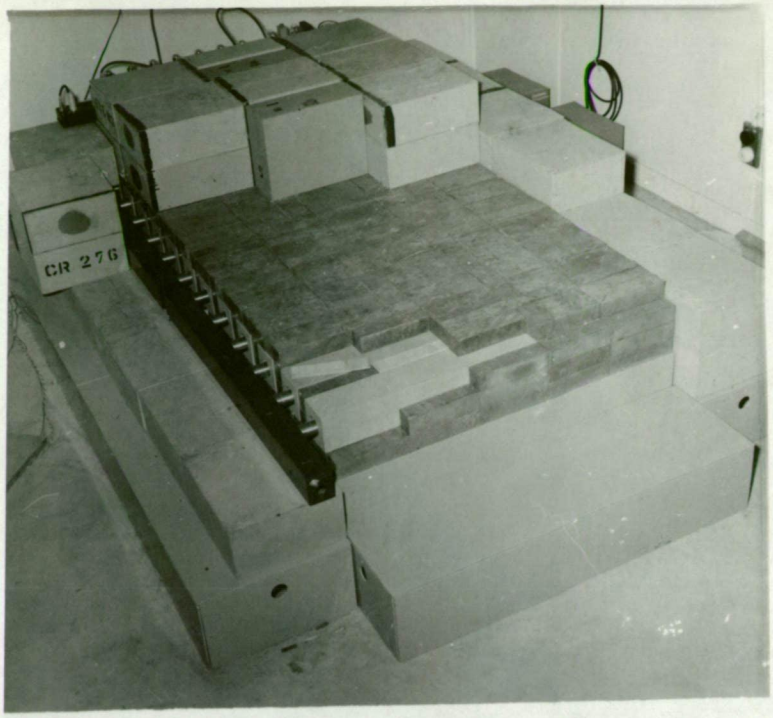

2A

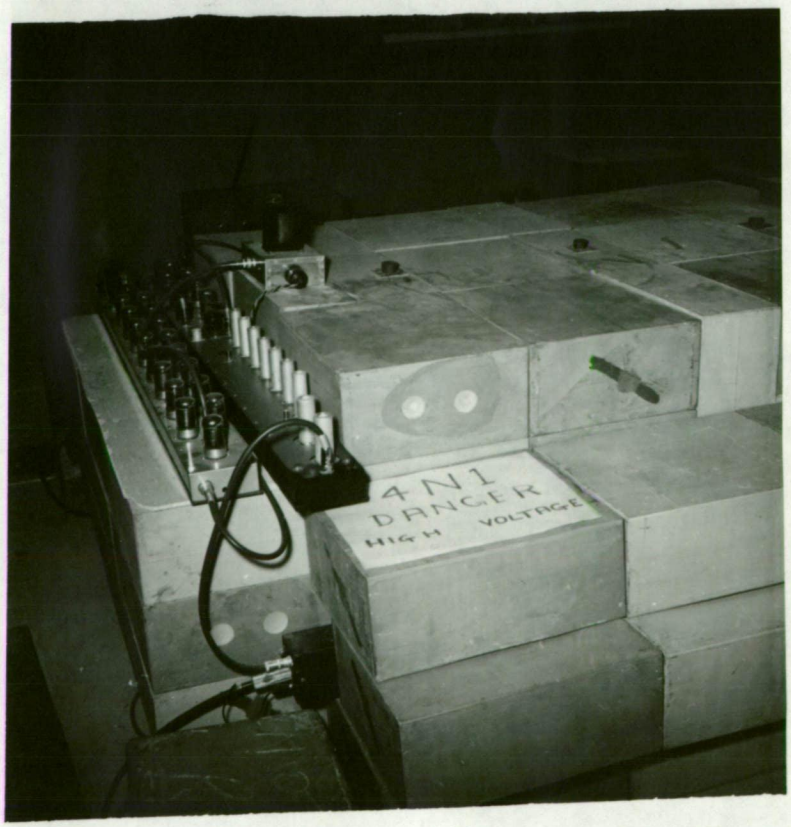

2B

for a long time. The requirement was imposed that every counter should, for at least one source position, contribute at least 20 percent of the counting rate.

1.6 Electronic circuits

To guard against complete loss of data through equipment failure, each monitor consists of two identical, independent sets of counters and electronic circuits. Fig. 1D indicates the manner in which the circuits have been divided up into units. The photograph, Fig. 2B, shows how the units are housed. The use of strip chassis for the amplifiers and scalers has proved to be very satisfactory, both from the design and maintenance point of view.

A brief description of the various units shown in the block diagram will now be given.

Counter connector box

The several counters in each section are connected together by this unit, which also contains the counter E.H.T. decoupling circuit, the counter anode load and the isolating condenser leading to the amplifier input (Fig. 3A). Connection to the amplifier is via coaxial cable. The shielding provided by the counter connector boxes against radio frequency pickup is quite adequate, even though the instruments at Mawson and Lae are in close proximity to high power telegraphy and pulse transmitters.

Considerable difficulty was experienced in achieving satisfactory insulation between the counter anode line and earth. Ceramic and polystyrene insulators proved to be quite unsatisfactory. The insulator shown in Fig. 3B, combining the excellent insulating properties of polyethylene with the mechanical stability of polystyrene has proved to be satisfactory.

Figure 3A - The counter connector box circuit. The NE51 neon gives a visual warning that the E.H.T. circuits are alive.

Figure 3B - The insulator used to support the anode lines in the counter connector boxes. The polyethylene component is a single length of the insulator used in PT11M coaxial cable.

Figure 3C - The circuit of the pulse amplifier and Schmitt trigger. Valves V_1 and V_2 are type EF86, valves V_3 to V_9 are type 6AU6.

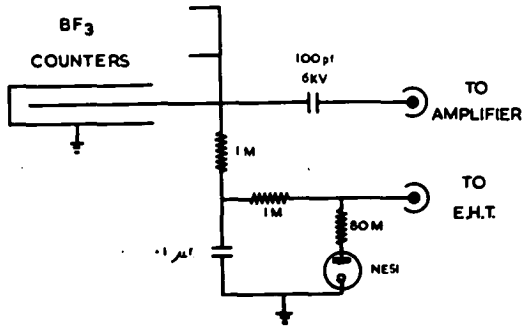
BF3
COUNTERS
100 pf
6KV
TO
AMPLIFIER
1 M
1M
TO
E.H.T.
80 M
·1 μf
NES1

3A

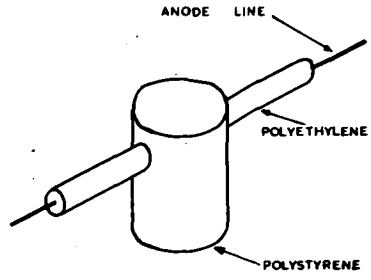
ANODE
LINE
POLYETHYLENE
POLYSTYRENE

3B

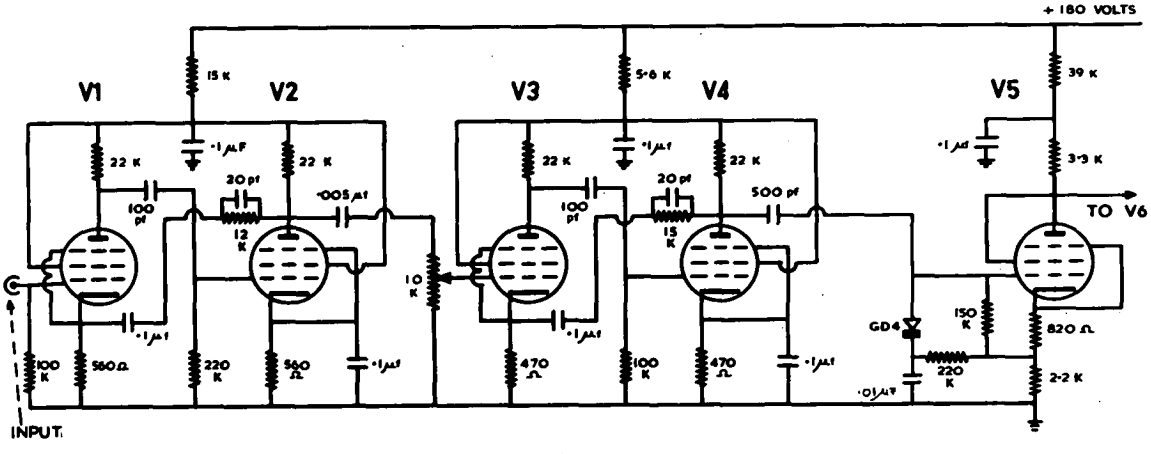
+ 180 VOLTS
V1
V2
V3
V4
V5
15 K
5·6 K
39 K
22 K
·1 μF
20 pf
·005 μf
100 pf
12 K
500 pf
15 K
3·9 K
TO V6
10 K
GD4
150 K
820 Ω
220 K
2·2 K
·01 μf
100 K
560 Ω
470 Ω
INPUT

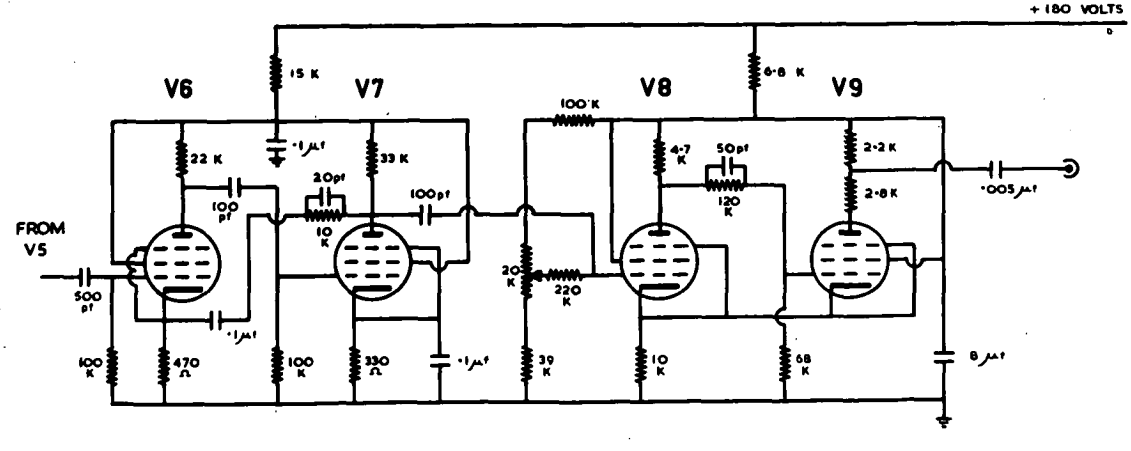
+ 180 VOLTS
V6
V7
V8
V9
15 K
6·8 K
100 K
·1 μf
22 K
33 K
4·7 K
50 pf
2·2 K
·005 μf
20 pf
100 pf
120 K
2·8 K
FROM
V5
10 K
20 K
220 K
500 pf
100 K
470 Ω
330 Ω
39 K
68 K
8 μf

3C

Amplifier and discriminator

It is necessary to select all pulses whose amplitudes exceed some predetermined level. The detection system must be stable, relatively unaffected by voltage change and valve aging.

This has been achieved by preceding a Schmitt trigger set to accept 8 volt pulses by a negative feedback pulse amplifier (Fig. 3C). The amplifier consists of three loops of two and a unit gain pulse inverter. The amplification factor of an amplifier using negative feedback is approximately $A' \doteq A(1 + xA)^{-1}$, where A is the amplification factor without feedback and x the fraction of the output voltage fed back to the input. If $xA \gg 1$, A' is largely independent of A. In the circuits used, $xA \approx 70$.

The Schmitt trigger is not stable to changes in valve characteristics, but this effect is minimised by the choice of a high threshold, 8 volts. The Schmitt threshold depends upon the high tension voltage, this being one reason why the 180 volt supply is stabilised.

Non microphonous valves, type EF86, are used in the first loop of two. This stage is built on a small, totally enclosed sub-chassis within the main chassis in order to minimise radio frequency pickup. Spurious pulses due to microphony and radio frequency pickup are much smaller than the neutron pulses in the remainder of the circuit, and no special precautions have been taken.

The amplifier gain is constant for frequencies between 85 and 500 Kc/sec. The gain is 3 db. down at 650 Kc/sec., hence the amplifier rise time is approximately 0.5 μs. The clipping time is 10 μs. The neutron pulses after amplification have some overshoot, but apart from this they are a fairly faithful reproduction of the input pulse. The Schmitt produces a standard 8 volt pulse of 5 μs duration every time it is triggered.

The threshold of the amplifier-discriminator combination

is stable to within ±2 percent for a ±15 percent change in filament voltage. As the operating threshold is upon the plateau of the bias curve, this stability is adequate. This was illustrated on two occasions when the Mt. Wellington mains stabiliser developed a fault, the A.C. voltage to the monitor changing from the normal 235v. to 210v. on one occasion and 280v. on the other. No significant change in counting rate was observed when the faults were rectified.

Scaler

The basic scaling and scaler output circuits are given in Figs. 4A and 4B. The number of binary scalers in cascade, and the number of output circuits varies from monitor to monitor, being determined by the type of recording apparatus employed.

The binary scaler is basically a direct coupled multivibrator using pentode valves. The input pulse is fed to the suppressors. The dead time of the whole scaling unit is 4 μs, and since the Schmitt output pulse is of 5μs duration, no pulses are lost in the scaler.

The binary scalers have proved to be extremely reliable. It was not necessary to match the components. The circuit functions reliably over a wide range of high tension and filament voltages, and is not affected by aging of the valves.

The scaler output circuit is essentially a self-quenching thyratron trigger circuit. Normally cut off, the thyratron conducts for approximately 0.5 sec. whenever the binary scaler valve to which it is connected is cut off. The pulse of current to the anode operates the recording equipment.

Power supplies

There is a separate stabilised high tension power supply

Figure 4A - The scaler input, and the binary scaling circuit. Valve V_2, a NE2 neon indicator, gives a visual indication of the operation of the circuit. Valves V_1, V_3 and V_4 are type 7C7. The cathodes of all the binary valves in a scaler connect to line L1, a resistor between L1 and earth biasing the cathodes 16 volts positive with respect to earth. The grid resistors of all binary valves such as V_4 connect to line L2. Opening S1 paralyses the scaler, and resets it to zero.

Figure 4B - The basic scaler output circuit. Valve V_5 is a thyratron, type 884. The grid circuit connects to the anode of a scaler valve such as V_3 in Fig. 4A.

Figure 4C - The flare alarm circuit. Valves V_6 and V_7 are type 6AU6, V_8 is a 90C1 gaseous regulator. The 25μF and 8μF condensers, and the associated resistors, comprise the "tank" circuit. The "bucket" condenser C is variable in steps, allowing the circuit to be adjusted for different counting rates.

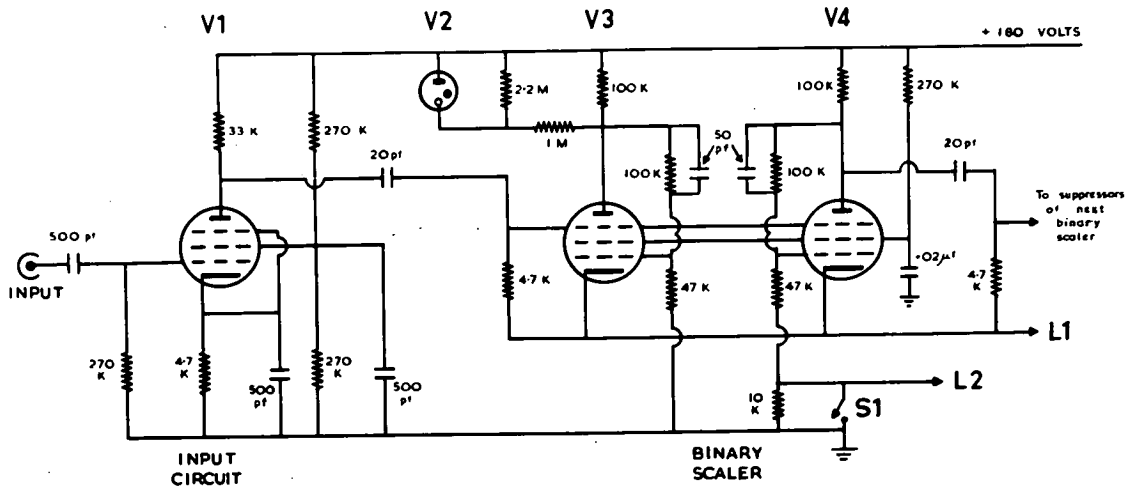
V1
V2
V3
V4
+180 VOLTS
33 K
270 K
2·2 M
100 K
1 M
50 pf
100 K
100 K
270 K
20pf
20pf
To suppressors of next binary scaler
500 pf
INPUT
4·7 K
47 K
47 K
·02μf
4·7 K
L1
270 K
4·7 K
500 pf
270 K
500 pf
L2
10 K
S1
INPUT CIRCUIT
BINARY SCALER

4A

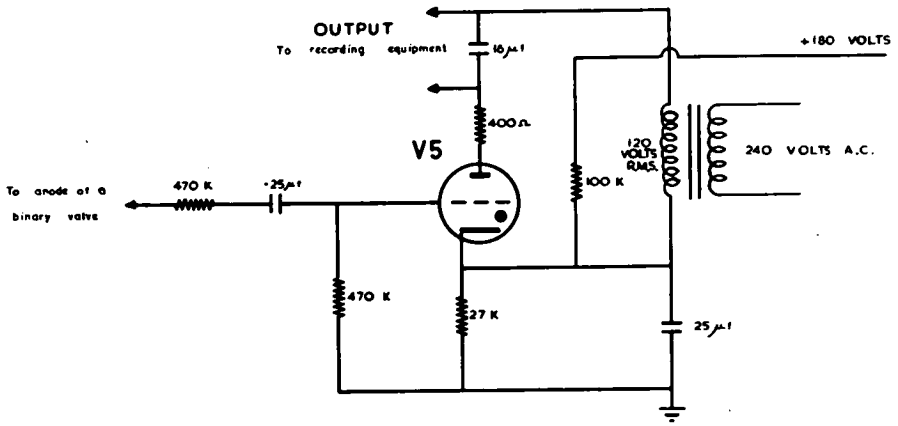
OUTPUT
To recording equipment
16μf
+180 VOLTS
400Ω
V5
120 VOLTS RMS.
240 VOLTS A.C.
To anode of a binary valve
470 K
·25μf
100 K
470 K
27 K
25μf

4B

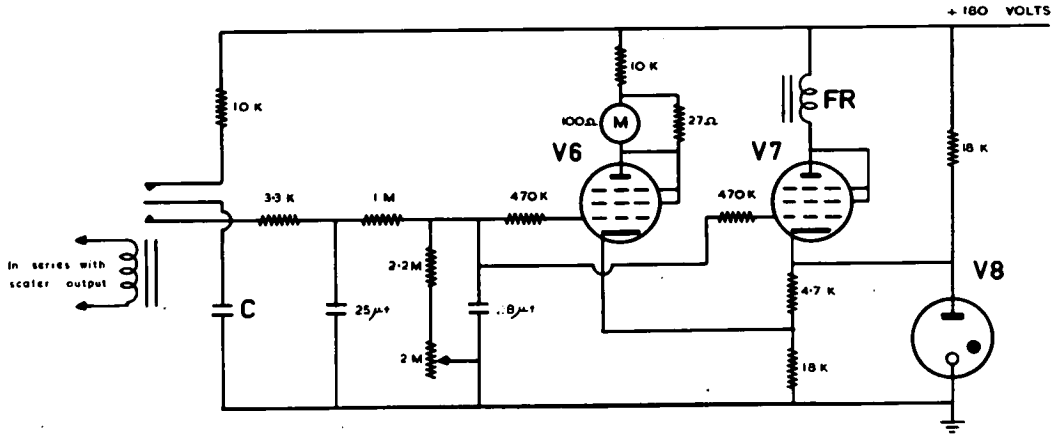
+180 VOLTS
10 K
10 K
100Ω
M
27Ω
FR
V6
V7
18 K
3·3 K
1 M
470K
470K
In series with scaler output
2·2M
C
25μf
·8μf
4·7 K
V8
2 M
18 K

4C

for each section of a monitor. A conventional series regulating circuit is used.

The E.H.T. supply for the proportional counters is regulated by a chain of G400/1K gaseous stabilising valves. The output voltage is variable in steps of 30 volts, and remains constant to within ±2 volts for a ±15 percent change of line voltage.

The stability of all circuits is improved by the use of electronic type A.C. mains stabilisers, manufactured by Stabilac Pty Ltd., Sydney.

Flare alarm

This unit is intended to initiate short term recording whenever the intensity exceeds the mean value by more than 50 percent. The circuit is given in Fig. 4C. There are independent circuits for the two halves of each monitor. The method of recording employed at Lae does not necessitate a Flare Alarm.

The scaler output pulse activates a relay, transferring charge from the "bucket condenser" to the "tank circuit". The time constant of the tank circuit is of the order of minutes, thus the voltage across the .8 μF condenser is relatively constant with time, the actual value being a function of the cosmic ray intensity. The 2×10^6 ohm potentiometer enables the tank circuit to be adjusted so that valve V_7 conducts whenever the counting rate exceeds the mean value for the station by 50 percent. This closes the relay in the V_7 anode circuit, initiating the short term recording programme.

The operating conditions of the meter valve V_6 have been chosen such that the minimum and maximum intensities encountered through atmospheric pressure variations produce meter readings of 0.1 and 0.8 of the full scale deflection. The flare alarm relay closes at 0.9 of the full scale deflection. For higher intensities, the meter valve draws grid current, and the meter reading is

virtually independent of the cosmic ray intensity.

The time delay between the commencement of an intensity increase and the closing of the flare alarm relay depends upon the rate at which the intensity increases, and the counting rate prior to the increase. In an unfavourable case when the intensity is at the minimum normally encountered at a station, the time delay for an instantaneous increase to 60 percent above the mean station intensity is 1.5 minutes.

As a more accurate measurement of the time of onset of a solar flare effect is very desirable (LUST and SIMPSON, 1957), chart recorders have recently been installed at Mt. Wellington and Mawson.

1.7 Recording apparatus

Different recording systems are used at the three stations. They are all designed to provide hourly counting rates, and counting rates for shorter intervals if required. The various systems are outlined below.

Mt. Wellington:- Two scaling factors, 64 and 512 are used. Counts from both are accumulated on mechanical registers. The registers, together with an aircraft altimeter and a clock are photographed every hour. The altimeter readings are converted to atmospheric pressure using an experimentally determined graph. In the event of a solar flare increase a second camera takes a photograph a few seconds after either flare alarm relay closes, and every two minutes thereafter, until both relays open again.

The scale of 512 output activates a pen on a multipen operations recorder, the chart speed being 4 inches per hour. This enables the counting rate over short time intervals to be determined, and also provides hourly data in the event of the camera failing.

This recording system is capable of yielding data for intensities up to 100 times above normal.

Mawson:- Each member of a bank of 48 mechanical registers is connected to the scale of 64 output for one hour every two days by a uniselector switch which steps on one position at the end of each hour. By reading the registers every day, hourly counting rates are obtained. Pressure data are obtained from a barograph situated in the nearby meteorological hut.

Five minute totals of the scale of 32 counting rate are provided by a bank of printing registers (FORD, 1958). At the end of each five minute period the number of counts accumulated is printed on to paper, and the registers reset to zero. When either flare alarm relay closes, the register prints every minute. A relay on the scaling circuit automatically changes the scaling factor to 128 when the scale of 32 pulse rate exceeds 100 per minute.

This recording system is capable of yielding data for intensities up to 60 times above normal.

Lae:- While the other observatories are in the charge of physicists thoroughly trained in the maintenance of the equipment, the Lae instrument is run by a Civil Aviation technician, and the time he can devote to the equipment is limited to one or two hours each week. Furthermore, postal delays, and the time taken in the reduction of the data means that some weeks may elapse before faulty operation is detected through inspection of the records.

An operations recorder was chosen as the most suitable recorder under these conditions. Hourly, or shorter term data are available, abnormal counting rates can be detected by the technician by glancing at the chart, and the recorder itself requires the minimum of maintenance.

A typical chart is shown in Fig. 5. Each scaler activates a pen, producing a series of pips. The scaler output, scaled by a further factor of ten, energises another pen. This second trace reduces the labour involved in reading the chart. Hour

SCALING FACTORS

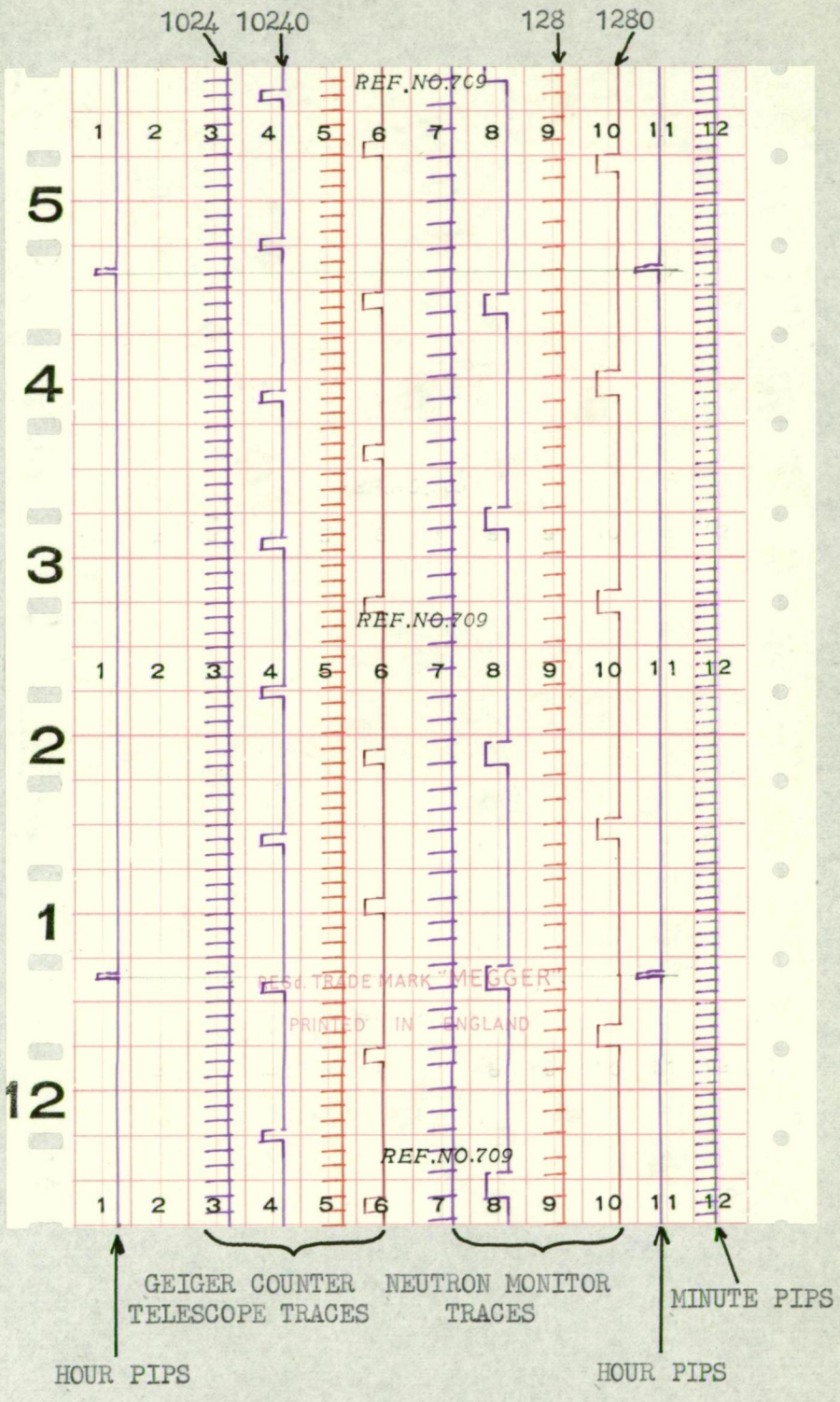

TYPICAL RECORDING CHART

FIG. 5

and minute pips on the outermost traces define the time scale.

Pressure data are obtained from a barograph in the nearby meteorological office.

1.8 Timing

Chronometers are used at all observatories to ensure long and short term stability. The instruments at Lae and Mt. Wellington are of the self winding variety, that is, they consist of a conventional chronometer movement which is maintained fully wound by an electro-mechanical system. Such a chronometer is not affected by reasonably long power breaks, and yet it requires no attention apart from occasional checks against the U.S.A.'s National Bureau of Standards time signal WWV. The chronometer rates have remained constant to within 0.01 percent.

1.9 Housing of the equipment

The instruments at Mt. Wellington and Mawson are installed in huts specially built as cosmic ray observatories, while the Lae equipment is inside an aircraft hanger which has been converted into offices. Table 1A summarises the characteristics of each observatory. Meson telescopes are installed at Hobart, Lae, Mawson and Macquarie Island. (Geographic co-ordinates; 54°S, 158°E).

TABLE 1A

Details of the observatories equipped with a neutron monitor. At all observatories the roof thickness is less than 10 gm cm^{-2}.

OBSERVATORY	GEOGRAPHIC		GEOMAGNETIC		ALTITUDE (m)	ATMOSPHERIC DEPTH (gm cm^{-2})	TEMP. (°C)	TOTAL COUNTING RATE (CTS/HR)
	LAT.	LONG.	LAT.	LONG.				
LAE	07°S	147°E	16°S	218°E	4	1030	20-35	8×10^3
MT. WELLINGTON	43°S	147°E	52°S	224°E	725	945	6-28	35×10^3
MAWSON	68°S	63°E	73°S	103°E	15	1010	10-30	33×10^3

A heater in the roof of the hut housing the Mt. Wellington detector is automatically turned on during cold weather in order to keep the roof free of snow. At Mawson, no snow can settle on the horizontal roof because of the incessant winds.

The air temperature and humidity at Lae are higher than recommended (SIMPSON, 1956). No evidence has been found that this produces spurious counts.

1.10 Testing procedures

The mains stabiliser output voltage, the counter E.H.T. voltage and the stabilised H.T. voltage are measured each week. At the same time the threshold of the amplifier-discriminator combination is determined using a pulse generator which produces facimile neutron pulses of variable amplitude.

By disconnecting the E.H.T. from the counters, spurious pulses due to radio frequency pick-up are detected. By disconnecting the counter anodes, pulses due to E.H.T. discharge or leakage across the isolating condenser leading to the amplifier are detected. These tests have been performed on both sections of the Mt. Wellington and Mawson monitors every week since installation. The equipment is regarded as satisfactory if the pulse count during 15 minutes is less than 0.05 of the standard deviation appropriate to a 15 minute cosmic ray count. In practice, it is unusual for any spurious pulses to be recorded in either test. Similar tests performed over a period of four months at Lae indicated that the Lae monitor was likewise free from spurious pulses.

The overall stability of the detection system is tested every three months by determining the counting rate with a Ra-Be neutron source inserted in the test keyways. At the same time the E.H.T. plateau is checked by determining the counting rate at voltages 60 volts above and below the operating value. No significant variations in the number of source neutrons detected

using the operating E.H.T. have been observed (standard deviation, 0.3 percent). A deterioration of plateaux is suspected, but as yet unconfirmed. During installation of the Lae monitor a rapid deterioration of one plateau was traced to one counter, for which the E.H.T. plateau had almost disappeared. The evidence was consistent with the theory that a slow air leak was introducing electronegative material into the counter.

Spurious pulses may originate within the BF_3 counters themselves. To test this possibility, a thin Cadmium sheath is slipped around a counter, all the other counters in the section being disconnected from the anode line. The amplifier threshold is set to the value appropriate to a single counter. Cadmium has a very high cross section for the capture of thermal neutrons, and so very few can enter the counter. The "cadmium background" counts are due to (1) stars in the counter walls, (2) response to non-thermal neutrons, (3) alpha particles emitted from the counter walls, (4) discharges inside the counter due to impurities or rough sections on the anode, (5) leakage across insulators, and (6) thermal neutrons entering the counter from either end. The contributions of the last three catagories are the most likely to change with time. The cadmium background averages 0.5 to 2 pulses per minute. No significant changes have been observed.

1.11 Equipment reliability

The electronic circuits have proved to be extremely reliable; for example, in the two years the Mt. Wellington monitor has been operating, only once has failure of an electronic circuit resulted in the loss of any data. Power valves are replaced every six months, all other valves every year. The greatest loss of data has been due to failure of the recording systems, the photographic system at Mt. Wellington being especially prone to failure. Loss of data at Mawson and Mt. Wellington has recently been minimised by the installation of two different, independent recording systems.

Diesel generators provide the A.C. power at Mawson and Lae, and as these units are quite small (35 K.V.A. and 100 K.V.A. respectively) voltage and frequency fluctuations are quite large, and complete failure for a few minutes at a time fairly common. One advantage of chart recording is that a period of a few minutes including a short power failure can be deleted without increasing the statistical error for the hour appreciably. Trees falling across the power line to Mt. Wellington occasionally result in the loss of up to twelve hours data.

CHAPTER 2

ROUTINE ANALYSIS OF NEUTRON DATA

2.1 Statistical fluctuations in the neutron counting-rate

The neutrons counted by one section of a monitor are not unrelated, there being two main causes of correlation.

(1) More than one nucleon of the cascade produced by a single primary cosmic ray may create a star in the monitor. The stars will not, in general, be produced simultaneously, as the initiating nucleons will be travelling with different velocities. Time delays in the emission of the nucleons from the stars responsible for the cascade action are completely negligible ($< 10^{-21}$ second per event. ROSSI, 1952, p.370). To estimate the order of time differences to be expected, consider (a) a high energy nucleon, and (b) a 50 Mev nucleon, both of which penetrate to ground level after being formed high in the atmosphere during the early stages of the development of a cascade. The upper limit of the velocity of particle (a) is the velocity of light, c, while the velocity of particle (b) is 0.31 c. Thus the time taken to travel from near the top of the atmosphere to ground level (20 Km) is $>$ 67 μsec and 212 μsec respectively. As few particles of energy $<$ 50 Mev produce stars, the time difference in this case, 145 μsec, should be close to the maximum possible.

(2) A number of neutrons are produced in each star and more than one of these may be detected. The mean life of thermal neutrons in paraffin wax is of the order of 140 μsec (GEIGER and ROSE, 1954) and therefore about 89 percent of the neutrons produced in a star will have been captured after 300 μs. Thus there will be few "multiples" in which the pulse separation is greater than 300 μsec.

When observing events occurring at random in time, the

number of events occurring in a fixed time interval follows a Poisson distribution which approximates to a normal distribution when the number of events is large. If the average number of events occurring in the time interval is n, the standard deviation is $\sqrt{n}$. The presence of correlated pulses ("multiples") in the output of a neutron monitor means that the counting rate does not follow a Poisson distribution.

Let X be the number of primary cosmic rays which produce one or more counts in a neutron monitor in a given time, while C is the total number of counts recorded. The multiplicity, m, is defined

$$C = mX \qquad 2(1)$$

The number of counts produced by a single primary is not affected by the arrival of other primaries at the top of the atmosphere. Hence m and X are independent variables. For a function of two independent variables

$$V\,g(YZ) \simeq \left(\frac{\partial g}{\partial Y}\right)^2 V(Y) + \left(\frac{\partial g}{\partial Z}\right)^2 V(Z) \qquad 2(2)$$

so
$$V(C) \simeq \bar{m}^2\, V(X) + \bar{X}^2\, V(m) \qquad 2(3)$$

where a bar indicates a mean value, and the variance of a quantity is indicated by V( ).

It is assumed that the arrival of primary particles is random in time. Hence $V(X) = \bar{X}$ and

$$V(C) \gtrsim \bar{m}^2 \bar{X} + \bar{X}^2\, V(m) > \bar{C}$$

It is immediately clear that an underestimate of the

standard deviation is obtained if the counting rate is assumed to follow a Poisson distribution.

An experiment was designed to measure $\bar{m}$ and $V(m)$*. A single shot multivibrator was connected to the output of a neutron monitor discriminator and adjusted so that pulses with a separation of less than 300 μsec gave a single output pulse. The multivibrator pulses were scaled and counted. As the majority of multiples were counted as single pulses, this gave the X count. The normal neutron monitor scaler gave the C count, and by applying equation 2(1), m was calculated. Using hourly data from a two counter monitor in which the two counters were connected in parallel, $\bar{m} = 1.11$, $V(m) = 4 \times 10^{-5}$ and $\bar{C} = 4.8 \times 10^{3}$ counts/hour. Thus for hourly data, $V(C) \approx 1.27\,\bar{C}$, and the standard deviation (written s.d.) is given by $\text{s.d.}(C) \approx 1.13\sqrt{\bar{C}}$.

A large monitor would be expected to have a somewhat higher multiplicity. As the evaporation neutrons from a star do not travel very far through matter (m.f.p. about 2 inches in paraffin), counters far away from a star will not be effective in the production of a multiple. Therefore the multiplicity of a large monitor is probably no more than about 1.2, and as a rough estimate $\text{s.d.}(C) \approx 1.2\sqrt{\bar{C}}$.

2.2 The ratio of the counting rates of two sections of a monitor

The functional relationship between the counting rate, primary intensity and meteorological variables will be the same for both sections of a monitor, as their geometries are identical. Hence the ratio of the counting rates should only vary because of statistical fluctuations in the two rates, and the mean ratio should remain constant with time.

---

* This experiment was performed by Dr. J. R. Storey.

Instrumental faults will, in general, occur in only one section at a time, and will produce a change in the ratio of the counting rates. The ratios therefore provide a continuous check on the reliability of the equipment. In the event of an adjustment being made to one section, comparison of long term ratios before and after the adjustment indicates whether any change in counting rate occurred, and enables correction to be made to the total counting rate. Greater reliance can then be placed in comparisons of data obtained many years apart. It is obviously very desirable that equipment alteration be carried out one section at a time.

Consider a monitor for which the counting rates of the two sections are C_1 and C_2. Since some of the counts included in C_1 and C_2 are due to the same primary cosmic rays, statistical fluctuations in C_1 and C_2 will not be completely independent. To determine the magnitude of the correlation between C_1 and C_2, the counting rate of one section of a twelve counter monitor was determined with and without the second section being in position.* It was found that approximately 4 percent of the neutrons counted by any one section originated in the adjacent section. The correlation between the statistical fluctuations is therefore quite small, and, as a first approximation it will be ignored.

From 2(2), the variance (V) of the ratio $\frac{C_1}{C_2}$ is given by

$$V\left(\frac{C_1}{C_2}\right) = \frac{1}{\bar{C}_2^2} V(C_1) + \frac{\bar{C}_1^2}{\bar{C}_2^4} V(C_2) \qquad 2(4)$$

If C_1 and C_2 are correlated, $V\left(\frac{C_1}{C_2}\right)$ is less than that given by

---

* This experiment merely gives the correlation due to the production of more than one neutron in a single star (class 2 in section 2.1). No information is available as to the correlation due to the two sections detecting two different members of the same nucleonic cascade.

the expression 2(4).

As the two sections are identical, $\bar{C}_1 = \bar{C}_2$ and $V(C_1) = V(C_2)$. Therefore

$$V\left(\frac{C_1}{C_2}\right) = \frac{2}{\bar{C}_2^2}\left(V(C_2)\right)$$

Thus the standard deviation of the ratio has an upper limit of $\sqrt{2} \cdot \frac{s.d.(C_1)}{\bar{C}_1}$. The correlation between C_1 and C_2 being small, the standard deviation of the monitor ratio is close to this upper limit.

For each of six months, the standard deviation of the Mawson daily ratio was calculated. The value to be expected from statistical fluctuations is listed in Table 2A along with the observed values. The differences are statistically significant.

TABLE 2A

Standard deviation (S.D.) of the Mawson daily ratio (Year 1957)

Month	April	May	June	July	August	Sept.	Expected
S.D. of ratio	0.0035	0.0025	0.0028	0.0033	0.0034	0.0029	0.0025

It is apparant that during most months there were minor equipment variations. In every month, the standard deviation of the ratio due to equipment change was <0.0025. This is equivalent to a standard deviation of 0.13 percent in the total counting rate when the assumption is made that all the variation was in one section.

2.3 The dependence of neutron counting rate upon atmospheric pressure

At atmospheric depths greater than 300 gm cm^{-2}, the relationship between the intensity of star producing nucleons and atmospheric depth is roughly exponential. (SIMPSON and FAGOT, 1953).

For a neutron monitor at ground level a change in atmospheric pressure is accompanied by an out of phase variation in counting rate. In order to compare neutron data obtained at times of different atmospheric pressure, it is the usual practice to estimate from the observed counting rate and pressure the counting rate which would have been observed if the pressure had been some other fixed value, p_o. This value is usually chosen to be close to the mean atmospheric pressure at the station. This method of compensating for pressure variations is known as "correction to the pressure level p_o".

Let the absorption mean free path of the nucleonic component in the units used to measure the atmospheric pressure be λ. If at time t the atmospheric pressure is p and the counting rate $R(t,p)$, then the intensity corrected to the p_o pressure level is given by

$$R(t) = R(t,p) \exp. \left(\frac{p - p_o}{\lambda}\right)$$

$$= R(t,p) \exp. \left(\frac{\partial p}{\lambda}\right) \qquad 2(5)$$

This may be rewritten

$$R(t) = R(t,p) + R(t,p) \left[\exp. \left(\frac{\partial p}{\lambda}\right) - 1 \right]$$

$$= R(t,p) + R(t) \left[1 - \exp. \left(-\frac{\partial p}{\lambda}\right)\right]$$

$$= R(t,p) + R(t) \left[\frac{\partial p}{\lambda} - \frac{1}{2!} \left(\frac{\partial p}{\lambda}\right)^2 + O(3) \right]$$

$$= R(t,p) + \frac{R(t)}{\lambda}(\partial p) - \frac{R(t)}{2\lambda^2} \cdot (\partial p)^2 + O(3) \quad .. 2(6)$$

In the correction of meson data for atmospheric change it has been the practice to use an additive correction. It can be

seen from 2(6) that if (a) primary variations are small, so that $R(t)$ on the right hand side can be replaced by R, the mean value of $R(t)$ over a long period, and (b) pressure variations are small, so that the $(\partial p)^2$ term is negligible, then the nucleonic correction equation can also be written in the linear form

$$R'(t) = R(t,p) + \left(\frac{R}{\lambda}\right) \partial p \qquad 2(7)$$

The quantity $R(t) - R'(t)$ is the error introduced by the use of equation 2(7). Values of this error, expressed as a percentage of $R(t)$, are listed in Table 2B for a number of values of ∂p and $R(t)$. The value of $R(t)$ is expressed in column one relative to the value of R adopted in 2(7).

TABLE 2B

Percentage Errors introduced into the corrected data by the use of a linear approximation to the correction equation.

$\frac{R(t)-R}{R(t)} \times 10^2$ \ ∂p (millibars)	-30	-20	-10	0	+10	+20	+30
0.0	-2.25	-1.00	-0.25	0.00	-0.25	-1.00	-2.25
-3.0	-1.62	-0.58	-0.04	0.00	-0.46	-1.43	-2.89
-6.0	-0.98	-0.15	+0.17	0.00	-0.68	-1.85	-3.53
-9.0	-0.34	+0.27	+0.39	0.00	-0.89	-2.28	-4.16

In some cases, these errors are considerably greater than the 0.6 percent and 1.2 percent standard deviations of the Mawson and Lae hourly counting rates. Thus neither condition (a) nor (b) is fulfilled in practice. For this reason, all the data accumulated since the inception of the neutron monitor programme have been corrected using the multiplicative correction equation 2(5).

The exponential nature of the pressure correction law means

that it is not strictly correct to group neutron data prior to correction. As such a procedure is less time consuming than correcting the data prior to grouping, the errors incurred will be calculated.

Let statistical and primary fluctuations be neglected. The hourly counting rates for N consecutive hours will be grouped. During the i^{th} hour, let the mean atmospheric pressure be p_i, and write $p_i - p_o = \partial p_i$.

For the rates of change of pressure encountered in practice, the following approximation is legitimate. (from 2(5))

$$R(p_i) = R(p_o) \exp. \left(- \frac{\partial p_i}{\lambda}\right)$$

Hence the mean counting rate for the N hours is given by

$$R = \frac{1}{N} \sum_{1}^{N} R(p_o) \exp. \left(- \frac{\partial p_i}{\lambda}\right)$$

It may be simply shown that this leads to

$$R(p_o) = R \exp. \left[\frac{P - p_o}{\lambda}\right] \left\{1 - \frac{1}{2N\lambda^2} \Sigma(p_i - P)^2 + 0_3\right\} \qquad 2(8)$$

where P is the mean of the p_i.

In the experimental case, R, p_i and P are known. From 2(8) the error introduced by grouping the data first, and then inserting the mean values R and P in the correction equation 2(5) is approximately

$$\frac{10^2}{2N\lambda^2} \Sigma (p_i - P)^2 \quad \text{percent.}$$

For each station, the above error function was evaluated for the day showing the greatest pressure variation since the inception of the recording programme. The results were:- Lae, 0.01 percent;

Mt. Wellington, 0.11 percent; Mawson, 0.24 percent. While the error at Lae is quite insignificant, those at the other two stations are comparable with the standard deviations due to statistical fluctuations.

Experience has shown that at Mawson and Mt. Wellington the statistical fluctuations in the hourly counting rates are small enough to allow primary variations of from 2 to 12 hours duration to be discerned. Consequently it has been desirable to correct the hourly values. The greater statistical fluctuations at Lae mask most short term phenomena, and so there is no point in correcting hourly values. It has been shown above that grouping prior to correction is permissible at Lae, and in practice daily mean values have been corrected.

2.4 Practical correction procedures

At the inception of the neutron recording programme, the best published value for the absorption mean free path, λ, was 145 gm cm^{-2}. (SIMPSON, FONGER and TREIMAN, 1953) . It appeared that for ground level stations (atmospheric depth $>$ 700 gm cm^{-2}) this value applied equally well at equatorial and high latitude stations, suggesting that it was relatively independent of primary spectrum. It was decided that all data would be corrected using the above value.

It is now clear that even at sea level the mean free path (m.f.p.) is latitude sensitive. This is shown by the fact that the latitude effects at 680 gm cm^{-2} and sea level are 2.55 and 1.77 respectively. (SIMPSON and FAGOT, 1953; ROSE et al, 1956) . Furthermore, it is probable that a better value at high latitudes would be λ = 138 gm cm^{-2}. (See Section 2.8). As the m.f.p. varies with latitude, it would be expected to be affected by spectral changes. This has been shown to be so (Section 6.2). It is consequently certain that there are still meteorological effects in the corrected data, although these can hardly exceed $\pm$1 percent at the

high latitude stations, and ±0.3 percent at Lae. We adhere to the original value of λ as a matter of convenience.

A table of exp. $(\frac{\partial p}{\lambda})$ was drawn up. This table is used in conjunction with the correction equation 2(5) to correct the Lae daily means. A less tedious method of correction is used to correct the hourly data at the other stations.

From 2(5)

$$\ln R(t) = \ln R(t,p) + \frac{\partial p}{\lambda}$$

A number of slide rules were prepared using this equation. In the earlier versions a conventional straight slide rule construction was employed. The scales were first drawn on white paper, then photographed and printed on a non-shrink photographic paper.

This design suffered from the disadvantage that the camera and enlarger lenses introduced distortions. A circular slide rule developed by Dr. J. R. Storey overcame this problem, and is now in general use. As shown in Fig. 6, circular, concentric scales are employed. Three logarithmic scales cover the range 100 to 1000 counts, and a fourth scale, calibrated in millibars and inches of mercury, covers the range 940 to 1045 millibars. By photographing the drawing of the scales with the axis of the lens concentric with the scales, distortion of angles was kept to a minimum.

The slide rule consists of a rigid body, a cursor and circular plate both free to rotate about the same axis, and a window of thin polystyrene sheet. The photographic scales are cemented on to the rotating plate concentric with the axis of rotation. A fine reference line on the polystyrene sheet is drawn through the axis of rotation.

The observed counting rate is set under the reference line on the window, and the cursor line is set over the observed pressure,

Figure 6 - Circular slide rule used in the correction of neutron data for changes in the atmospheric pressure.

barometric pressure
inches of mercury
millibars
neutron intensity

Rotation of the scale plate until the reference pressure p_o is under the cursor line brings the corrected counting rate under the reference line on the window.

Table 2C is a typical data analysis sheet. The counting rates of the two sections (C_1,C_2) and the atmospheric pressure (P) are entered, and the ratio C_1/C_2 evaluated. The ratios are plotted on graph paper, and if they show no anomalous variation, the sum $C_1 + C_2$ is entered and corrected to the standard pressure adopted for the observatory. Graphs of the corrected hourly data are prepared and examined for unusual variations.

Monthly summary sheets of the uncorrected counting rate ($C_1 + C_2$), the pressure, and the corrected counting rate are duplicated (Table 2D). These sheets are used for all subsequent analyses, and are circulated to other cosmic ray groups.

2.5 Errors in the corrected counting rate

The errors inherent in the measurement (statistical fluctuations) and the errors which can be introduced by unsuitable data handling procedures have been discussed. In the present section the errors due to the limited accuracy of the recording systems are considered.

(a) Scaling and rounding off errors

The scaling factor is chosen such that (a) the register count is relatively low, to avoid excessive wear, and (b) the statistical fluctuations in the scaled counting rate are still sufficiently large for the content of the scaler at the end of each hour to be safely ignored.

Let C_1 and C_2 be the number of unscaled counts recorded each hour by the two sections of a monitor. Let X_1 and X_2 be the number of scaled counts recorded each hour, and F the scaling factor.

TABLE 2C

Typical data analysis sheet

RECORD OF THE COSMIC RAY NEUTRON COMPONENT

Form 108

AUSTRALIAN NATIONAL ANTARCTIC RESEARCH EXPEDITION

Station MT. WELLINGTON

Monitor BN 2

Scale Factor 64

C_1 = Section No.1 Count

C_2 = Section No.2 Count

C^1 = Corrected Count

P = Pressure

DATE	25 11 57 / 26 11 57						27 11 57 / 28 11 57						29 11 57 / 30 11 57					
HOUR GMT	C_1	C_2	C_1/C_2	C_1+C_2	P	C^1	C_1	C_2	C_1/C_2	C_1+C_2	P	C^1	C_1	C_2	C_1/C_2	C_1+C_2	P	C^1
01	288	297	970	585	27.03	536	240	247	972	487	27.50	499	270	273	989	543	27.14	510
02	287	296	969	583	03	534	243	251	968	494	48	504	274	275	996	549	14	516
03	289	298	970	587	03	538	241	247	976	488	47	496	271	281	964	552	13	518
04	289	299	966	588	03	538	242	249	972	491	46	498	273	280	975	553	12	518
05	T	297		586 s	03	537 s	237	242	979	479	46	486	268	281	954	549	11	512
06	T	T		T	04	T	240	243	988	483	45	489	271	277	978	548	10	510
07	290	290	1000	580	05	534	242	244	992	486	44	491	276	277	996	553	09	514
08	285	294	969	579	06	534	242	248	976	490	44	495	271	281	964	552	09	513
09	289	292	990	581	09	540	241	247	976	488	44	493	270	277	975	547	08	507
10	287	292	983	579	12	542	240	246	976	486	43	490	272	284	958	556	08	515
11	277	288	962	565	14	531	241	247	976	488	43	492	273	279	986	554	09	514
12	280	288	972	568	15	535	242	246	984	488	43	492	268	281	954	549	11	512
13	278	282	986	560	16	529	247	247	1000	494	42	496	271	275	986	546	12	511
14	281	285	986	566	17	536	245	252	972	492	41	498	269	275	975	543	12	508
15	281	290	969	571	18	542	251	254	988	505	39	504	268	271	978	536	14	504
16	275	281	979	556	19	529	244	256	953	500	38	498	269	272	989	541	15	510
17	273	280	975	553	20	527	251	255	984	506	36	501	267	275	971	542	16	512
18	279	282	989	561	22	538	249	255	976	504	35	498	259	273	949	532	17	504
19	272	279	975	551	25	532	251	259	969	510	35	504	263	270	974	533	19	507
20	267	278	960	545	28	530	253	263	962	516	34	508	262	267	981	529	21	506
21	265	274	967	539	31	528	251	263	954	514	34	507	257	263	977	520	23	499
22	262	270	970	532	35	526	253	260	973	513	33	504	253	264	958	517	26	500
23	263	269	978	532	37	528	247	260	950	507	32	497	254	258	984	512	29	499
24	263	269	978	532	39	531	258	262	985	520	31	509	254	257	988	511	31	500
Total	6130	6876		12979	2787	12275	5891	6043		11934	2373	11949	6401	6866		12967	2763	12219
Mean				5643	27.161	533.7				497.3	27.405	497.9				540.3	27.151	509.1
Check	6120	6876				5336	5891	6043		11934		4979	6401	6566		12967		509.3
01	259	268	966	527	27.40	527	258	261	988	519	27.30	507	256	262	977	518	27.33	509
02	258	270	956	528	41	529	252	264	955	516	30	504	268	267	1004	535	34	518
03	268	270	993	538	42	540	258	262	985	520	30	508	265	267	993	532	35	516
04	263	265	992	528	43	532	256	261	981	517	31	506	265	260	1019	525	36	520
05	258	265	974	523	43	527	254	259	981	513	31	502	259	265	977	524	37	520
06	255	265	962	520	45	526	260	262	992	522	30	510	258	269	959	527	38	525
07	250	262	954	512	45	520	254	270	941	524	30	512	258	261	989	519	39	518
08	253	260	973	513	46	520	248	264	943	513	30	501	259	262	989	521	41	522
09	243	250	972	493	48	502	264	259	981	513	30	501	256	263	973	519	42	522
10	241	242	996	483	50	494	253	261	969	514	30	502	252	257	981	509	44	514
11	237	245	967	482	51	495	257	264	973	521	29	508	248	260	954	508	45	514
12	238	246	967	484	53	499	257	267	963	524	28	509	248	259	958	507	46	514
13	234	237	987	471	53	486	255	267	955	522	26	505	253	259	977	512	46	520
14	240	244	984	484	52	498	261	267	978	528	24	508	250	258	969	508	46	516
15	237	245	967	482	50	494	269	273	985	542	22	519	252	259	973	511	45	517
16	245	243	1008	488	49	498	268	271	989	539	19	513	251	256	980	507	44	512
17	236	253	933	489	48	498	266	275	967	541	17	512	258	263	981	521	44	526
18	244	246	992	490	47	498	263	272	967	535	16	505	259	267	970	526	44	531
19	244	253	964	497	47	505	267	276	967	543	15	512	260	264	985	524	45	530
20	246	247	996	493	48	503	268	276	971	544	15	513	255	261	977	516	47	522
21	247	248	996	495	49	506	268	275	975	543	15	512	258	262	985	520	45	526
22	245	248	988	493	50	505	266	276	964	542	15	511	258	265	974	523	43	527
23	237	244	971	481	50	493	266	271	982	537	15	506	259	263	985	522	43	525
24	241	247	976	488	51	501	268	276	971	544	14	512	255	265	962	520	42	522
Total	5919	6063		11982	3541	12196	6247	6429		12676	2972	12198	6160	6294		12454	3401	12506
Mean				499.3	27.475	508.2				528.2	27.238	508.3				518.9	27.417	521.0
Check	5919	6063		11982		508.2	6247	6429		12676		508.1	6160	6294		12454		520.9

C.D.O. 2001

TABLE 2C

Typical data analysis sheet

TABLE 2D

Monthly summary sheet of the pressure corrected neutron counting rate observed at Mt. Wellington.

COSMIC RAY DATA. PHYSICS DEPARTMENT, UNIVERSITY OF TASMANIA.

STATION: MT. WELLINGTON (HOBART), TASMANIA. (42° 55'S, 147° 14'E). Altitude 725 metres. NOVEMBER, 1957.

RECORDER: DUPLEX NEUTRON MONITOR. Scale Factor, 64. Barometer Coefficient -9·44 percent/cm. Hg.

TABULATED: HOURLY COUNT TOTALS CORRECTED TO STANDARD PRESSURE OF 27·40 inches of Hg.

Hour GMT.	Date. 01	02	03	04	05	06	07	08	09	10	11	12	13	14	15	16	17	18	19	20	21	22	23	24	25	26	27	28	29	30	31
01	535	535	539	541	543	549	553	564	557	560	558	563	567	557	565	569	558	562	539	554	549	565	553	540	536	527	499	507	510	509	
02	545	546	539	537	547	554	555	563	543	554	559	561	574	561	557	558	555	549	557	550	559	564	556	535	534	529	504	504	516	528	
03	537	540	537	550	547	553	549	565	548	552	555	568	559	563	570	557	556	563	555	548	544	552	556	533	538	540	496	508	518	526	
04	541	542	548	542	552	553	555	560	546	556	555	557	560	561	564	555	552	556	559	547	551	555	552	537	538	532	498	506	518	520	
05	541	550	543	550s	550	549	562	558	557	553	T	550	565	561	558	561	556	554	555	556	553	556	545	545	537s	527	486	502	512	520	
06	532	544	534	T	557	551	555	565	557	554	559s	560	553	559	567	558	564	557s	560	549	551	554	550	533	T	526	489	510	510	525	
07	538	544	549		549	546	557	565	559	559	553	556	566	561	563	549	560	555s	556	553	552	556	552	537	534	520	491	512	514	518	
08	537	541	543		550	543	554	561	551	551	557	551	567	560	559	559	553	561	555	553	549	559	545	536	534	520	495	501	513	522	
09	536	542	535	545	552	550	550	563	553	554	553	555	564	556	561	555	551	553	553	555	557	553	545	542	540	502	493	501	507	522	
10	543	539	539	548	547	549	551	559	555	553	556	557	564	556	558	551	555	557	557	552	554	555	545	537	542	494	490	502	515	514	
11	537	530	542	540	543	550	557	559	549	552	556	561	552	560	554	552	557	556	552	550	557	554	544	547	531	495	492	508	514	514	
12	535	539	539	543	RF	555	549	561	553	545	550	561	561	564	552	554	550	553	554	544	552	559	551	539	535	499	492	509	512	514	
13	537	541	542	538	545	555	554	554	555	552	555	561	557	559	553	549	562	551	553	548	558	553	537	536	529	486	496	505	511	520	
14	540	543	547	538	547	558	554	554	556	557	553	562	565	555	560	547	557	560	547	553	560	547	541	536	536	498	498	508	508	516	
15	538	548	536	539	544	549	557	565	550	551	550	570	564	560	554	551	564	557	546	554	550	552	538	537	542	494	504	519	504	517	
16	543	537	542	534	548	549	558	565	554	549	551	556	559	559	552	553	560	559	548	551	547	559	534	547	529	498	498	513	510	512	
17	533	545	539	537	547	553	556	558	561	553	557	562	558	553	557	554	556	555	551	547	552	555	538	537	527	498	501	512	512	526	
18	538	535	540	542	543	547	555	563	555	547	555	555	556	553	553	557	560	560	545	546	557	551	550	536	538	498	498	505	504	531	
19	538	539	539	537	550	550	561	567	551	552	557	557	556	554	549	564	558	553	553	539	560	555	549	533	532	505	504	512	507	530	
20	534	532	532	533	548	553	565	562	551	553	559	556	555	555	551	552	556	555	559	553	551	560	552	539	530	503	508	513	506	522	
21	533	535	533	537	545	559	560	553	554	557	549	558	553	561	554	559	555	561	550	550	553	555	546	535	528	506	507	512	499	526	
22	537	532	537	543	543	555	570	557	559	556	551	558	553	559	553	548	553	555	546	548	549	548	531	535	526	505	504	511	500	527	
23	541	541	537	537	551	556	572	565	551	561	557	558	564	567	556	559	556	555	549	551	547	551	543	538	528	493	497	506	499	525	
24	543	537	540	539	561	553	563	553	559	553	559	561	557	560	547	552	563	556	554	559	553	552	547	533	531	501	509	512	500	522	
SUM	12912	12951					13372	13284					13449	13367	13367	13253	13265	13100								11949	12219				
MEAN	538.0	539.6					557.2	553.5					560.4	557.0	557.0	552.2	552.7	545.8								497.9	509.1				
	12957				13239		13459	13284			13414		13414		13323		13353		13210		13320		12903		12196		12198		12506		
	539.9				551.6		560.8	553.5			558.9		558.9		555.1		556.4		550.4		555.0		537.6		508.2		508.3		521.1		

T = Testing. RF = Recording failure. ___s = Derived from Single Section.

At the beginning and end of each hour, a fraction of the F counts necessary to generate the next scaled count will have arrived at the scaler. Let n_{1B} and n_{1E} be the fractions appropriate to the section 1 scaler, and n_{2B} and n_{2E} those appropriate to section 2.

Then

$$X_1 + X_2 = \frac{C_1}{F} + \frac{C_2}{F} + n_{1B} + n_{2B} - n_{1E} - n_{2E}$$

If the pressure correction factor is α, equation 2(5) shows that the corrected count, R, is given by

$$R = \alpha \left[X_1 + X_2 \right]$$

The figure tabulated is the value of R rounded off to the nearest integer. Let the rounding off value be n_3. The tabulated value R_T is

$$R_T = \frac{\alpha}{F} \left[C_1 + C_2 \right] + \alpha \left[n_{1B} + n_{2B} - n_{1E} - n_{2E} \right] + n_3$$

Statistical fluctuations in C_1 and C_2 have been shown to be practically independent. n_{1B}, n_{2B}, n_{1E}, n_{2E} are independent variables uniformly distributed over the range (0,1). n_3 is an independent variable uniformly distributed in the ideal case over the range (- 1/2, + 1/2) (CRAMER, 1951) .

Indicating the mean value and variance of a quantity by the symbols M.V.( ) and V( ) respectively, then

$$M.V.\left(R_T \right) = M.V.\left(\frac{\alpha}{F}(C_1 + C_2) \right) + 0$$

$$V\left(R_T \right) = V\left(\frac{\alpha}{F}(C_1 + C_2) \right) + \frac{4\alpha^2}{12} + \frac{1}{12}$$

From the first equation, it can be seen that in the ideal case scaling and correction does not introduce a systematic error. In actual fact, if the primary intensity and pressure remain approximately constant, the rounding off error n_3 also remains constant, introducing a systematic error. This represents a $\pm$0.1 percent error at Mawson and Mt. Wellington. For the same stations, insertion of the appropriate values in the second equation shows that scaling and rounding off errors increase the standard deviations above those due to statistical fluctuations by no more than 5 percent.

(b) Barometric pressure errors

Errors will be introduced by (a) the limited accuracy of the pressure recording instruments, and (b) the approximations used to derive the mean hourly pressure from the observations.

Twenty four hour barographs are in use at Lae and Mawson. At each station, spot pressure readings taken with mercury column barometers are used to correct for instrumental variations, and hence systematic errors are largely eliminated. As the detailed pressure-time relationship during each hour is recorded, the errors in the determination of the mean pressure are small. It is believed that the Mawson hourly means are correct to within $\pm$0.3 mb, that is, the standard deviation of the hourly counting rates due to this cause is about 0.1 percent. This does not allow for the effect of winds (LOCKWOOD and CALAWA, 1957) which may be considerable, but indeterminate.

The pressure accuracy at Lae is estimated to be $\pm$0.7 m.b. Hence the daily means have a standard deviation of about 0.1 percent due to this cause.

At Mt. Wellington, systematic errors are present in the pressure data. On some days these may be as great as $\pm$0.5 m.b. The maximum error from this cause in both the hourly and daily

values is ±0.35 percent. The distribution of the error is not known. As a rough estimate this error is assigned a standard deviation of 0.2 percent.

2.6 The accuracy of the tabulated data

The estimated standard deviations of the tabulated values due to the various causes are listed in Table 2E. The various errors are largely independent, allowing an estimate of the standard deviation due to all causes to be made.

TABLE 2E

Standard deviation of the tabulated data due to various causes, expressed as a percentage of the mean counting rate.

TYPE OF ERROR	LAE		MT. WELLINGTON		MAWSON	
	Hourly Mean	Daily Mean	Hourly Mean	Daily Mean	Hourly Mean	Daily Mean
Statistical fluctuations of the unscaled counts	1.30	0.27	0.64	0.13	0.66	0.13
Statistical fluctuations plus scaling error	1.30	0.27	0.67	0.13	0.69	0.14
Rounding off error	0.10	0.0	0.10	0.10	0.10	0.10
Errors inherent in the pressure data	0.25	0.05	0.20	0.20	0.10	0.02
Standard deviation due to above causes	1.32	0.28	0.70	0.26	0.70	0.17
Error due to poor choice of m.f.p.		0.15		0.50		0.50

It may be seen that the greatest errors are being introduced through imperfect pressure correction. In the comparison of hourly data obtained a few hours apart, the errors due to imperfect pressure correction are the same, and therefore of no consequence. When comparing data obtained many days apart, errors due to

equipment variation may also be present.

2.7 Experimental determination of the standard deviations of the daily mean intensities

A period of 30 days was found in which the corrected counting rate of all recorders approximated to a linear function of time. For each instrument, the linear change was removed from the data, leaving statistical fluctuations, errors and possibly some small primary changes. The standard deviations of these data were determined (Table 2F). These values will be used

TABLE 2F

Standard deviations (in percent) of various daily data after correction for meteorological effects.

INSTRUMENT	Lae Neutron	Mt. Wellington Neutron	Mawson Neutron	Lae Cubical	Hobart Cubical	Hobart Ionization
STANDARD DEVIATION	0.31±0.04	0.42±0.06	0.39±0.05	0.16±0.02	0.39±0.05	0.32±0.05

in this thesis when discussing the significance of results. It can be seen that the values for the Mt. Wellington and Mawson neutron intensities are greater than those listed in row five of Table 2E, confirming that other errors, such as those due to a poor choice of absorption m.f.p. (row six) are present.

2.8 Determination of the absorption m.f.p.

Experiment A. When the prototype monitor was transferred from Hobart to Mt. Wellington, a small two counter monitor was operating at Hobart. This enabled the change in prototype counting rate to be freed from the effects of primary fluctuations. From the observed change in pressure and counting rates, the m.f.p. was calculated independently for the two sections of the monitor. The

values obtained were 134 ± 2 and 139 ± 2 gm cm^{-2}. The greatest errors are probably due to the slight differences in geometry before and after the move. It has been reported that the counting rate of a monitor of similar construction is reproducible to within $\pm 2\frac{1}{2}$ percent (SIMPSON et al, 1953) . Hence the mean of the above values, 136.5 gm cm^{-2}, is probably within ±4 gm cm^{-2} of the true value. A standard deviation cannot be assigned.

Experiment B. The large primary fluctuations in recent years precluded a determination of the m.f.p. by a simple intensity against pressure correlation analysis. It was necessary to introduce a third variable into the analysis in order to allow for these primary changes. A multiple correlation analysis between the corrected Mt. Wellington count, Mt. Wellington pressure and corrected Mawson count was performed. The partial regression coefficient of the Mt. Wellington count upon pressure gave the dependence of counting rate upon pressure with the effect of the primary variations removed. A similar analysis was performed between the corrected Mawson counting rate and Mawson pressure, using the corrected Mt. Wellington data to allow for the primary changes. Seven different intervals of a month each were used for each analysis.

Every one of the fourteen computations showed that the corrected data were still correlated with pressure, and that the m.f.p. was less than 145 gm cm^{-2}. The weighted means of the values found for the m.f.p. were 138.2 ± 1.1 for Mawson and 139.6 ± 1.2 for Mt. Wellington.

Experiment C. The monthly mean corrected intensities and pressures at Mt. Wellington and Mawson were calculated for the period April, 1957 to January, 1958. Write them as I_W, I_M, P_W, P_M where I_W and I_M are expressed as percentages of the mean value for the whole period. As both stations are at a high latitude, the percentage variations due to primary changes will be very nearly the same. Let them be represented by $Q(t)$. Suppose that the

m.f.p. used to correct the data was in error. As a first approximation, assume that the m.f.p. is the same at both stations. Then, indicating mean values by a bar,

$$\left.\begin{aligned} I_W &= Q(t) + \alpha(P_W - \bar{P}_W) \\ I_M &= Q(t) + \alpha(P_M - \bar{P}_M) \end{aligned}\right\} \quad \alpha = \text{constant}$$

and therefore

$$I_M - I_W = \alpha(\partial P_M - \partial P_W) \quad \text{where} \quad \partial P_M = P_M - \bar{P}_M$$

$(I_M - I_W)$ and $(\partial P_M - \partial P_W)$ are plotted against time in Fig. 7, and a marked similarity is evident. A correlation analysis showed that the quantities were strongly correlated ($r = 0.89$) and yielded a m.f.p. of 133.5 ± 2.1 gm cm^{-2}.

All three experiments agree that the m.f.p. is less than 145 gm cm^{-2}. The weighted mean of the values found in experiments B and C is 138.1 ± 0.8 gm cm^{-2}, a value which is in good agreement with experiment A.

Figure 7 - Illustrating the dependence of corrected neutron intensity upon atmospheric pressure. $I_M - I_W$ and $\partial P_M - \partial P_W$ are plotted as functions of time.

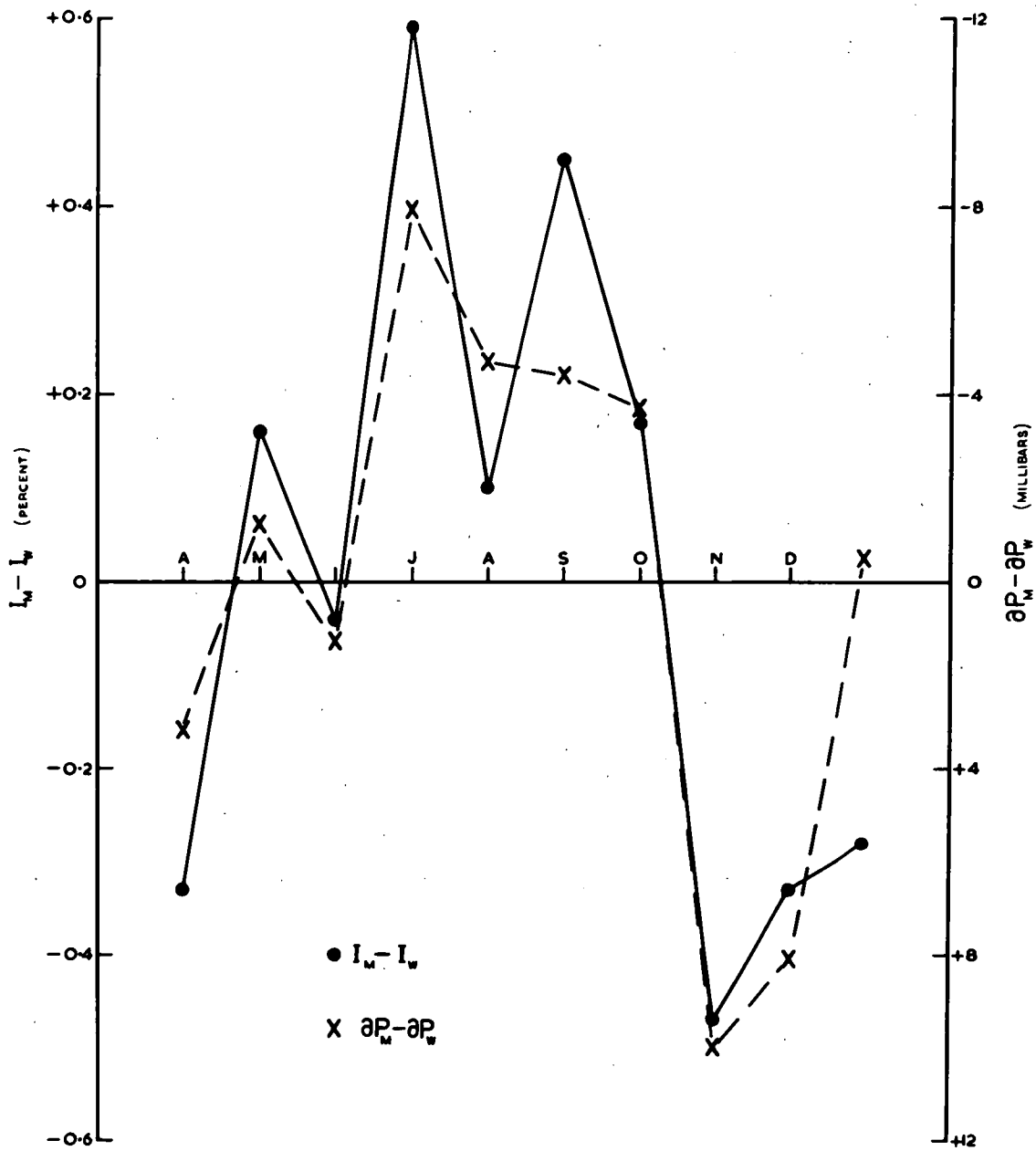
+0·6
+0·4
+0·2
0
−0·2
−0·4
−0·6
$I_M - I_W$ (PERCENT)
-12
-8
-4
0
+4
+8
+12
$\partial P_M - \partial P_W$ (MILLIBARS)
A
M
J
A
S
O
N
D
● $I_M - I_W$
X $\partial P_M - \partial P_W$

CHAPTER 3

THE MESON DETECTORS

3.1 The ionization chamber

The ionization chamber itself is similar to the well known Carnegie Type C chamber (COMPTON et al, 1934). It consists of a 23 litre spherical steel shell and a concentric spherical collection electrode, and employs voltage and current compensation. It is filled with commercial nitrogen to a pressure of 60 atmospheres, and is shielded on the top and at the four sides by 10 cm. of Lead.

The collection electrode is connected to a vibrating condenser electrometer (Fig. 8A). The A.C. output from the electrometer energises one coil of an induction motor, a reference signal 90° out of phase being fed to the other coil. The motor drives a pen across the recording chart, and, at the same time, a roller on the pen carriage picks a D.C. voltage off a precision wound resistance strip. A fraction of this voltage is fed back on to the vibrating condenser. The circuits have been arranged so that the pen always moves to the point where the feedback voltage cancels out the voltage on the vibrating condenser. Thus the voltage across the insulator between the collection electrode and the earthed guard ring is always very small, and the leakage of ionization charge negligible. The chamber E.H.T. and the voltage applied across the feedback resistance strip are checked against a standard cell every day.

The chart speed is 8 cm/hour. Each hour the collection electrode and the feedback line are connected to earth for half a minute. A typical trace is depicted in Fig. 8B. At the beginning and end of each chart, the pen position corresponding to zero charge on the vibrating condenser is determined, and used as the origin from which the hourly pen deviations are measured. The deviations are measured to the nearest millimeter and any bursts (Fig. 8B) subtracted.

Figure 8A - Block diagram of the Hobart ionization chamber. The chart deflection produced by a given change in cosmic ray intensity is determined by the setting of the sensitivity control.

Figure 8B - Portion of the ionization chamber record obtained on the 23rd February, 1956. The sudden discontinuity at about 0150 U.T., called a "burst", is due to the production of heavily ionizing particles in the walls of the chamber. Such events are quite common.

The trace was quite normal up to 0341 U.T. At this time the intensity started to increase, the rate of increase becoming very great at about 0343 U.T. This increase in intensity was due to the generation of cosmic radiation in a solar flare (FENTON et al, 1956).

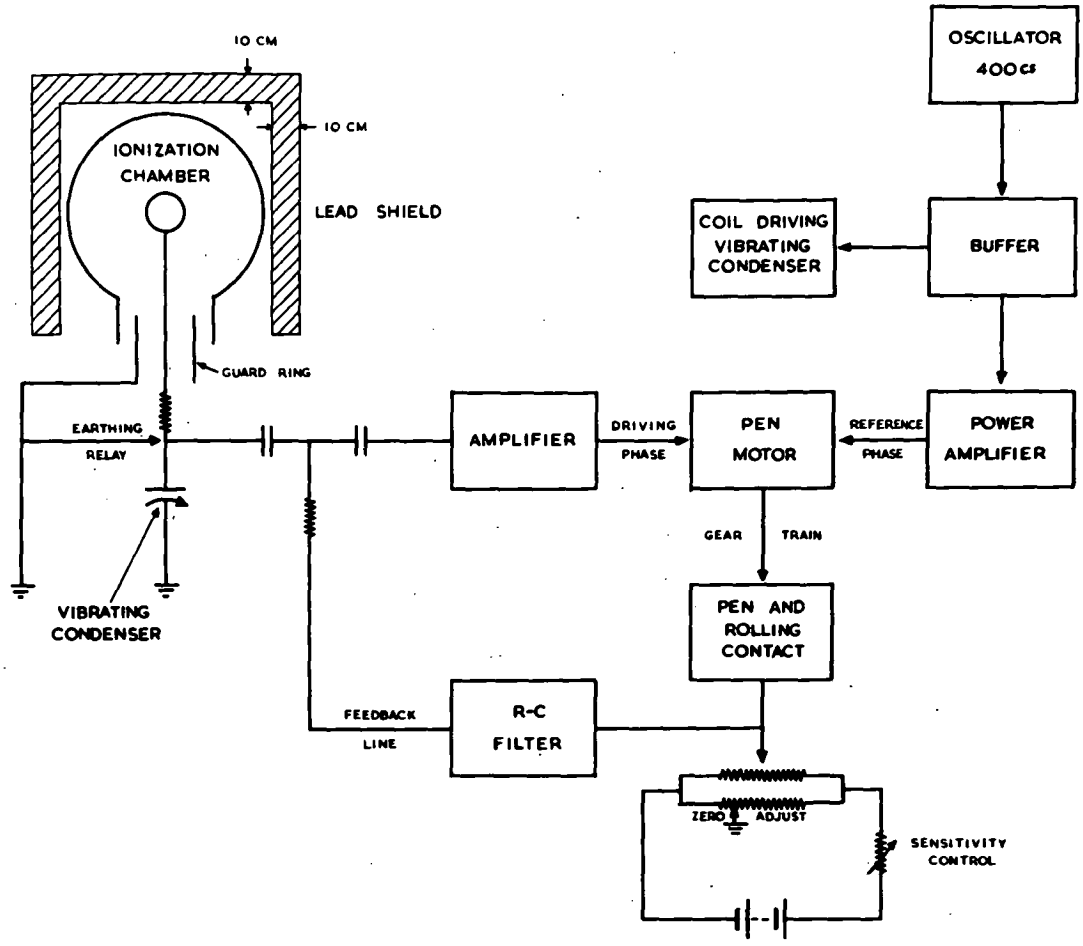
10 CM
10 CM
IONIZATION CHAMBER
LEAD SHIELD
GUARD RING
OSCILLATOR 400 cs
COIL DRIVING VIBRATING CONDENSER
BUFFER
EARTHING RELAY
AMPLIFIER
DRIVING PHASE
PEN MOTOR
REFERENCE PHASE
POWER AMPLIFIER
GEAR TRAIN
VIBRATING CONDENSER
PEN AND ROLLING CONTACT
FEEDBACK LINE
R-C FILTER
ZERO ADJUST
SENSITIVITY CONTROL

8A

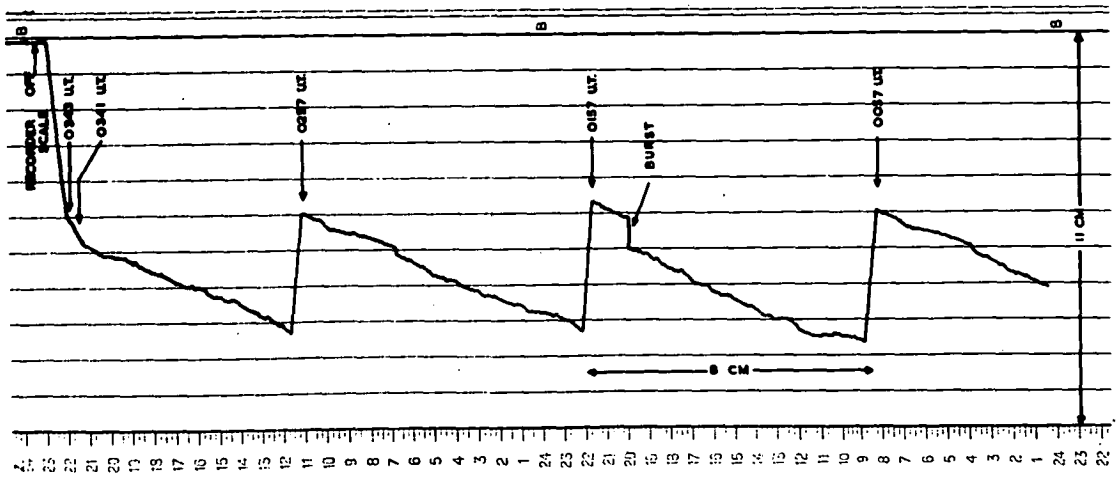
B
B
B
RECORDER SCALE
0.940 U.T.
0.341 U.T.
0.017 U.T.
0.157 U.T.
0.017 U.T.
BURST
8 CM
11 CM

8B

3.2 Balance current and residual ionization

The current due to the collection of ions in the main chamber (I_A) is partially balanced by a time invariant balance chamber current (I_B). The very great advantages gained by the use of this system have been enumerated (COMPTON et al, 1934).

Cosmic radiation and radioactive contamination of the chamber and its surroundings ionize the gas in the main chamber. Hence the main chamber current, I_A, is the sum of a current due to cosmic ray ionization, I_C, and the radioactive contamination (or residual) current, I_R. I_R is substantially constant in a shielded chamber, all variation of the chart deflection being due to changes in I_C. Knowing I_B and I_R, the percentage change in I_C represented by an observed change in chart deflection can be calculated.

A method similar to that used by COMPTON et al (1934) was used to determine I_R and I_B. Whereas these investigators took their chamber into a mine where the cosmic ray intensity was negligible, and therefore the main chamber current wholly due to contamination, the cosmic ray intensity was still appreciable in the tunnel used in the case of the Hobart instrument.

Denoting underground measurements by a dash

$$\left.\begin{aligned} I_A &= I_C + I_R \\ I'_A &= I'_C + I'_R \end{aligned}\right\} \qquad 3(1)$$

Two large semi-cubical telescopes were in operation in the tunnel at the time, and as they had been operated at the University during initial tests, the ratio of the intensity in the tunnel to that at the University (α) could be determined. As the zenith angle dependence of a semi-cubical telescope is similar to that of an ionization chamber at all but large zenith angles (for which the

thickness of earth was great), α must be a good approximation to $\frac{I'_C}{I_C}$.

In a totally shielded chamber, for which the γ rays from contamination of the surroundings are nearly all absorbed in the shield, the residual current is almost wholly due to contamination of the chamber and its shield, and therefore $I_R \approx I'_R$. The Hobart chamber is only shielded by 2 to 3 cm. of iron at the bottom, and consequently contamination of the laboratory floor does contribute to the residual current. In the absence of information to the contrary, it is assumed that the contamination of the floors at the two sites was approximately the same, so that $I_R = I'_R$. This assumption probably introduces the greatest error into the determination.

Thus from 3(1)

$$I_R = \frac{1}{1 - \alpha} \quad (I'_A - \alpha I_A)$$

The rate of change of centre electrode potential is a measure of the current flowing to it. The chart deflection is proportional to the centre electrode voltage, and so all currents have been measured in units of millimeters drift/hour. Table 3A lists the values found. The standard deviations given were derived from the scatter of the observations.

TABLE 3A

(a) Values observed during the deviation of I_R

(b) The parameters of the ionization chamber

	a			b		
Symbol	α	I_A	I'_A	I_B	I_R	$I_B - I_R$
Observed Value	0.129	683±3	243±2	637±3	178±2	459±4

To obtain the mean cosmic ray current over any period, the mean deflection from balance is added to $(I_B - I_R)$.

3.3 The meson telescopes

These have been described elsewhere (PARSONS, 1957). Briefly they consist of three equally spaced square trays of counters. The tray separation is now equal to the sensitive length of the counters (that is, a cubical geometry), although prior to May, 1957, it was 1.5 times this figure. Between the bottom two trays is 10 cm. of lead absorber. The threefold counting rate of the Hobart instrument is 130,000 counts/hour, and that of each of the two Lae instruments 48,000 counts/hour.

3.4 Correction of the meson data for atmospheric effects

(a) At Lae, a daily radio sonde indicates that day to day changes in the temperature distribution of the atmosphere are small. Pressure variations are also small, rendering an experimental determination of the barometer coefficient difficult. For the present thesis, all data have been corrected using Trefall's theoretical coefficient of -2.31 percent/cm.Hg. (TREFALL, 1955).

(b) At Hobart, the day to day changes in pressure and atmospheric structure are considerable. Simple correction for atmospheric pressure change leaves a large seasonal wave, and marked day to day changes of atmospheric origin.

For the present thesis, the ionization chamber and meson telescope data have been corrected using mass and decay coefficients. As in the case of the neutron data, the large primary variations in recent years interfered with the experimental determination of the coefficients. To avoid having to perform a fourfold correlation analysis to allow for the primary changes, the corrected neutron data were examined, and all days for which the intensity lay within a range of 4 percent chosen. For these days, threefold correlations

between the daily mean meson intensity, the daily mean atmospheric pressure, and the mean height of the 125 millibar level were performed. See Table 3B.

TABLE 3B

Mass and decay coefficients for the Hobart meson telescopes and ionization chamber.

Detector	1 x 1 x 1.5 Telescope	Cubical Telescope	Ionization Chamber
Number of days in analysis	86	85	161
Mass Coefficient (percent/inch Hg)	-4.16 ± 0.37	-4.14 ± 0.40	-4.58 ± 0.22
Decay Coefficient (percent/Km)	-4.66 ± 0.63	-4.88 ± 0.94	-5.02 ± 0.34

The standard deviations of all meson data after correction are listed in Table 2F.

CHAPTER 4

VARIATIONS IN THE COSMIC RAY SPECTRUM. (METHODS OF ANALYSIS)

4.1 Comparison of data.

The geomagnetic field prevents primary cosmic radiation of rigidity less than 10 Bv from reaching the top of the atmosphere near the equator. The geomagnetic cut-off decreases with increasing latitude, until at high geomagnetic latitudes ($\lambda > 55^{\circ}$) primaries with rigidities as low as 2 Bv are detected by a sea level neutron monitor.

It has been shown by FONGER (1953) that a neutron monitor is more sensitive than a meson telescope to low rigidity primary radiation. Thus at $\lambda = 55^{\circ}$, approximately 45 percent of the neutron, and 10 percent of the meson counting rates at sea level are due to primaries whose rigidities are too low to enable them to reach the earth in equatorial regions. (Derived from figures given by ROSE et al, (1956)).

By comparing the variations in the counting rates of (1) two similar detectors, one near the equator and the other at a high latitude, and (2) a neutron monitor and a meson telescope, both at the same latitude, the energy dependence of the cosmic ray variations can be calculated. In the following chapters a number of such comparisons are detailed. Further information is gained from a study of meson data recorded underground.

4.2 Summary of the types of cosmic ray variations

After correction for variations in meteorological conditions, the cosmic ray intensity is still time dependent. There are a number of distinct modes of variation, each characterised by its dependence on time.

The Forbush decrease is characterised by an abrupt decrease in intensity, followed by a gradual recovery during the subsequent 3 to 6 days to an intensity near the pre-event value. There are often enhanced diurnal variations during the event. The event is observed by widely separated recorders, however, there are often significant differences in the times of onset, and in the intensity fluctuations during the first few days of an event. The event often occurs in close time association with a geomagnetic storm. A more detailed examination of this type of event is made in Chapter 9.

There is an eleven year periodicity which is out of phase with the variation in solar activity (FORBUSH, 1954). The changes in intensity are most pronounced at low rigidities. (MEYER and SIMPSON, 1955, 1957). The primary cut-off which has a value of about 1 Bv at sunspot maximum goes to a very low value at sunspot minimum, 100 Mev protons having been detected (NEHER, 1957).

A quasi-periodicity with a period of approximately 27 days is often observed. (for example, VAN HEERDEN and THAMBYAHPILLAI, 1955). The variations would appear to be produced by some feature on the sun, the rotation of the sun resulting in the observed 27 day periodicity. It is undecided whether the variations are recurrent depressions, enhancements or are due to a modulation of the mean level. As yet the solar feature responsible for the variations has not been positively identified. The variations may persist for more than six solar rotations, and at any time two or more recurrence sequences may be apparent.

There is a weak variation of period 24 hours, the phase and amplitude varying from day to day (for example, FIROR et al, 1954). The diurnal variation exhibits 27 day and 11 year changes in character. There is a correlation between the diurnal variation and geomagnetic disturbance, the amplitude increasing and the time of maximum intensity changing on days when the magnetic elements are disturbed.

On a number of occasions a sudden intensity increase has been observed soon after the occurrence of a large solar flare (for example, p514, DORMAN, 1957). The intensity reaches its maximum value within 5 to 15 minutes, and then gradually returns to the pre-event level within the next 6 to 24 hours. The amplitude of the increase is strongly dependent upon latitude and longitude, being consistent with a very steep energy spectrum and a source in the direction of the sun. After the first 30 minutes of a flare increase the longitude dependence becomes less pronounced, indicating that the radiation incident on the earth has become roughly isotropic. This means that there is a mechanism within the solar system capable of deflecting the radiation produced in the sun through considerable angles.

The comparison of the temporal dependence and the amplitudes of cosmic ray phenomena recorded by different instruments is complicated by the superposition of the different modes of variation. For example, in the period 1st October to 31st December 1957, a 27 day recurrence sequence, three Forbush decreases, diurnal variations and portion of the 11 year intensity variation were superposed (Fig. 9). In order to study the various modes by themselves and to see whether different specimens of the one mode exhibit different characteristics, and furthermore, to minimise the effect of long term equipment and residual meteorological effects, the data have been split up into small groups prior to analysis.

4.3 Comparison of the amplitudes of variations

Let the intensities observed by recorders 1 and 2 during simultaneous recording periods be X_1 and X_2. It is necessary to find the functional relationship between X_1 and X_2 giving the "best fit" to N observed (X_1,X_2) pairs. Statistical fluctuations and systematic errors are present in X_1 and X_2, and while conventional regression analysis defines two regression functions

which are applicable to practical cases where either one or the other of the variates is free from error, there is no reason to prefer either function in the present case.

Statisticians have considered this problem, a useful review being given by ROOS (1937). While he presents a criterion yielding a mathematically satisfactory line of "best fit", the computation of the gradient of the line is rather complicated. It must be acknowledged, however, that a method such as this, employing weights which reflect the errors likely in the data, will give the most satisfactory line of best fit.

In what follows, any coefficient relating a variation in X_1 to that in X_2 will be called a measure of the "relative amplitude" of the variation. In every case, X_1 and X_2 will be expressed as a percentage of the respective mean value for the whole period considered. The following standard symbols will be used quite frequently:- σ_i (standard deviation of the N values of X_i); b_{ij} (regression coefficient of data i upon data j); r_{ij} (correlation coefficient between data i and data j). Less common symbols will be defined when they appear.

Various measures of relative amplitude have been used by earlier cosmic ray investigators. Thus b_{12}, $\frac{1}{b_{21}}$, $\frac{1}{2}(b_{12} + \frac{1}{b_{21}})$, $\frac{\sigma_1}{\sigma_2}$, $\frac{\partial X_1}{\partial X_2}$ (where ∂X_1 and ∂X_2 are the changes in X_1 and X_2 which occur between two specified times), and regression coefficients derived by assigning weights to the data have all been used. When the correlation coefficient between X_1 and X_2 is exactly unity, all the (X_1, X_2) points lie on the one straight line, and all the above measures yield the same value for the relative amplitude. As the correlation coefficient decreases, the points become scattered, and the values obtained for the various measures diverge from one another. The following discussion investigates

their separation for a number of values of the correlation coefficient.

From the definitions,

$$b_{12} = r_{12} \frac{\sigma_1}{\sigma_2}$$

$$\frac{1}{b_{21}} = \frac{1}{r_{12}} \frac{\sigma_1}{\sigma_2}$$

and therefore $$\frac{1}{2}\left(b_{12} + \frac{1}{b_{21}}\right) = \left(\frac{1 + r_{12}^2}{2r_{12}}\right) \cdot \frac{\sigma_1}{\sigma_2}$$

For most practical cases, the ratio of the weights appropriate to data 1 and 2 will be roughly one or two, for when high counting rate equipment is used, the residual meteorological effects and equipment variations result in the standard deviations of all individual daily means being approximately 0.3 percent (Table 2F). Taking Roos' line of"best fit" (ROOS, 1937) as representative of methods that weight the data, and assigning equal weights to the data 1 and 2, then for $r_{12} > 0$,

$$X_1 = \left(\frac{\sigma_1 + \sigma_2 r_{12}}{\sigma_1 r_{12} + \sigma_2}\right) \frac{\sigma_1}{\sigma_2} X_2 + \text{const.}$$

That is, $\left(\frac{\sigma_1 + \sigma_2 r_{12}}{\sigma_1 r_{12} + \sigma_2}\right) \frac{\sigma_1}{\sigma_2}$ is the measure of the relative amplitude based upon Roos' line of best fit.

It is difficult to relate $\frac{\partial X_1}{\partial X_2}$ to $\frac{\sigma_1}{\sigma_2}$. In general, the

standard error of $\frac{\partial X_1}{\partial X_2}$ will be greater than that of any other measure, as it is based upon less data.

Table 4A compares the various measures of relative amplitude for three values of the correlation coefficient. In practice, the correlation coefficient is usually greater than 0.8. As most of the analyses in this thesis were performed using about 25 (X_1, X_2) pairs, the standard error of b_{12} derived from

$$\text{S.E.}\,(b_{12}) = \frac{\sigma_1}{\sigma_2}\sqrt{\frac{1 - r_{12}^2}{N - 2}}$$ for $N = 25$ is given as an indication of the reliance that can be placed in any individual value of the relative amplitude.

TABLE 4A

Comparison of the various measures of relative amplitude

r_{12}	b_{12}	$1/b_{21}$	$\frac{1}{2}(b_{12} + 1/b_{21})$	Roos' coefficient		S.E.(b_{12})
				$\sigma_1 \approx \sigma_2$	$\sigma_1 \approx 2\sigma_2$	
0.95	$0.95\,\frac{\sigma_1}{\sigma_2}$	$1.05\,\frac{\sigma_1}{\sigma_2}$	$1.001\,\frac{\sigma_1}{\sigma_2}$	$\frac{\sigma_1}{\sigma_2}$	$1.02\,\frac{\sigma_1}{\sigma_2}$	$0.06\,\frac{\sigma_1}{\sigma_2}$
0.90	$0.90\,\frac{\sigma_1}{\sigma_2}$	$1.11\,\frac{\sigma_1}{\sigma_2}$	$1.006\,\frac{\sigma_1}{\sigma_2}$	$\frac{\sigma_1}{\sigma_2}$	$1.04\,\frac{\sigma_1}{\sigma_2}$	$0.09\,\frac{\sigma_1}{\sigma_2}$
0.80	$0.80\,\frac{\sigma_1}{\sigma_2}$	$1.25\,\frac{\sigma_1}{\sigma_2}$	$1.025\,\frac{\sigma_1}{\sigma_2}$	$\frac{\sigma_1}{\sigma_2}$	$1.08\,\frac{\sigma_1}{\sigma_2}$	$0.12\,\frac{\sigma_1}{\sigma_2}$

As mentioned before, a relative amplitude based upon a method which weights the data is probably the most satisfactory. However, it is clear from Table 4A that for $|r_{12}| > 0.8$ either $\frac{\sigma_1}{\sigma_2}$ or $\frac{1}{2}(b_{12} + \frac{1}{b_{21}})$ approximate to such a measure quite well, while for

$|r_{12}| < 0.9$ neither b_{12} nor $\frac{1}{b_{12}}$ are satisfactory. The measure $\frac{\sigma_1}{\sigma_2}$ has the property that

$$(\frac{\sigma_1}{\sigma_2}) \cdot (\frac{\sigma_2}{\sigma_3}) = (\frac{\sigma_1}{\sigma_3})$$

thus the relative amplitudes of variates 1 and 2, 2 and 3, and 1 and 3 are consistent. This is only roughly true for the other definitions. In the majority of the investigations reported in this thesis, $\frac{\sigma_1}{\sigma_2}$ has been used as the measure of relative amplitude.

4.4 Functional dependence of counting rate upon primary change

In theory it is possible to relate changes in the counting rate of a cosmic ray detector to the changes in the primary radiation. For simplicity, the heavy particle component will be neglected. The primary proton differential spectrum is written $j(E)$. For component "i" recorded at geomagnetic latitude λ and atmospheric depth x, the counting rate due to primaries arriving from within an elementary solid angle of $\partial\omega$ about the vertical direction is given by

$$N_v^i(\lambda,x).\partial\omega = \int_{E_v(\lambda)}^{\infty} j(E) \cdot \partial\omega \cdot S(E,x)dE \cdots 4(1)$$

where $E_v(\lambda)$ is the vertical cut-off energy, that is, the minimum energy a proton must have in order to arrive at the earth from the vertical direction. $N_v^i(\lambda,x)$ is called the vertical counting rate. The function $S(E,x)$, the specific yield function of FONGER (1953), relates the intensity of radiation of energy E to the counting rate it produces.

The counting rates of the commonly encountered detectors are

due largely to radiation incident at an angle to the vertical. However, by using the Gross transformation * it may be shown that their counting rates are approximately proportional to the vertical counting rates (p.139, JANOSSY, 1950; TREIMAN, 1953).

Neglecting changes due to any simultaneous variation in the vertical cut-off energy, or of atmospheric origin, the change in vertical counting rate produced by a change in spectrum is

$$\partial N_v^i(\lambda,x) = \int_{E_v(\lambda)}^{\infty} \partial j(E) \cdot S(E,x)\,dE \quad \cdots\cdots 4(2)$$

This may be rewritten

$$\frac{\partial N_v^i(\lambda,x)}{N_v^i(\lambda,x)} = \int_{E_v(\lambda)}^{\infty} \frac{\partial j(E)}{j(E)} \cdot \frac{j(E).S(E,x)}{N_v^i(\lambda,x)}\,dE$$

$$= \int_{E_v(\lambda)}^{\infty} \frac{\partial j(E)}{j(E)} \cdot W_{\lambda,v}^i(E,x)\,dE \quad \cdots\cdots 4(3)$$

where $W_{\lambda,v}^i(E,x)$ is the "coupling constant" of DORMAN (1957). This function relates the fractional variations in the i^{th} component to the fractional variations in the primary spectrum. Using either 4(2) or 4(3), the counting rate variations produced by a given primary spectrum change can be calculated, or conversely, the observed variations in a number of components (or at a number of latitudes) can be used to deduce the energy dependence of a spectral change.

---

* A number of assumptions are necessary in the derivation of the Gross transformation. SIMPSON et al (1952a) have investigated these and find that they do not introduce serious errors.

A difficulty in the application of 4(2) or 4(3) lies in the determination of $S(E,x)$ or $W(E,x)$. In theory, the geomagnetic effect should enable these functions to be determined for E within the range 2 to 15 Bev; for differentiating 4(1) with respect to $E_v(\lambda)$,

$$\frac{\partial N_v^i(\lambda,x)}{\partial E_v(\lambda)} = -j\left\{E_v(\lambda)\right\} \cdot S\left\{E_v(\lambda),x\right\}$$

and as $j(E)$ is known from photographic emulsion studies at high altitudes, $S(E,x)$ can be obtained from the dependence of intensity upon vertical cut-off energy. Hence $W(E,x)$ can be determined.

For $E > 15$ Bev, there is at present no method whereby either function can be determined experimentally, and our knowledge of the production and propagation of the secondary radiation is insufficient to allow a theoretical determination. Thus it is necessary to extrapolate the functions found at low energies, with the restriction that

$$N_v^i(\lambda,x) = \int_{E_v(\lambda)}^{\infty} j(E) \cdot S(E,x)\, dE$$

At present, the determination of $S(E,x)$ or $W(E,x)$ in the range 2 to 15 Bev is subject to considerable error, as our knowledge of the geographic distribution of vertical cut-off energies is poor. It is the usual practice to calculate vertical cut-off energies on the assumption that the geomagnetic field at the earth's surface gives a true indication of the field effective in the deflection of cosmic rays. Thus an equivalent dipole field is derived, and the vertical cut-off energies are calculated from this.

The inadequacy of this method is illustrated in Table 4B, where a number of values of the rate of change of neutron intensity

with change in vertical cut-off energy are listed. These values were derived from a voyage during 1954-55 (ROSE et al, 1956) and one during 1956-57 (KODAMA and MIYAZAKI, 1957). These voyages are not strictly comparable in that part of the long term, latitude sensitive intensity decrease (Chapter 5) occurred prior to the Indian Ocean determinations. As the long term effect was a rapidly decreasing function of energy, it must have resulted in a reduction in the latitude effect, and in the rates of change of intensity with cut-off energy. Thus the Indian Ocean values are probably lower than they were in 1954-55.

TABLE 4B

Percentage change in intensity per Bev change in vertical cut-off energy calculated from the eccentric dipole field.

Region of earth \ Vertical cut-off energy	3.1	7.1	9.0
Pacific Ocean	-3 -5	-7 -5	-7 -7
Atlantic Ocean	-4 -6	-9 -4	-2 -4
Indian Ocean	0	-9	-9

A wide scatter of values is evident in Table 4B. It is thus clear that the vertical cut-off energies based on the eccentric dipole are in error. High altitude emulsion studies support this contention (WADDINGTON, 1956). Ad hoc adjustment of the magnetic dipole to yield the correct position of the cosmic ray equator aggravates the errors (ROSE et al, 1956).

Depending on which latitude survey is used, different $S(E,x)$ for $2 < E < 15$ Bev will be obtained. This inaccuracy at low energies renders the extrapolation to high energies less reliable. Thus at present only rough evaluations of $S(E,x)$ or $W(E,x)$ can be

made. This must be the situation until the cut-off energies along the path of a latitude survey have been determined more accurately (e.g. by high altitude observation of the primary radiation itself).

The errors in the functions appropriate to the meson component are even greater than those for the neutron component owing to the smaller latitude effect, and the consequently greater dependence on the correctness of the extrapolation to high energies. Furthermore, as has been pointed out by KUPFERBERG (1948), portion of the observed meson latitude effect is due to the atmosphere being warmer in equatorial regions than at high latitudes. As our understanding of the dependence of counting rate upon atmospheric structure is not yet complete, the correction for this effect is not perfect, and so a further error is introduced into the specific yield function.

CHAPTER 5

THE LONG TERM VARIATION

The daily mean neutron intensity at Mt. Wellington for the period August 1956 to January 1958 is plotted as a function of time in Fig. 9A. As shown in Fig. 9B, all the other ground level detectors maintained by the University of Tasmania recorded similar variations.

One striking feature of the data is the manner in which the intensity suffered a permanent change during the period November 1956 to January 1957. The fact that during the greater part of March and May 1957 the intensity was constant, and not showing any tendency to return to the October 1956 value suggests that a drastic, long lived change occurred in the primary intensity. It seems reasonable to identify this as part of the eleven year periodicity reported by FORBUSH (1954).

There were a large number of short term variations of from 3 to 30 days duration superposed on the long term change. A selection was made of those days on which the Mt. Wellington neutron intensity was unaffected by short term variations. In the selection, the view was taken that disturbed days were (1) those during the onset and recovery from Forbush decreases, (2) those during which the intensity was showing a systematic trend which resulted in intensity changes in excess of 3 percent within a period of 3 days, and (3) those on which the intensity was depressed below adjacent maxima by more than 3 percent. Figure 10A indicates the class to which each day within the period 1st October to 31st December, 1957 was assigned.

For each month within the period July 1956 to January 1958, the mean of the neutron intensities observed on the undisturbed days was calculated for Lae, Mt. Wellington and Mawson. These means will

Figure 9A - The daily mean, pressure corrected neutron intensity at Mt. Wellington as a function of time. The standard deviation of each point is 0.4 percent. The double headed arrows indicate the subintervals used in the analyses detailed in Chapter 6.

Figure 9B - Pressure corrected daily mean intensities observed by six different cosmic ray detectors during September-December, 1957. The standard deviation of the Lae telescope data is 0.16 percent, while those of all other data are about 0.4 percent.

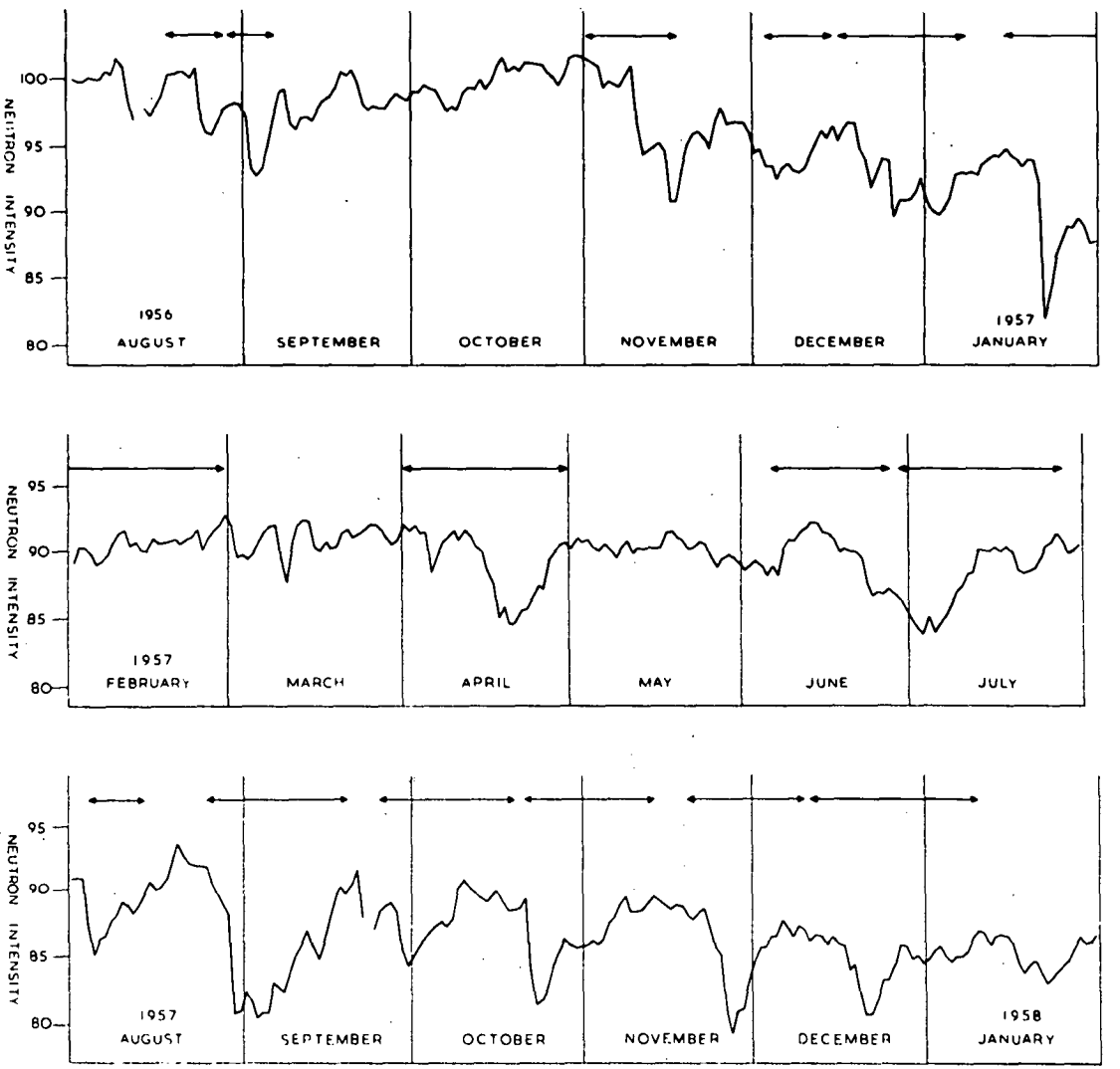
NEUTRON INTENSITY
100
95
90
85
80
1956
AUGUST
SEPTEMBER
OCTOBER
NOVEMBER
DECEMBER
1957
JANUARY
NEUTRON INTENSITY
95
90
85
80
1957
FEBRUARY
MARCH
APRIL
MAY
JUNE
JULY
NEUTRON INTENSITY
95
90
85
80
1957
AUGUST
SEPTEMBER
OCTOBER
NOVEMBER
DECEMBER
1958
JANUARY

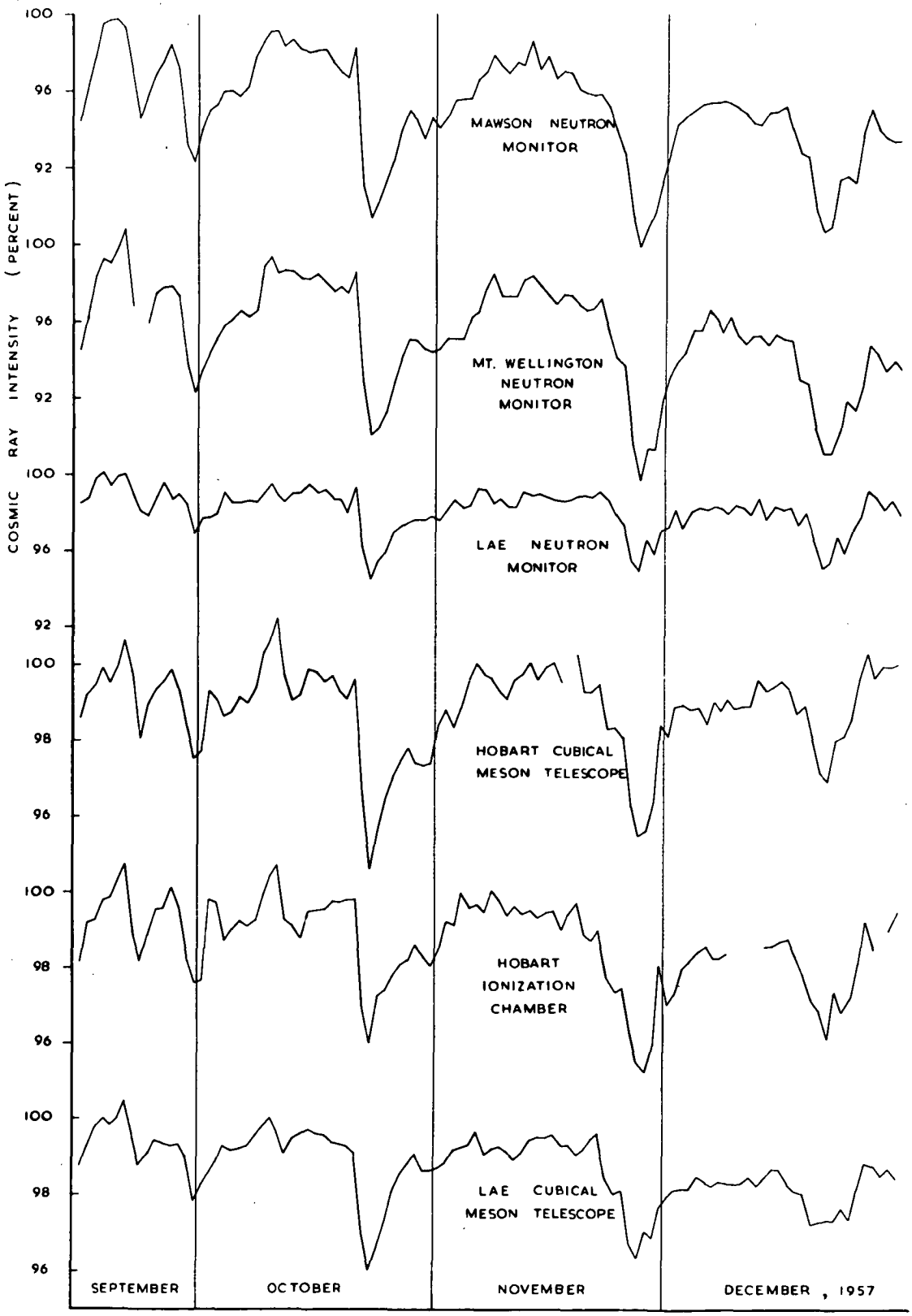
COSMIC RAY INTENSITY (PERCENT)
MAWSON NEUTRON MONITOR
MT. WELLINGTON NEUTRON MONITOR
LAE NEUTRON MONITOR
HOBART CUBICAL MESON TELESCOPE
HOBART IONIZATION CHAMBER
LAE CUBICAL MESON TELESCOPE
SEPTEMBER
OCTOBER
NOVEMBER
DECEMBER , 1957

9B

Figure 10A - Illustrating the selection of "disturbed" and "undisturbed" days. The data obtained on undisturbed days are indicated by filled in circles, those obtained on disturbed days by open circles. Daily mean neutron intensities recorded at Mt. Wellington are plotted.

Figure 10B - The undisturbed neutron intensity recorded at Mt. Wellington during the period July 1956 to January, 1958.

Figure 10C - The undisturbed Mawson neutron intensity plotted against the Lae undisturbed neutron intensity (open circles), and against the Mt. Wellington undisturbed neutron intensity (filled in circles). The data were obtained during the period August, 1957 to January, 1958.

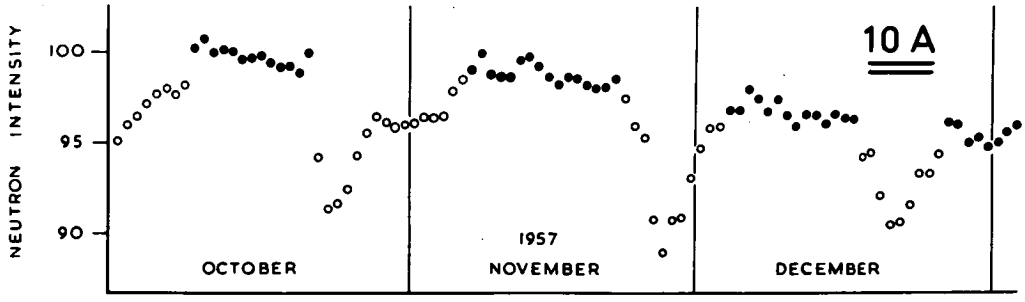
NEUTRON INTENSITY
100
95
90
OCTOBER
1957
NOVEMBER
DECEMBER
10 A

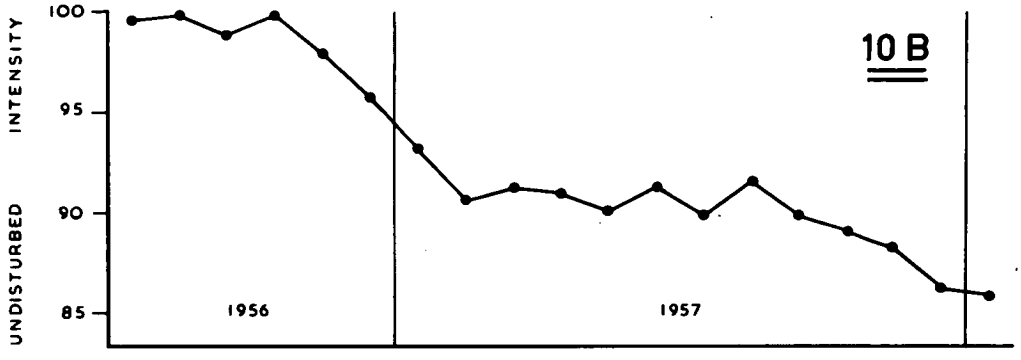
UNDISTURBED INTENSITY
100
95
90
85
1956
1957
10 B

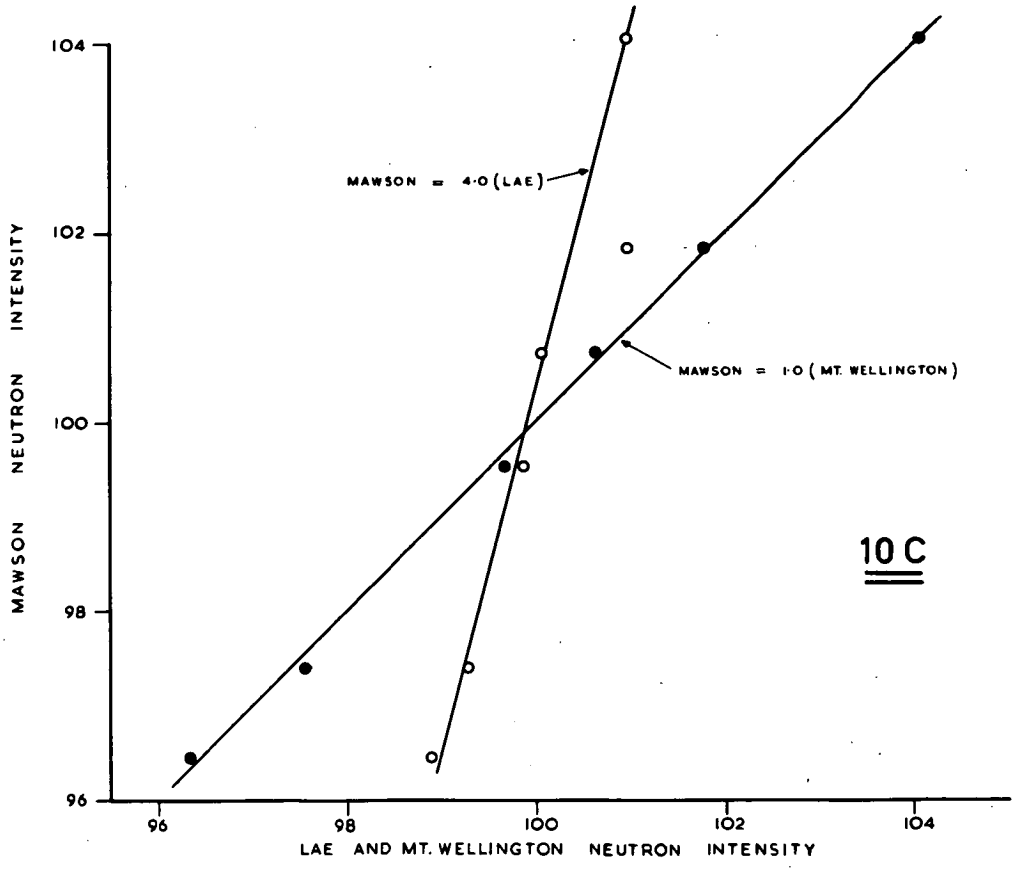
MAWSON NEUTRON INTENSITY
104
102
100
98
96
MAWSON = 4·0 (LAE)
MAWSON = 1·0 (MT. WELLINGTON)
10 C
96
98
100
102
104
LAE AND MT. WELLINGTON NEUTRON INTENSITY

be referred to as the "undisturbed" neutron intensities for the month.

In Fig. 10B the Mt. Wellington undisturbed intensity is plotted as a function of time. The effects of short term fluctuations having been eliminated, this graph indicates the manner in which the long term change affected the Mt. Wellington neutron intensity. It is clear that the undisturbed intensity decreased during November and December 1956 and January 1957, remained practically constant from February to September 1957, and then decreased slowly until January 1958.

In Fig. 10C, the undisturbed Mawson intensity* is plotted against those for Lae and Mt. Wellington* for the period August 1957 to January 1958. The percentage variation at Mawson is four times greater than that at Lae, and equal to that at Mt. Wellington. The value of 4.0 for the Mawson-Lae relative amplitude indicates that the eleven year periodicity is much more pronounced at low than at high rigidities.

Comparison of the long term variations in neutron and meson intensity is more difficult owing to the incomplete correction of the meson data for changes in atmospheric structure. By comparing the data obtained during a period in which the primary intensity was changing rapidly, the error introduced into the relative amplitude by residual atmospheric structure effects is minimised.

Fig.9A shows that while the two periods 1-9 November 1956 and 21-30 November 1956 were relatively free of short term variations, the mean neutron intensities for the two periods differed by 4 percent. Fig.9A suggests that this was part of the long term variation. The difference in meson intensity was calculated, yielding a value of 3.8 for the neutron-meson relative amplitude. The magnitude of the error introduced into this value by incomplete

---

* Corrected using the best m.f.p. available, viz. 138 gm cm^{-2} (Section 2.8).

correction for change in atmospheric structure is not known. A similar determination using data from high latitude stations in the northern hemisphere yielded a figure of 4 to 5 (FENTON et al, 1958). These investigators quoted the monthly mean intensities for their recorders, and as October 1956 and May 1957 were both practically "undisturbed" months, the method used in this thesis could be applied. This yielded values of 2.8 and 4.4 for Ottawa and Resolute respectively. It is suggested that the lack of agreement is due to inadequate correction of the meson data. From the data available, the neutron-meson relative amplitude appears to have a value of about 4.0.

CHAPTER 6

SHORT TERM VARIATIONS

6.1 Introduction

From consideration of the manner in which the intensity changed with time, the variations of 3 to 30 days duration evident in Fig.9A were classified as Forbush decreases, 27 day variations and combinations of these events (Chapter 8). A number of subintervals were chosen, each containing one major intensity fluctuation. The subintervals are indicated in Fig. 9A. The frequent superposition of a 27 day variation and a Forbush decrease prevented these phenomena from being studied separately, and they were considered under the broad title of "short term variations".

Let the intensities observed by recorders 1 and 2 during simultaneous recording periods, when expressed as percentages of the mean for the subinterval, be written as X_1 and X_2. For each subinterval, scatter diagrams of (X_1, X_2) were prepared for a number of definitions of X_1 and X_2. Four such diagrams are given in Figs. 11 A and B. A good correlation between X_1 and X_2 was evident for most scatter diagrams, the majority of the points defining a straight line quite well. An occasional exception occurred when comparing data obtained at widely separated longitudes. Most of the anomalous points represented data obtained during the first one or two days of a Forbush decrease. If a diagram as a whole showed a poor correlation, no further analysis was performed. There was no evidence that the gradients of the scatter diagrams appropriate to Forbush and 27 day events were markedly different.

For those subintervals for which the scatter diagrams were satisfactory, the standard deviations

Figures 11A and 11B - Scatter diagrams of Mt. Wellington neutron intensity against Hobart meson intensity. Intensities are expressed relative to the mean for the whole period. Standard deviations are shown.

Figure 11C - Various relative amplitudes plotted as functions of time. Standard errors are shown. The undisturbed neutron intensity recorded at Mt. Wellington is plotted for comparison with the Hobart neutron-meson relative amplitude.

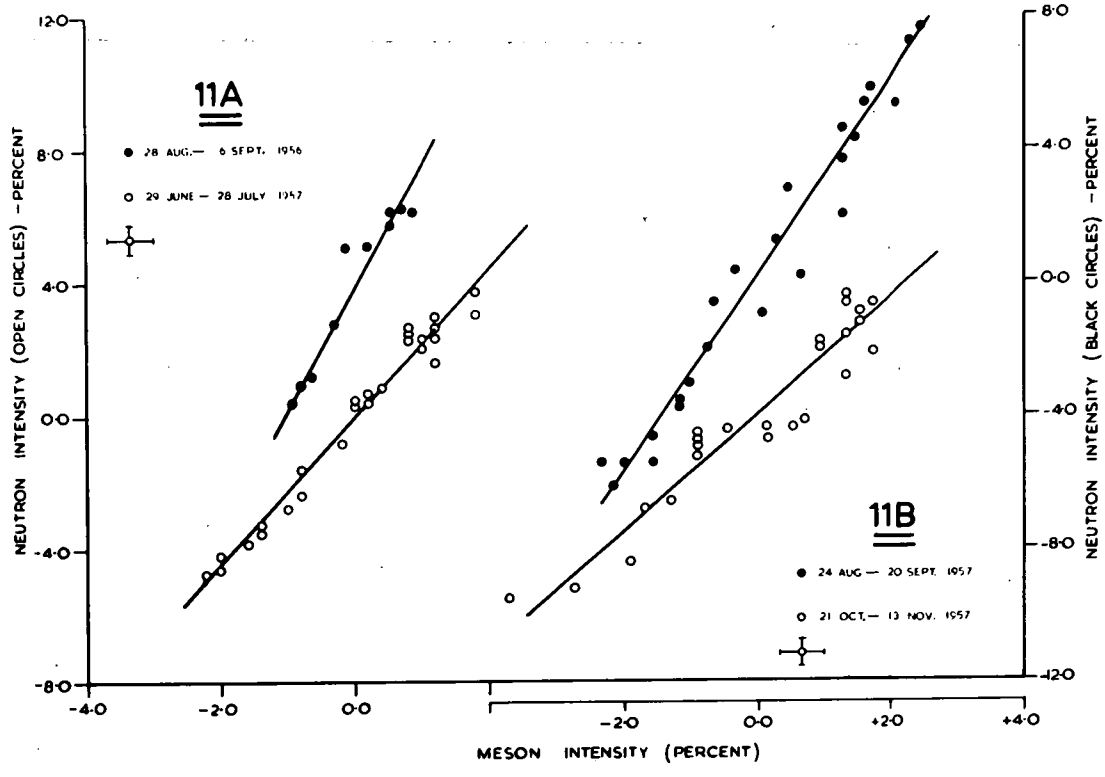
11A
28 AUG.— 6 SEPT. 1956
29 JUNE — 28 JULY 1957
11B
24 AUG — 20 SEPT. 1957
21 OCT.— 13 NOV. 1957
NEUTRON INTENSITY (OPEN CIRCLES) — PERCENT
NEUTRON INTENSITY (BLACK CIRCLES) — PERCENT
MESON INTENSITY (PERCENT)
12·0
8·0
4·0
0·0
-4·0
-8·0
-12·0
-4·0
-2·0
0·0
+2·0
+4·0

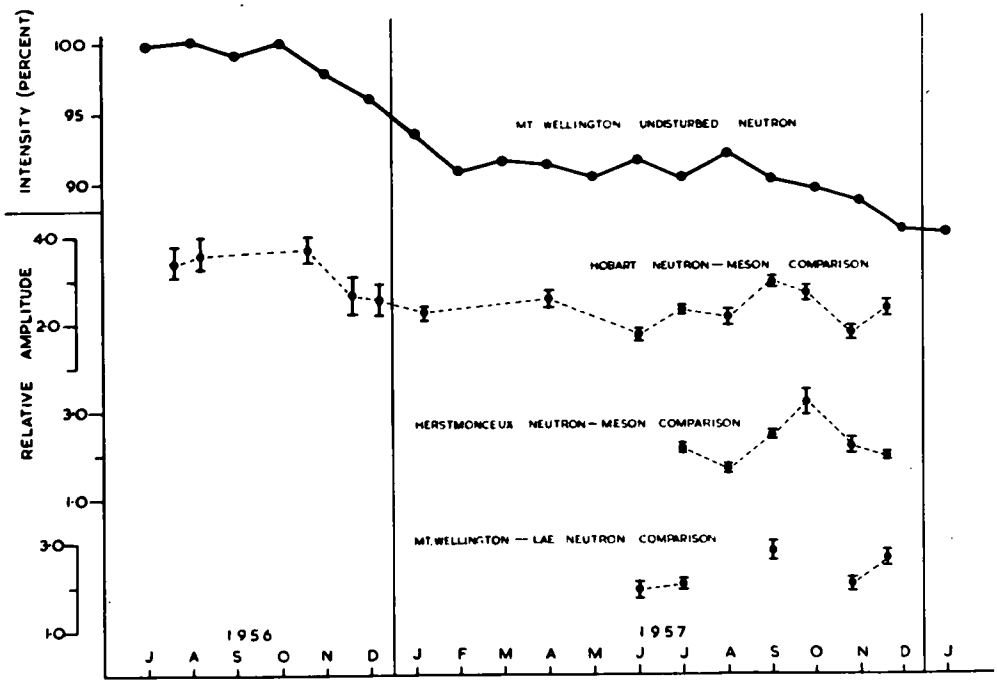
INTENSITY (PERCENT)
100
95
90
MT WELLINGTON UNDISTURBED NEUTRON
RELATIVE AMPLITUDE
4·0
2·0
3·0
1·0
3·0
1·0
HOBART NEUTRON — MESON COMPARISON
HERSTMONCEUX NEUTRON — MESON COMPARISON
MT. WELLINGTON — LAE NEUTRON COMPARISON
1956
1957
J A S O N D J F M A M J J A S O N D J

11C

$$\sigma_1 = \sqrt{\frac{1}{N-1} \cdot \Sigma(X_1 - \bar{X}_1)^2}$$

$$\sigma_2 = \sqrt{\frac{1}{N-1} \cdot \Sigma(X_2 - \bar{X}_2)^2}$$

and the correlation coefficient

$$r_{12} = \frac{\Sigma(X_1 - \bar{X}_1) \cdot (X_2 - \bar{X}_2)}{\sqrt{\Sigma(X_1 - \bar{X}_1)^2 \cdot \Sigma(X_2 - \bar{X}_2)^2}}$$

were calculated, N being the number of (X_1, X_2) pairs used in the analysis, and a mean value being indicated by a bar. The quantity $\frac{\sigma_1}{\sigma_2}$, the estimate of the amplitude of the variation in X_1 relative to that in X_2 was then calculated. The choice of this quantity as the measure of the relative amplitude has been discussed in section 4.3. The standard error of the regression coefficient of X_1 upon X_2 was calculated as a rough estimate of the standard error of the relative amplitude. The results of these analyses are given in Tables 6B-6E and 6J.

By comparison of data obtained at the observatories listed in Table 6A, the following were determined

(1) the variation of event amplitude with altitude,

(2) the variation of event amplitude with geomagnetic latitude,

(3) the neutron monitor-cubical meson telescope relative amplitude and the ionization chamber-cubical telescope relative amplitude.

The following sections are devoted to the presentation and discussion of the results of these studies.

TABLE 6A

The geomagnetic latitudes and altitudes of the stations whose data are compared in Tables 6B-6E and 6J. The data from the stations marked with an asterisk were obtained through private exchange of data (See Preface).

Station	Geomagnetic Latitude	Altitude (metres)	Station	Geomagnetic Latitude	Altitude (metres)
Banff *	58°N	2280	Mt. Norikura *	26°N	2840
Herstmonceux *	54°N	20	Mt. Wellington	52°S	725
Hobart	52°S	20	Resolute *	83°N	17
Lae	16°S	4	Tokyo *	26°N	20
Mawson	73°S	15	Uppsala *	58°N	<100

6.2 Dependence of event amplitude upon altitude

In Table 6B are given the amplitudes of the neutron variations at a number of observatories relative to those at the sea level observatory at Herstmonceux. As event amplitude is a function

TABLE 6B

The dependence of event amplitude upon altitude for the neutron component. All stations are at approximately the same geomagnetic latitude. Year 1957.

Relative Response \ Period		29 June-28 July	24 Aug-20 Sept	21 Sept-19 Oct	20 Oct-13 Nov	14 Nov-10 Dec
Uppsala -	$\frac{\sigma_1}{\sigma_2}$	1.00±0.02	1.06±0.03	1.12±0.08	1.02±0.03	1.10±0.04
Herstmonceux	r_{12}	1.00	0.99	0.93	0.99	0.99
Mt. Wellington -	$\frac{\sigma_1}{\sigma_2}$	1.12±0.04	1.09±0.02	1.22±0.07	1.02±0.04	1.19±0.05
Herstmonceux	r_{12}	0.99	0.99	0.96	0.99	0.98
Banff -	$\frac{\sigma_1}{\sigma_2}$	1.31±0.04	1.26±0.03	1.47±0.13	1.09±0.04	1.31±0.05
Herstmonceux	r_{12}	0.99	0.99	0.92	0.99	0.98

of geomagnetic latitude (section 6.3), this analysis has been restricted to data from observatories at approximately the same geomagnetic latitude. All observatories are above the "knee" in the intensity against latitude curve. The values given in Table 6B are plotted as functions of altitude in Fig. 12. From these graphs it is clear that event amplitude is a function of altitude, and that the dependence is noticeable at quite low altitudes (e.g. 725 metres). Comparison of Fig. 12D with the remainder of the graphs suggests that the altitude dependence varies from event to event.

The ratio of the high latitude to equatorial neutron intensity varies with altitude, being 1.77 at sea level (ROSE et al, 1956) and 2.55 at 3,300 metres (SIMPSON et al, 1953). This means that a neutron monitor's response to low rigidity primaries increases with altitude. The event amplitude increasing with altitude is consistent with the hypothesis that the change in primary intensity is greatest at low rigidities. The variability of the altitude dependence indicates that the dependence of event amplitude upon rigidity varies from event to event.

For most events, the relative amplitude varied by about 12 percent per 1000 metres altitude. That is, the absorption m.f.p. increases during an event. This is not unexpected as the m.f.p. is presumably a function of primary energy. During a large event (10 percent depression) the m.f.p. changes by about 2 percent.

The dependence of event amplitude upon altitude means that some care must be taken when investigating the rigidity dependence of variations by means of the comparison of data obtained at different latitudes. Clearly, indiscriminate comparison of high altitude (3000 metres) and sea level data will introduce considerable errors.

6.3 The latitude dependence of event amplitude

The results of the analyses comparing the counting rate variations at different geomagnetic latitudes are listed in Tables 6C

Figures 12A to 12F - Relative amplitude plotted as a function of altitude. The amplitudes are all relative to those observed at the sea level station of Herstmonceux. All the data were obtained during 1957. Standard errors are shown.

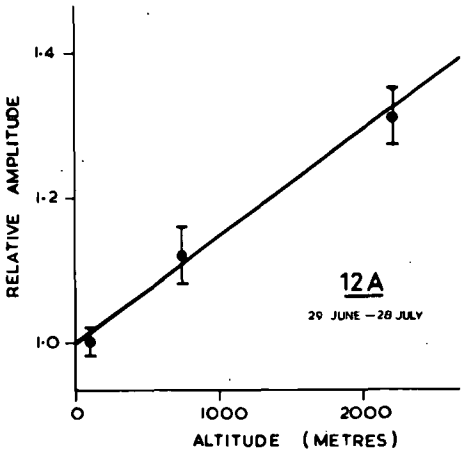
RELATIVE AMPLITUDE
1·4
1·2
1·0
0
1000
2000
ALTITUDE (METRES)
12A
29 JUNE – 28 JULY

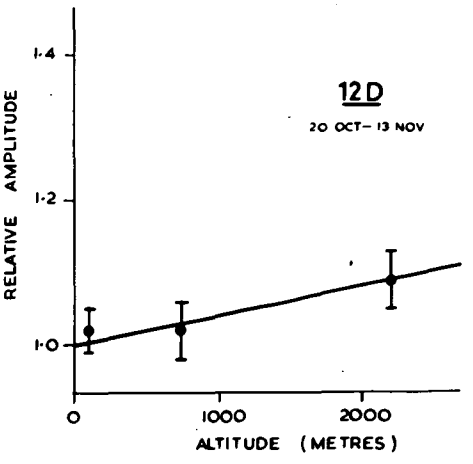
RELATIVE AMPLITUDE
1·4
1·2
1·0
0
1000
2000
ALTITUDE (METRES)
12D
20 OCT – 13 NOV

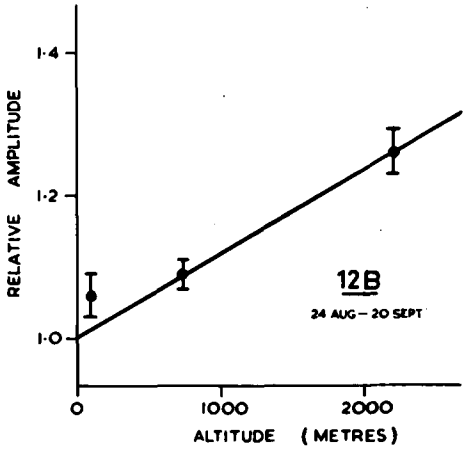
RELATIVE AMPLITUDE
1·4
1·2
1·0
0
1000
2000
ALTITUDE (METRES)
12B
24 AUG – 20 SEPT

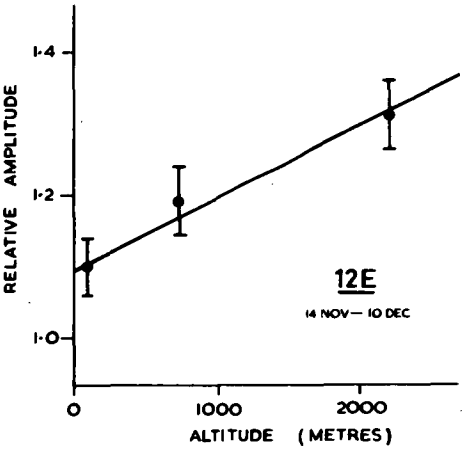
RELATIVE AMPLITUDE
1·4
1·2
1·0
0
1000
2000
ALTITUDE (METRES)
12E
14 NOV – 10 DEC

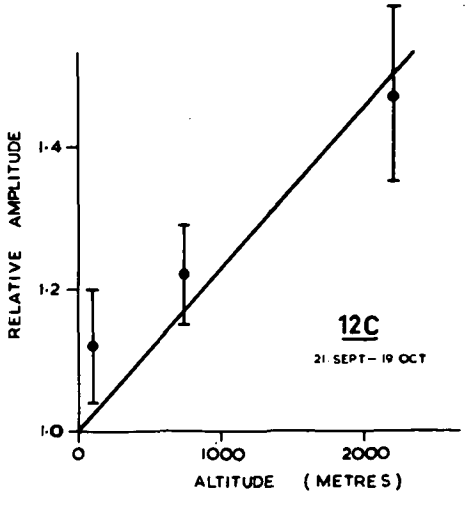
RELATIVE AMPLITUDE
1·4
1·2
1·0
0
1000
2000
ALTITUDE (METRES)
12C
21 SEPT – 19 OCT

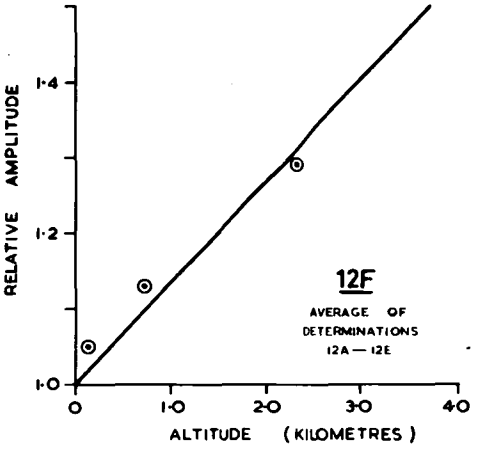
RELATIVE AMPLITUDE
1·4
1·2
1·0
0
1·0
2·0
3·0
4·0
ALTITUDE (KILOMETRES)
12F
AVERAGE OF DETERMINATIONS 12A – 12E

12A–F

and 6D. Only those data which were obtained near sea level (altitude $<$ 100 metres) have been used in these analyses. The average of the values of the Mawson-Lae relative amplitude of the neutron variations is 2.3, and that of the Hobart-Lae relative amplitude of the meson variations is 1.5. These values, indicating that short term variations are more pronounced at low than at high rigidities, will be discussed in Chapter 7.

TABLE 6C

The dependence of event amplitude upon latitude for the neutron component. All stations are near sea level. Year 1957. Herst. stands for Herstmonceux.

Relative Response \ Period		1 June–28 June	29 June 28 July	24 Aug–20 Sept	21 Sept–19 Oct	20 Oct–13 Nov	14 Nov–10 Dec
Mawson–Lae	$\frac{\sigma_1}{\sigma_2}$	1.95±0.21	2.03±0.11	2.80±0.24		2.07±0.17	2.66±0.25
	r_{12}	0.89	0.96	0.91		0.92	0.88
Herst. – Mawson	$\frac{\sigma_1}{\sigma_2}$	0.92±0.05	0.99±0.03	0.93±0.02	0.90±0.05	1.06±0.04	0.95±0.04
	r_{12}	0.98	0.99	0.99	0.95	0.98	0.98
Uppsala–Mawson	$\frac{\sigma_1}{\sigma_2}$	1.15±0.06	0.98±0.03	0.98±0.03	1.05±0.08	1.12±0.05	1.04±0.05
	r_{12}	0.96	0.99	0.99	0.93	0.98	0.97
Resolute–Mawson	$\frac{\sigma_1}{\sigma_2}$	1.17±0.07	1.02±0.05	1.02±0.04	1.04±0.07	1.18±0.04	1.06±0.05
	r_{12}	0.97	0.98	0.98	0.95	0.98	0.97

TABLE 6D

The Hobart-Lae relative amplitude for the meson component. (cubical telescopes). Both stations are near sea level. Year 1957.

	1 June-28 June	29 June-28 July	29 July-23 Aug	24 Aug-20 Sept	21 Sept-19 Oct	20 Oct-13 Nov	14 Nov-10 Dec
$\frac{\sigma_1}{\sigma_2}$	1.43±0.14	1.48±0.04	1.37±0.08	1.43±0.09	1.57±0.32	1.50±0.10	1.83±0.17
r_{12}	0.91	0.99	0.97	0.96	0.78	0.97	0.94

In Fig. 13, relative amplitude is plotted as function of latitude for $\lambda > 50^{\circ}$. From these graphs, it appears that during 1957 the event amplitudes were slightly greater at $\lambda = 58^{\circ}$ than at $\lambda = 54^{\circ}$. Above $\lambda = 58^{\circ}$, the event amplitude was independent of latitude.

Observations made at sea level and aircraft altitudes indicate that the "knee" in the neutron intensity against geomagnetic latitude curve was at $\lambda = 55^{\circ}$ during 1954. (ROSE et al, 1956; MEYER and SIMPSON, 1957). As solar activity increased, the knee observed at aircraft altitudes shifted to a lower latitude, being in the vicinity of $\lambda = 52^{\circ}$ in 1957 (MEYER and SIMPSON, 1957; STOREY et al, 1958). Presumably the knee in the sea level curve would also have been at $\lambda = 52^{\circ}$ during 1957. That is, all sea level neutron monitors above $\lambda = 52^{\circ}$ recorded the same spectrum in 1957. Consequently, a change in the primary spectrum would be expected to have produced the same percentage change in counting rate at all geomagnetic latitudes greater than 52°.

The preceding remarks apply only if the changes in spectrum were the same for primary radiation reaching the earth from all directions in space. If the effect of a depressive mechanism were more pronounced in some directions than in others, the percentage

Figures 13A to 13F - Relative amplitude plotted as a function of geomagnetic latitude. The amplitudes are all relative to those observed at Mawson. All data were obtained during 1957. Standard errors are shown.

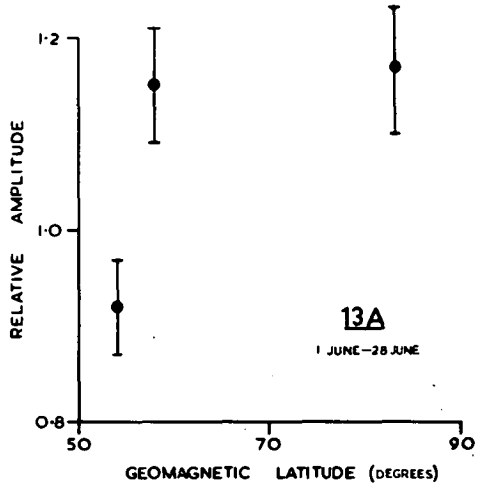
1·2
1·0
0·8
RELATIVE AMPLITUDE
13A
1 JUNE–28 JUNE
50
70
90
GEOMAGNETIC LATITUDE (DEGREES)

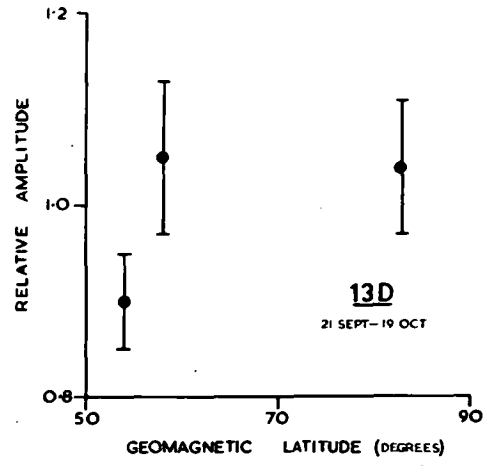
1·2
1·0
0·8
RELATIVE AMPLITUDE
13D
21 SEPT–19 OCT
50
70
90
GEOMAGNETIC LATITUDE (DEGREES)

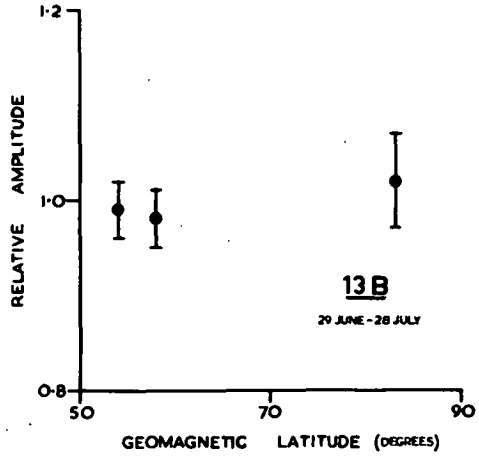
1·2
1·0
0·8
RELATIVE AMPLITUDE
13B
29 JUNE–28 JULY
50
70
90
GEOMAGNETIC LATITUDE (DEGREES)

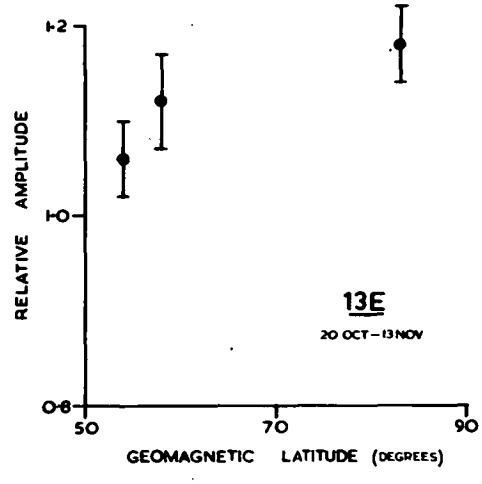
1·2
1·0
0·8
RELATIVE AMPLITUDE
13E
20 OCT–13 NOV
50
70
90
GEOMAGNETIC LATITUDE (DEGREES)

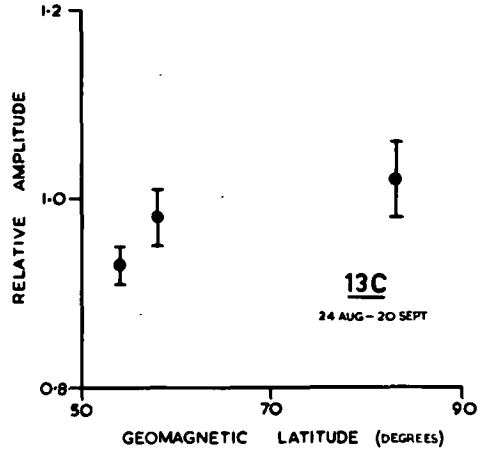
1·2
1·0
0·8
RELATIVE AMPLITUDE
13C
24 AUG–20 SEPT
50
70
90
GEOMAGNETIC LATITUDE (DEGREES)

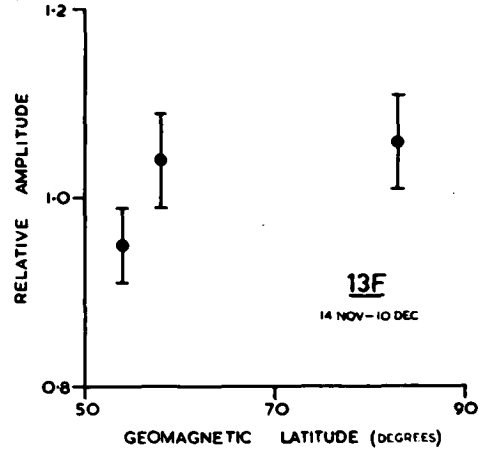
1·2
1·0
0·8
RELATIVE AMPLITUDE
13F
14 NOV–10 DEC
50
70
90
GEOMAGNETIC LATITUDE (DEGREES)

13A–F

Changes in intensity would be different for different particle trajectories. Consequently, the event amplitude could be a function of latitude even at latitudes above $\lambda = 52^{\circ}$.

To be specific, suppose that the depressive mechanism were sited outside the geomagnetic field. Reference to published data on the deflection of cosmic radiation by the geomagnetic field (BRUNBERG, 1953; BRUNBERG and DATTNER, 1953; JORY, 1956) reveals that whereas a neutron monitor near $\lambda = 52^{\circ}$ responds to radiation coming from asymptotic directions * within about 30° of the geographic equatorial plane, a monitor at $\lambda > 80^{\circ}$ responds largely to radiation coming from asymptotic geographic latitudes between 50° and 90°. If then, the extent to which the intensity were depressed were a function of asymptotic latitude, the event amplitudes at $\lambda = 52^{\circ}$ and $\lambda > 80^{\circ}$ would be different. Likewise, a mechanism sited within the geomagnetic field could produce a dependence of event amplitude upon latitude for $\lambda > 52^{\circ}$.

The relatively weak dependence of event amplitude upon latitude for $\lambda > 52^{\circ}$ indicates that the depressive mechanism affects radiation coming from all directions to about the same extent. If anything, the greatest depression of the intensity occurs in directions making large angles with the equatorial plane. SINGER (1958, p.319), from an analysis of meson data from a single event, finds that the event amplitude at $\lambda = 89^{\circ}$N is considerably (about two times) greater than that at $\lambda = 57^{\circ}$N. The conflict between this result and the present one may be due to either (a) the fact that a meson telescope responds to higher energy primaries than does a neutron monitor, or (b) the fact that the data analysed by Singer were not corrected for atmospheric structure.

In Chapter 5 it was shown that in the case of the long term variation, the Mt. Wellington-Mawson relative amplitude was unity. Thus the magnitude of the long term variation is also virtually independent of asymptotic direction.

---

* The asymptotic direction of arrival of a cosmic ray particle is that direction from which the particle is coming before it enters the geomagnetic field.

6.4 The variability of the neutron-meson relative amplitude

The neutron monitor-meson telescope relative amplitudes derived from data obtained at a number of observatories are listed in Table 6E. The scatter diagrams of four events observed at Mt. Wellington and Hobart are given in Fig. 11. Differences in slope are evident.

TABLE 6E

Neutron-cubical meson telescope relative amplitude. Year 1957. The following abbreviations are used:- Well = Mt. Wellington; Hob = Hobart; Herst = Herstmonceux.

		1 June-28 June	29 June-28 July	29 July-24 Aug	24 Aug-20 Sept	21 Sept-19 Oct	20 Oct-13 Nov	14 Nov-10 Dec
Well-Hob	$\frac{\sigma_1}{\sigma_2}$	1.76±.10	2.30±.07	2.16±.20	2.94±.12	2.67±.21	1.79±.13	2.32±.19
	r_{12}	0.98	0.99	0.92	0.98	0.95	0.95	0.95
Herst	$\frac{\sigma_1}{\sigma_2}$		2.17±.12	1.72±.22	2.44±.05	3.19±.33	2.23±.19	1.94±.06
	r_{12}		0.97	0.95	0.99	0.92	0.94	0.99
Lae	$\frac{\sigma_1}{\sigma_2}$	1.30±.13	1.36±.09	1.10±.11	1.38±.06	1.31±.16	1.30±.10	1.58±.23
	r_{12}	0.93	0.95	0.91	0.98	0.87	0.94	0.89

Neutron-non cubical meson telescope relative amplitude. (telescope geometry:- tray area 1m x 1m, tray separation 1.5m)

		18.8 - 28.8.56	29.8 - 6.9.56	1.11 - 17.11.56	3.12 - 15.12.56	16.12.56-8.1.57	15.1 - 28.2.57	1.4 - 30.4.57
Well-Hob	$\frac{\sigma_1}{\sigma_2}$	3.40±.40	3.55±.38	3.70±.32	2.66±.45	2.56±.35	2.24±.16	2.56±.21
	r_{12}	0.94	0.96	0.95	0.90	0.85	0.91	0.93

The variability of the slope could be due to

(a) the rigidity spectrum of the primary radiation prior to passage through the depressive mechanism being different from event to event, or

(b) the rigidity dependence of the spectral changes being different from event to event. These possibilities will be considered in turn.

(a) Whenever the primary spectrum changes, the counting rate of at least one of the monitors at Lae and Mt. Wellington must change. The variations in the Mt. Wellington and Lae undisturbed intensities (defined in Chapter 5) during the period June-September 1957 were quite small, indicating that there was little change in the primary spectrum during this time apart from those occurring during the short term events. During the period there were marked differences in the neutron-meson relative amplitude, and consequently possibility (a) can be excluded.

(b) The remaining alternative is that the manner in which the mechanism affects the spectrum varies from event to event. Thus for some events the percentage change at low rigidities would be much greater than that at high rigidities, resulting in high values of the neutron-meson relative amplitudes. For other events, the high and low ends of the spectrum would be affected to roughly the same extent and the values of the relative amplitude would be close to unity.

It has been shown (Section 6.3) that the short term mechanism is not strongly dependent upon asymptotic direction. Hence (b) requires that the values of the neutron-meson relative amplitude at widely separated stations, and the Mawson-Lae relative amplitude of the neutron component, should exhibit similar fluctuations. The neutron-meson relative amplitudes for Hobart and Herstmonceux, and the Mawson-Lae relative amplitudes for the neutron component, are

plotted in Fig. 11C. While the graphs exhibit similarities it is not certain at this stage whether this is fortuitous. Comparison with the values found at other stations during the International Geophysical Year will probably determine whether the effect is world wide, and hence whether (b) is plausible. Until such comparisons are made, it is assumed that (b) is correct.

6.5 Short term variations observed underground.

It has been shown (TAYLOR, 1958) that Forbush decreases affect the primary spectrum at quite high energies. Taylor's equipment consisted of two semi-cubical telescopes, each of sensitive area 1 metre by 1 metre. They were situated in a tunnel a few miles from Hobart, the earth and rock above them being estimated to be the equivalent of 40 metres of water (40 m.w.e.). The total absorber above them was therefore 50 m.w.e.

Using the barometric and positive temperature coefficients found by Taylor (-0.85 percent/cm.Hg. and 0.07 percent/^{o}C respectively) the daily mean counting rates were corrected for atmospheric change. While equipment variation rendered much of the data useless and precluded any long term investigations, apparently reliable results were obtained at the times of three large Forbush decreases. Table 6F compares the changes in intensity observed underground with those observed by the Hobart cubical telescope and the Mt. Wellington neutron monitor.

Comparison of the last two rows of Table 6F reveals an interesting result. While the ratio of the changes in the neutron and ground level meson counting rates varied from event to event, in good agreement with the relative amplitudes listed in Table 6E, there were no significant changes in the neutron-underground meson relative amplitude. Thus it would seem that the variability in spectral change only occurred at medium energies (about 30 Bev). This result cannot be regarded as conclusively proven as undetected

TABLE 6F

Intensity changes observed by the Mt. Wellington neutron monitor, the Hobart cubical telescope and the Hobart underground telescope.

Event	29 August, '57	21 October, '57	19 December, '57
Period prior to event	26-29 Aug.	18-21 Oct.	17-19 Dec.
Period during event	30-31 Aug.	22-24 Oct.	21-22 Dec.
% change neutron	9.3±0.2	7.0±0.2	4.6±0.2
% change cubical	3.2±0.1	3.9±0.1	2.0±0.1
% change underground	1.3±0.1	1.0±0.1	0.5±0.1
neutron/ cubical	2.9±0.2	1.8±0.2	2.3±0.2
neutron/ underground	7.3±0.6	7.3±0.7	8.9±0.8

equipment variation may have contributed to the variations observed underground.

A muon must have an energy of >15 Bev to penetrate 50 m.w.e. of absorber (p. 413, GEORGE, 1952). DORMAN (1957, p.119) states that the little evidence available suggests that the initial energy of the muon is about one tenth of the energy of the initiating primary. On the basis of this figure the minimum primary energy necessary to ensure detection in the tunnel is 150 Bev. Thus the Forbush mechanism was effective for $E > 150$ Bev. for at least three events during 1957.

In Fig. 14A the data for one event are plotted as a function of time. It is clear that the time variations at $E > 150$ Bev. were similar to those at $E \approx 10$ Bev. In particular, the event started at about the same time in both sets of data. The large standard deviation of the underground data precludes a precise determination of the onset time.

The observation of a Forbush decrease underground is contrary to the findings of Mac Anuff (p.422, GEORGE, 1952), who found no significant variation at 60 m.w.e. during an event which produced a 5 percent change in the ground level meson intensity. The higher "cut-off" energy of his recorder, 210 Bev, could conceivably be the cause of this discrepancy, and this will be investigated more fully in Section 7.1.

6.6 Comparison with the literature.

A number of investigators have published comparisons of the data obtained using different recorders. A careful study of their results is necessary, as some of them appear to disagree with those presented in this thesis.

As discussed in section 4.3, the quantities b_{12}, $\frac{1}{b_{21}}$, $\frac{1}{2}(b_{12} + \frac{1}{b_{21}})$, $\frac{\sigma_1}{\sigma_2}$, $\frac{\partial X_1}{\partial X_2}$ and regression coefficients derived by weighting the two data have all been used as measures of the relative amplitude. Further, it was shown that for $r > 0.8$, the three measures $\frac{1}{2}(b_{12} + \frac{1}{b_{21}})$, $\frac{\sigma_1}{\sigma_2}$ and a weighted regression coefficient are in good agreement, while the agreement with b_{12} and $\frac{1}{b_{21}}$ is poor for $r_{12} < 0.9$. Thus when an author lists either b_{12} or $\frac{1}{b_{21}}$ as the measure of relative amplitude, and also gives r_{12}, $\frac{\sigma_1}{\sigma_2}$ has been calculated ($b_{12} = r_{12} \frac{\sigma_1}{\sigma_2}$).

The majority of relative amplitude determinations have employed ionization chamber data. In order to convert the observed changes in centre electrode current into percentage changes in cosmic ray intensity, the contribution to the centre electrode current made by radioactive contamination must be known (e.g. Section 3.2). Clearly an error in this value will introduce an error into relative amplitudes calculated from the data from the chamber.

The stations dealt with in the literature are listed in Table 6G.

TABLE 6G

Stations from which relative amplitude data have been reported.

Station	Geomagnetic Latitude	Altitude (metres)	Station	Geomagnetic Latitude	Altitude (metres)
Canberra	45°S	800	Huancayo	1°S	3350
Cheltenham	50°N	72	Manchester	57°N	<100
Christchurch	49°S	8	Ottawa	57°N	101
Climax	48°N	3350	Resolute	83°N	17
Freiburg	49°N	240	Syowa(Antarctica)	68°S	$\approx$ 2
Godhavn	80°N	9	Teoloyucan	30°N	2285
Hafelekar	48°N	2300	Tokyo	26°N	20

It is to be expected that the amplitude of an intensity change in the meson component will increase with altitude. Table 6H summarises the data available on this effect at high latitudes. It is clear that the event amplitude is greater at Hafelekar (2300 m) than at sea level. Extrapolation of this meagre data indicates that the ionization chamber variations at 3350 m. would be about 1.6 to 2.0 times those at sea level.

TABLE 6H

Comparison of high latitude ionization chamber data.

Investigator	Detector 1	Detector 2	$\frac{\sigma_1}{\sigma_2}$
FONGER, 1953	Freiburg	Cheltenham	0.77
YOSHIDA and KAMIYA, 1953	Christchurch	Cheltenham	0.81 ± 0.21
	Godhavn	Cheltenham	1.17 ± 0.13
	Canberra	Cheltenham	1.01 ± 0.15
	Hafelekar	Cheltenham	1.40 ± 0.03

To determine the altitude effect at low latitudes, the ionization chamber data from Mt. Norikura (26°N, 2840 metres) were compared with those from Tokyo (26°N, 20 metres), the resulting values of $\frac{\sigma_1}{\sigma_2}$ being given in Table 6J. The mean relative amplitude is 1.7. Unfortunately, while both chambers were shielded by 10 cm Pb, the Tokyo chamber was situated under a 40 cm. concrete shield (1.1 m.w.e.), presumably increasing the relative amplitude. As a rough estimate, taking the concrete shield to be the equivalent of 1.1 m.w.e. of the atmosphere, the event amplitude at 3350 metres would be about 1.6 times that at sea level.

Thus at high and low latitudes, there is a marked dependence of event amplitude upon altitude.

TABLE 6J

Miscellaneous relative amplitudes. Year 1957.

The following abbreviations are used:- A = Hobart ion chamber-Hobart cubical telescope relative amplitude; B = Mt. Wellington neutron-Hobart ion chamber relative amplitude; C = Mt. Norikura ion chamber-Tokyo ion chamber relative amplitude.

		1 June-28 June	29 June-28 July	29 July-23 Aug	24 Aug-20 Sept	21 Sept-19 Oct	20 Oct-13 Nov	14 Nov-10 Dec
A	$\frac{\sigma_1}{\sigma_2}$	1.09±.06	0.92±.05		1.07±.08	0.98±.08	0.74±.05	0.90±.07
	r_{12}	0.97	0.96		0.95	0.93	0.95	0.95
B	$\frac{\sigma_1}{\sigma_2}$		2.46±.17	2.12±.19	3.08±.25	2.48±.30	2.52±.18	2.49±.16
	r_{12}		0.93	0.91	0.92	0.87	0.94	0.95
C	$\frac{\sigma_1}{\sigma_2}$	1.99±.14	1.63±.31	1.49±.14	1.75±.12	1.95±.20	1.75±.13	1.68±.10
	r_{12}	0.95	0.71	0.92	0.95	0.90	0.95	0.97

The published data on the dependence of event amplitude upon latitude are given in Table 6K. These data (in particular, the Cheltenham-Huancayo relative amplitude) have led a number of investigators to conclude that event amplitude is only slightly latitude dependent (e.g. SARABHAI and NERURKAR, 1956).

TABLE 6K

The dependence of event amplitude upon latitude for ionization chamber data. Long and short term variations.

Investigator	Variation	Detector 1	Detector 2	$\frac{\sigma_1}{\sigma_2}$
FORBUSH, 1938, 1954; FONGER, 1953	Short	Cheltenham	Huancayo	1.11,1.06,1.1
FORBUSH, 1938	Long and Short	Teoloyucan	Huancayo	1.58
FORBUSH, 1938	Short	Hafelekar	Huancayo	1.59
YOSHIDA and KAMIYA, 1953	Short	Tokyo	Cheltenham	0.91
FORBUSH, 1938, 1954	Long	Cheltenham	Huancayo	1.11,0.98

From the altitude effect for ionization chamber data deduced earlier, and taking the Cheltenham-Huancayo relative amplitude to be 1.1, the high latitude variations at 3350 metres are estimated to be between $1.1 \times 1.6 = 1.7$ and $1.1 \times 2.0 = 2.2$ times those at Huancayo (3350 metres). Thus the value of 1.6 for the Teoloyucan-Huancayo relative amplitude is reasonable, whereas earlier investigators (Forbush and Fonger) have regarded it with suspicion.

As there is still a marked altitude effect at low latitudes, the variations recorded at sea level at the equator will be less than those at Huancayo. Assuming that the value of 1.6 found for the altitude effect at $\lambda = 26^{\circ}$ applies at the equator, the sea level variations are estimated to be $\frac{1}{1.6}$ times those at Huancayo. From

the observed value of 1.1 for the Cheltenham-Huancayo relative amplitude, the high latitude-low latitude relative amplitude at sea level is estimated to be about 1.1 x 1.6 $\approx$ 1.7. Bearing in mind the uncertainties in the derivation of this result, it is not inconsistent with the value of 1.5 found from the comparison of cubical telescope data (Table 6D).

It is concluded that the data in the literature indicate that the amplitude of short term events is more latitude dependent than previously thought.

It is seen from Table 6K that the Cheltenham-Huancayo relative amplitude for the long term variation is the same as that for the short term variation. Making the reasonable assumption that the long term variation is altitude dependent leads to the conclusion that the long term variation is also latitude dependent.

Table 6L lists the various values obtained for the neutron-meson relative amplitude. While all meson detectors were situated near sea level, a number of the determinations were based upon neutron data obtained at mountain altitudes. To permit comparison of the determinations, the values of the relative amplitude which would have been observed at sea level have been estimated using the average altitude effect found in section 6.2.

There is good agreement between the values found for Hobart, Herstmonceux, Ottawa, Resolute and Manchester. All these determinations employed meson telescope data. The majority of the values found using ionization chamber data are somewhat higher. Those reported by KODAMA and MIYAZAKI (1957), NEHER and FORBUSH (1952), and the Climax-Cheltenham value of FONGER (1953) can be reconciled to the values found for telescope data by taking into account the value of 0.95 for the average ionization chamber-cubical telescope relative amplitude found at Hobart (Table 6J), and the fact that this is somewhat variable.

TABLE 6L

Average of the values found for the neutron-meson relative amplitude. When neutron data have been obtained at mountain altitudes the relative amplitude which would have been observed if the monitor had been at sea level has been estimated. (written $(\frac{\sigma_1}{\sigma_2})_s$).

Investigator	Detector 1	Detector 2	$\frac{\sigma_1}{\sigma_2}$	$(\frac{\sigma_1}{\sigma_2})_s$
FONGER, 1953	Climax neutron	Freiburg ion	5.5	3.8
FONGER, 1953	Climax neutron	Cheltenham ion	4.0	2.8
KODAMA and MIYAZAKI, 1957	Syowa neutron	Syowa ion	2.8	
VAN HEERDEN and THAMBYAHPILLAI, 1955	Manchester neutron	Manchester telescope	2.3	
NEHER and FORBUSH, 1952	Climax neutron	Cheltenham ion	3.0	2.1
FENTON et al, 1958	Ottawa neutron	Ottawa telescope (cubical)	1.9	
FENTON et al, 1958	Resolute neutron	Resolute telescope (cubical)	2.2	
McCRACKEN	Mt. Wellington neutron	Hobart telescope (cubical)	2.4	2.2
McCRACKEN	Herstmonceux neutron	Herstmonceux telescope (cubical)	2.3	
McCRACKEN	Mt. Wellington neutron	Hobart ion	2.5	2.3

Some doubt must be thrown upon the reliability of one or the other of FONGER's results, for although they were determined over the same period in 1951, there is a considerable difference between them. As the Freiburg chamber had by far the best statistical accuracy* and further, as the data were corrected for the mass, decay and positive temperature effects (SITKUS, 1946), it would appear that

* The volume of the Freiburg chamber is 500 litres, compared with 20 litres for the Cheltenham chamber.

the Climax-Freiburg value should be the more accurate. This would suggest that either (a) the neutron-ion chamber relative amplitude changed between 1951 and 1957, or (b) the Freiburg corrections for residual ionization were in error.*

Considering possibility (a), Fig. 11C indicates that a decrease in neutron-meson relative amplitude occurred at the time of the marked decrease in "undisturbed intensity" during 1956 (Chapter 5). This suggests that the neutron-meson relative amplitude varies in phase with the eleven year periodicity in cosmic ray intensity. The primary spectrum varies during the sunspot cycle (MEYER and SIMPSON, 1955; 1957), the low rigidity end being considerably enhanced during the period of minimum solar activity, and this would be expected to result in a variation in the neutron-meson relative amplitude. On the other hand, MEYER and SIMPSON (1954) report that there is no evidence that the neutron-meson relative amplitude varies with time. Their analysis suffered from the disadvantage that the neutron and meson data which they analysed were obtained many years apart, and an indirect comparison was necessary. Direct comparison of the neutron and meson data accumulated since 1951 by overseas groups should enable this question to be settled conclusively.

With one exception then, the results reported in the literature are in agreement with the results given in Tables 6B-6E and 6J. As the variations during 1957 were quite large, and as the instruments operated by the University of Tasmania are of high statistical accuracy, it is proposed that considerable reliance can be placed in the results presented in these tables.

---

* No statement that the Freiburg data have been corrected for residual ionization has been found, although it is presumed that this will have been done. If it has not, the tabulated percentage changes will be too small, and the neutron-meson relative amplitude too big, as is observed.

CHAPTER 7

THE ENERGY DEPENDENCE OF VARIATIONS AND COMPARISON WITH THEORY

7.1 Calculation of the energy dependence

Table 7A lists the mean values of some of the relative amplitudes which are given in Tables 6B-6E and 6J.

TABLE 7A

Mean relative amplitudes for short and long term events. Where necessary they have been corrected for altitude.

Relative amplitude	Short term variations	Long term variation
Mawson neutron-Lae neutron	2.3	≈ 4.0
Hobart cubical-Lae cubical	1.5	
Mt. Wellington neutron-Hobart cubical	2.2	≈ 4.0
Lae neutron-Lae cubical	1.3	
Hobart ion chamber-Hobart cubical	0.95	
Mt. Wellington neutron-Hobart ion	2.3	
Mt. Wellington neutron-Hobart underground	7.0	

Unless there is a statement to the contrary, the alpha particle and heavy particle components of the primary radiation are neglected in this chapter.

There is no doubt that for both the high latitude neutron-low latitude neutron and the neutron-meson relative amplitudes the value applicable to the long term variation is greater than that applicable to the short term variation. Thus the two energy dependences are different, the long term variation being more pronounced at low energies. This suggests that the mechanisms responsible are different.

From Table 7A, a determination of the energy dependence of the two types of event can be made. Consider a dependence of the form

$$\frac{\partial j(E)}{j(E)} = \alpha(1 + E)^{-\beta}$$

where α and β are constants and E is the proton kinetic energy, (in Bev).

Using Dorman's coupling constants (see section 4.4 of this thesis and DORMAN, 1957) the intensity variations at high and low latitudes, and the variations under 50 m.w.e. of absorber were calculated for various values of the exponent β. A graphical method was used in the integration of equation 4(3). The integrand was evaluated for a number of values of E and plotted on graph paper, then the area under the curve through the points was measured with a planimeter. This method is accurate to within 1 percent, this being quite adequate for the present investigation. From the variations calculated in this manner, the various relative amplitudes listed in Table 7B were calculated.

Dorman's coupling constants for the meson component were calculated from a series of latitude surveys using ionization chambers. As yet no surveys have been reported using cubical telescopes, however RATHGEBER (1950) reports that while a very wide angle telescope showed a latitude effect of 13 percent, in reasonable agreement with ionization chamber surveys (MONTGOMERY, 1949, p.137), a vertical telescope of opening angle 26° x 33° showed a latitude effect of 20 percent. It therefore appears that the coupling constants of a narrow angle, vertical pointing telescope are different from those applicable to an ionization chamber. It was not deemed worthwhile calculating new constants until a survey has been made with a

TABLE 7B

Values of the relative amplitudes calculated for a spectral variation of the form $\frac{\partial j}{j} = \alpha(1+E)^{-\beta}$

Relative amplitude \ β	0.6	0.8	1.0	1.2	2.0	Observed	
						short	long
High latitude neutron-Low latitude neutron	2.0	2.4	3.0	3.6	10.6	2.3	≈4.0
High latitude neutron-High latitude meson (ion chamber)	2.1	2.7	3.4	4.2		2.3 (ion)	≈4.0 (telescope)
High latitude neutron-Underground	6.9	13.9	26.1	51.8	1000	7	
High latitude meson-Low latitude meson (ion chambers)	1.2	1.3	1.3	1.4		1.5 (telescope)	
Low latitude neutron-Low latitude meson (ion chamber)	1.3	1.4	1.4	1.6		1.3 (telescope)	

cubical telescope*. On the basis of the results reported by RATHGEBER (1950), it can be seen that a narrow angle telescope is more sensitive to low energy primaries than is an ionization chamber. Hence the variations in the telescope counting rate at high latitudes will be greater than those for an ionization chamber (as is observed), and the high latitude-low latitude relative amplitude will be greater than that applicable to an ionization chamber.

Referring to Table 7B, it is seen that exponents of 0.6 and 0.8 yield values for the relative amplitudes which are in reasonable agreement with those observed for short term variations. As predicted in the previous paragraph, the high latitude-low latitude relative amplitude calculated for the meson component is lower than that observed.

---

* In the event of no such survey being made in the near future, the survey reported by ROSE et al (1956) could be used.

For the long term variation, an exponent of 1.2 fits the observations quite well. An exponent of 1.0 fits neither variation satisfactorily, while an exponent of 2.0 is clearly greatly in error, the neutron-underground relative amplitude being in error by two orders of magnitude.

For a detector with a primary"cut-off" of 210 Bev (i.e. Mac Anuff's instrument, section 6.5), the ground level meson-underground meson relative amplitude for $\beta = 0.8$ has been calculated to be 6.4, thus, as a 5 percent variation was observed at ground level during the period considered by Mac Anuff, a 0.8 percent variation should have been observed underground. Such a variation could well be masked by the statistical fluctuations in Mac Anuff's data, for the standard deviation of his six hourly totals was 0.5 percent (p.422, GEORGE, 1952). Therefore, his results are not inconsistent with the proposed exponent of $\beta = 0.8$.

Summarising, three properties of the short term variation are:-

(a) Within the range 2.5 Bev $< E <$ 150 Bev, the energy dependence approximates to the law $\frac{\partial j}{j} = \text{const.}(1+E)^{-\beta}$, where $\beta = 0.6$ or 0.8.

(b) The energy dependence is variable from event to event. (Section 6.4).

(c) Short term variations occur at energies >150 Bev (Section 6.5).

These three facts will now be used to test the validity of a number of models.

7.2 Geocentric disordered magnetic fields

PARKER (1956) has proposed that the cosmic ray intensity is depressed by clouds of solar matter which are captured by the gravitational field of the earth. Some of these clouds, by virtue of

their high electrical conductivity, are permeated by disordered magnetic fields whose decay times are of the order of days or even months. Cosmic rays will be scattered by such clouds, which therefore form a semi-permeable barrier around the earth. As the cosmic rays inside the barrier are being continually removed by collision with the earth, the radiation intensity inside the barrier is less than that outside the barrier. The intensity at the earth will decrease immediately the barrier is established, and then slowly return to the pre-event value as the fields within the barrier decay.

The energy dependence of the intensity decrease depends upon whether the Larmor radii of the cosmic ray trajectories are large or comparable with the size of the clouds. For energies for which the deflection in each cloud can be $\geq \frac{\pi}{2}$, the barrier depresses the intensity equally at all energies. Such a barrier will not produce a low energy cut-off, the phenomenon upon which PARKER's theory is largely based. PARKER shows that a barrier of scattering clouds (deflections $< \frac{\pi}{2}$) produces a spectrum at the earth given by

$$j(E) = j_{\infty}(E) \cdot \frac{E(E+2)}{C + E(E+2)}$$

where $j_{\infty}(E)$ is the spectrum outside the barrier, and C is a quantity determined by the properties and number of scattering clouds making up the barrier. A value of 2.65 for C yields a spectral maximum at 1 Bev, as is observed during the period of maximum solar activity.

Having derived this model to explain the observed changes in spectrum, PARKER suggests that it may explain Forbush decreases. Consider a short term change in C produced by the arrival of clouds from the sun. Let C change from C_o to $C_o + \partial C$. For $\partial C < 3$ and $E > 3$

$$\frac{\partial j(E)}{j(E)} \approx - \frac{\partial C}{C_o + E(E + 2)}$$

$$\approx - \partial C(E + 1)^{-2.0}$$

It has been shown (Section 7.1) that the relative amplitudes calculated for an exponent of 2.0 are greatly in error.

This result was checked another way. The specific yield function for the sea level neutron component

$$S_Z(E) = A_Z(1 + E)^{0.27} \ln(\frac{1 + E}{2.2}) \quad \text{for} \quad E > 1.2 \text{ Bev}$$

$$= 0 \quad \text{for} \quad E < 1.2 \text{ Bev}$$

where A_Z is the atomic weight of the primary particles of kinetic energy E Bev per nucleon and charge Z, was derived from the sea level neutron intensity against latitude curves reported by ROSE et al (1956). Using this specific yield function, and taking into account the alpha and heavy particle components of the primary radiation (KAPLON et al, 1952), the Hobart-Lae relative amplitude for the neutron component was calculated to be 8.1, whereas the observed value is 2.3.

Thus it is concluded that the Parker mechanism does not fit the observed facts. A similar conclusion has been reached by BROWN (1958).

7.3 Geocentric Electric Fields

NAGASHIMA (1953) has proposed that intensity variations are produced by a varying potential between the earth and infinity. On the basis of our present knowledge, the high electrical conductivity of interplanetary space throws doubt upon the existance of such a field.

Nevertheless, the cosmic ray effects of such a field will be calculated. FONGER (1953) shows that for an electric field outside the geomagnetic field,

$$\frac{\partial j(E)}{j(E)} \sim \frac{1}{1+E}\left\{\frac{2}{1-\frac{1}{(1+E)^2}} + \text{const}\right\} \text{ where const} \approx 2.0$$

$$\sim \frac{1}{1+E}\left\{\frac{1}{(1+E)^2} + \text{const}\right\} \quad \cdots\cdots 7(1)$$

where E is the energy per nucleon, (in Bev).

For $E > 3$, this approximates to a $(1+E)^{-1.0}$ energy dependence. It has been shown in section 7.1 that such a law does not give a good fit to the observed facts. However, the discrepency is not as great as in the case of the Parker hypothesis, in fact, on some occasions values of the relative amplitudes have been observed which are close to thosepredicted for $\beta = 1.0$.

Using the same specific yield function which was employed to test the Parker hypothesis, the Hobart-Lae relative amplitude for the neutron component was calculated to be 3.1. Such a value has been observed (Table 6C).

If a geocentric electric field were to exist outside the region containing the earth's magnetic field, the energy dependence of the intensity variations would always be given by 7(1), and no variability of relative amplitude would be possible. However, an electric field in the same region as the geomagnetic field would alter the distribution of cut-off energies upon the surface of the earth, and thereby alter the latitude dependence of relative amplitude. A study of this type of mechanism has been reported (SIMPSON, 1954). It is stated that an electric field at a distance of about 4 earth radii does result in a smaller latitude dependence of relative amplitude than when the field is either closer to, or further away

from the earth.

There is thus a qualitative agreement between the variable latitude dependence of relative amplitude and the geoelectric hypothesis. Further computation is necessary to determine whether the theory is in quantitative agreement with the observations.

7.4 Ordered fields associated with streams of solar matter

DORMAN (1957) postulates a mechanism in which the magnetic field associated with a stream of matter from the sun is ordered. Fig. 14B is the idealised diagram which he gives. As seen from the earth, such a stream will produce two distinct effects, (1) the prevention of radiation from reaching the earth from some directions, and (2) the acceleration of some of the radiation which does reach the earth.

The radius of curvature $\rho(E)$ of the trajectory of a proton of energy E ev in a field of H gauss is given by

$$\rho(E) = \frac{E}{300\ H} \text{ centimeters } (E > 10^{10} \text{ev.})$$

Let the width of the solar stream at the orbit of the earth be 1, and consider the case in which the earth is in the middle of the solar stream (Figs. 14B). Consider asymptotic directions of arrival at the earth which are perpendicular to $\bar{H}$. It is clear from Fig. 14B(1) that for

$E < 75\ 1\ H$, all orbits are trapped within the solar stream. Thus no cosmic rays from outside the solar stream can reach the earth from these directions if $E < 75\ 1\ H$.

Consider Fig. 14B(2). For $75\ 1\ H < E < 150\ 1\ H$, some orbits terminating at the earth are trapped, and so some directions are forbidden directions of access for cosmic radiation from outside the solar stream. For $E > 150\ 1\ H$, all directions of access are

Figure 14A - The meson intensity observed 40 m.w.e. underground, and the neutron intensity observed at Mt. Wellington as a function of time for the period 20-24 October, 1957. Four hourly means are plotted.

Figure 14B - Illustrating Dorman's mechanism. The earth is in the centre of a solar stream, the magnetic field within the stream being the same at all points near the earth.

Figure 14C - Illustrating Dorman's mechanism in the case where the earth is near the edge of a solar stream. As seen by an observer at the earth, the stream has an electric field $\bar{E}$ associated with it. Particles moving along trajectory A' are decelerated, and those moving along A" are accelerated by this field.

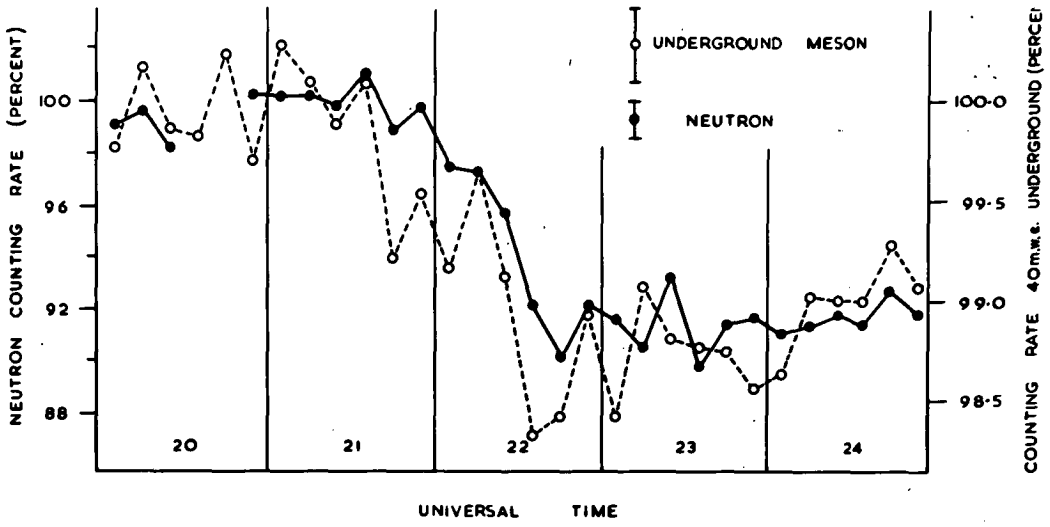

14 A

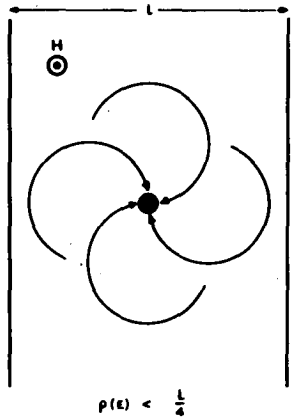

$\rho(E) < \frac{L}{4}$
ALL DIRECTIONS FORBIDDEN

14 B(1)

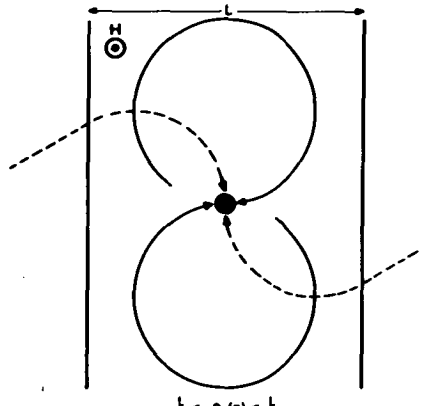

$\frac{L}{4} < \rho(E) < \frac{L}{2}$
SOME DIRECTIONS ALLOWED
SOME DIRECTIONS FORBIDDEN

14B(2)

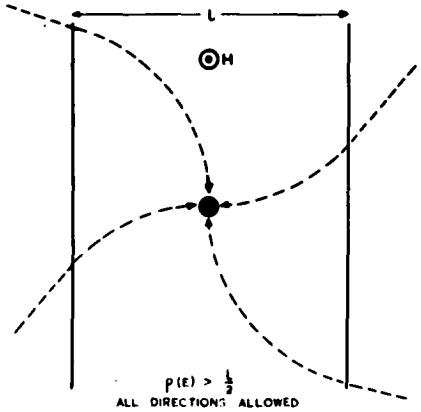

$\rho(E) > \frac{L}{2}$
ALL DIRECTIONS ALLOWED

14 B(3)

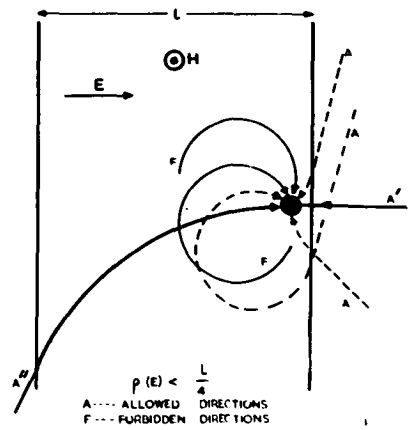

$\rho(E) < \frac{L}{4}$
A---- ALLOWED DIRECTIONS
F--- FORBIDDEN DIRECTIONS

14C

allowed (Fig. 14B(3)).

For asymptotic directions which are not perpendicular to $\bar{H}$, the cosmic ray trajectories are spirals. Depending upon the field configuration outside the solar stream, and upon how far past the earth the field remains ordered, some such directions will be allowed, and others forbidden. Neglecting the accelerating effect of electric fields associated with the solar stream, the cosmic ray intensity at the earth from allowed directions will be the same as that outside the stream (Liovilles Theorem), while it will be zero from forbidden directions. Thus when the earth is within the solar stream, there is complete exclusion of some radiation. The screening mechanism is most effective at low energies, and has no effect above a certain energy (150 lH electron volts).

If the lines of force of the ordered magnetic field are not parallel to its direction of motion, the solar stream will be electrically polarised when viewed by an observer who is not moving with the stream. This will result in acceleration of the radiation which arrives at the earth from some directions, and retardation of that from other directions. Thus a diurnal variation in intensity will be produced.

For a Forbush decrease to the observed 40 m.w.e. underground as a "classical" Forbush decrease, and not as an enhanced diurnal variation, some directions of arrival of particles for which $E > 150$ Bev must be forbidden. That is,

$$150 \times 10^9 < 150\ lH$$

$$\text{or } H > \frac{10^9}{l}$$

Estimates of l based upon magnetic data range from 2×10^{12}cm. to 10^{13}cm. (CHAPMAN and BARTELS, 1951). From these two estimates, $H > 5 \times 10^{-4}$ or $H > 10^{-4}$ gauss. Various estimates

based upon the properties of the sun do in fact yield an upper limit for H of about 10^{-4} gauss (DORMAN, 1957, p.438 obtains 3×10^{-4} gauss; PARKER, 1956, obtains 1.4×10^{-4} gauss), and so it is possible that the mechanism could operate.

Without making arbitrary assumptions regarding the configuration of the fields outside the solar stream, it is not possible to calculate the latitude dependence of the relative amplitude.

Now consider the earth situated near the edge of the same solar stream which was considered in Figs. 14B. Fig. 14C illustrates this case, and shows the trajectories of particles of the same energy as those shown in Fig. 14 B(1). It can be seen that, whereas in the case illustrated in Fig. 14 B(1) all directions perpendicular to $\bar{H}$ are forbidden, only about a quarter of these directions are forbidden in the case shown in Fig. 14 C. Thus for the earth near the edge of a solar stream, there will be relatively few forbidden directions at high energies.

In crossing the stream, high energy particles will be accelerated (or decelerated). Thus at high energies, the main effect of a solar stream is to produce intensity enhancements or depressions which are observed by a recorder on the earth every 24 hours (compare trajectories A" and A'). At low energies however, there may still be many forbidden directions, and the "classical" Forbush decrease may still be observed. Thus the variations predicted at high and low energies by Dorman's theory can be different.

A very marked Forbush decrease was observed at low energies on 22 October, 1957. There was a very active solar centre situated 35°-40° West of the central solar meridian the previous day, and it seems likely that the flare responsible for the cosmic ray event occurred in this centre. Thus the earth must have been very close to the edge of the solar stream ejected by the flare (flares so far from the central meridian seldom produce magnetic storms or Forbush decreases). This view is supported by the very short duration of the

magnetic effect accompanying the Forbush decrease (BARTELS, 1957). In such a case, the meson variations observed underground would be expected to be either recurrent enhancements or depressions. Fig. 14A shows that such was not the case, a "classical" Forbush decrease being observed. This suggests that the Dorman theory may not be correct.

CHAPTER 8

TIME VARIATIONS OF THE COSMIC RAY INTENSITY

8.1 The investigation of time variations

Study of the time and energy dependence of the variations in the cosmic ray intensity enables a number of different modes of variation to be identified. In searching for the mechanism responsible for any such mode, a very definite advance is made when a correlation with some other phenomenon is established. It has been found that the correlations are not always clear cut, and that a statistical analysis of a number of individual events is often necessary. It is obvious that only those variations which belong to the same class should be considered in any such analysis.

In such a manner, it has been found that the majority of cosmic ray variations are produced by solar controlled mechanisms. In the case of the solar flare effect and the Forbush decrease, a definite correlation with a particular solar event (the solar flare) has been possible. In the case of 27 day variations, diurnal variations, and the eleven year periodicity, it has not been possible to identify the solar feature most closely linked to the cosmic ray phenomenon. This is at least partly due to the correlation between the various types of solar activity.

The time delay between the occurrence of the solar and the cosmic ray event indicates the nature of the solar-terrestrial link. Thus in the case of the solar flare effect, the delay is of the order of 10 to 20 minutes, indicative of a radiation travelling at, or close to, the speed of light. The 24 to 48 hour delay in the case of the Forbush decrease suggests that a depressive mechanism is established in the vicinity of the earth by slowly moving solar matter ejected by the flare.

The rate at which the intensity changes imposes restrictions

upon the type of mechanism which may be acting. The duration of the event, when compared with the periods of axial rotation of the earth and sun, and the period of orbital motion of the earth, imposes limits upon the spatial extent of the mechanism.

In the following sections, an attempt will be made to exploit some of these techniques in the study of short term variations.

8.2 Classification of short term events

In Chapter 6 the cosmic ray variations of 3 to 30 days duration were classified as short term variations. An examination of hourly intensities reveals that there are two distinct types of short term variation, examples being given in Fig. 15. The obvious properties of the two classes are summarised below.

Forbush Decreases. Fig. 15A.

(1) The intensity decreases suddenly, minimum intensity occurring within24 to 48 hours of the onset. The greater part of the decreasing phase usually occupies a period of from 3 to 12 hours duration.

(2) The intensity slowly returns to near the pre-event value. The rate of change of intensity during this phase is considerably less than that during the intensity decrease.

(3) The effect is world wide, although there may be very considerable differences in the time variations at different points on the earth during the period of decreasing intensity. (See Chapter 9).

The Symmetrical Decrease. Fig. 15B

(1) The intensity decreases slowly, minimum being reached after about 3 to 4 days. There is no sudden onset.

(2) The intensity may remain near the minimum value for a day or two.

(3) There is a slow recovery to the pre-event intensity, the

Figure 15 - Examples of short term variations in the cosmic ray intensity. Four hourly totals of the pressure corrected Mt. Wellington counting rate are plotted. Standard deviations are shown. The lines have been drawn by eye to emphasise the properties of the events. Times are measured on the universal time scale.

Figure 15A - A Forbush decrease

Figure 15B - A symmetrical decrease

Figure 15C - A Forbush decrease superposed upon a symmetrical decrease.

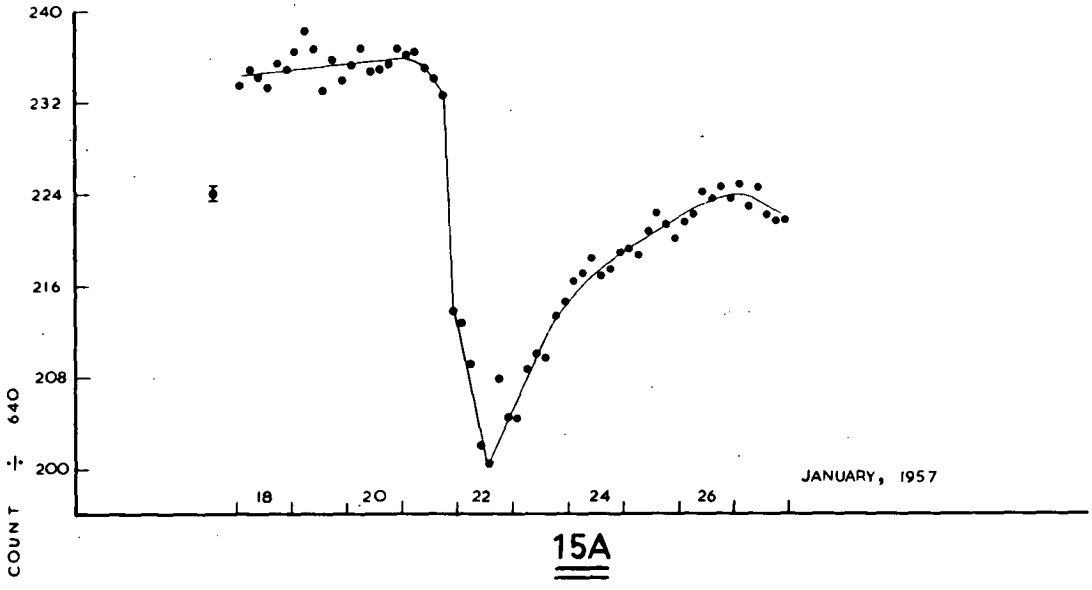
240
232
224
216
208
200
COUNT ÷ 640
18
20
22
24
26
JANUARY, 1957

15A

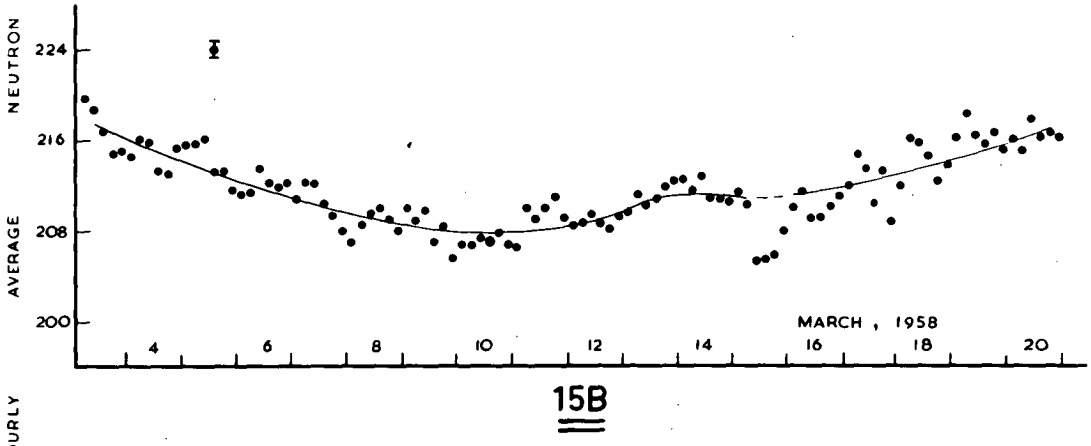
NEUTRON
AVERAGE
224
216
208
200
4
6
8
10
12
14
16
18
20
MARCH , 1958

15B

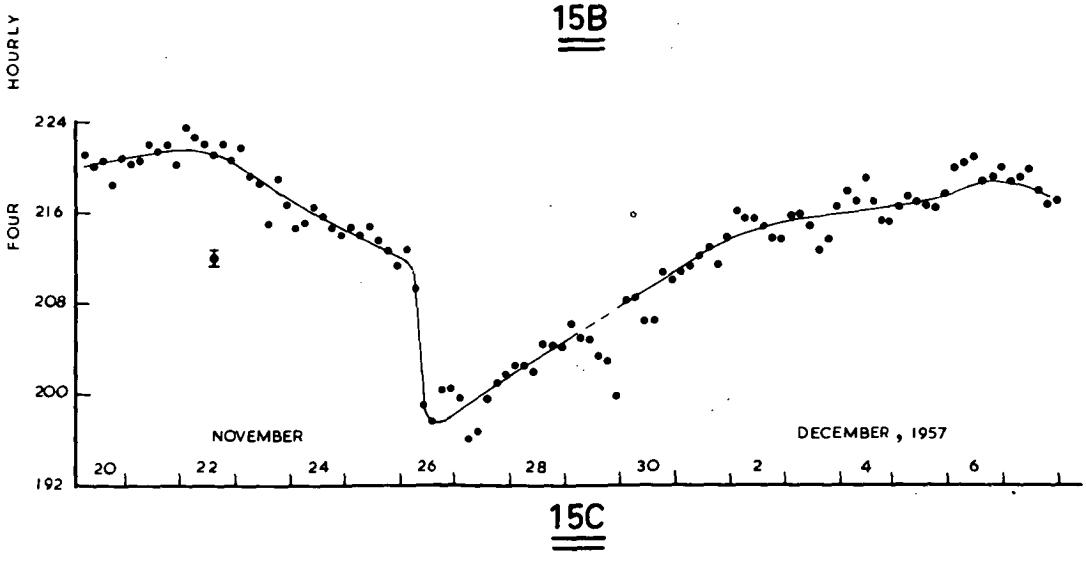
HOURLY
FOUR
224
216
208
200
192
NOVEMBER
DECEMBER , 1957
20
22
24
26
28
30
2
4
6

15C

rate of change of intensity being about the same as that during the decreasing intensity phase.

(4) The effect is world wide.

It is clear that the behaviour during the decreasing intensity phase typifies the event.

The view is taken here that the symmetrical events are recurrent intensity decreases, as against the alternative possibilities of recurrent increases or modulation of the mean level. This view is supported by the results of VAN HEERDEN and THAMBYAHPILLAI (1955), and of VENKATESAN (1958). Further, consider the period October-December, 1957, during which three Forbush decreases and three symmetrical events occurred (Fig. 16A). This period is shown more clearly in Fig. 10A. In this latter figure, all the black points lie very close to a single straight line, suggesting that they represent the "undisturbed" cosmic ray intensity, the Forbush decreases and symmetrical events being depressions below this undisturbed value. This view is further supported by the results reported in this chapter, for it is shown that the correlations of disturbance of the geomagnetic field with (1) Forbush decreases, and (2) symmetrical events show considerable similarities, suggesting that both types of event are produced by similar mechanisms.

The superposition of events

Some events appear to exhibit the characteristics of both classes of variation. Thus the event shown in Fig. 15C had

(1) an initial phase, during which the intensity decreased slowly,

(2) a phase during which the intensity decreased suddenly, the intensity-time relations at Mawson and Mt. Wellington being markedly different, and

(3) a gradual recovery to pre-event intensity.

It is proposed that this type of event is due to the superposition of a Forbush and a symmetrical decrease.

8.3 The recurrence of symmetrical events and the duration of Forbush decreases

The hourly intensities for the two periods 20 October, 1956 - 30 March, 1957 and 1 October, 1957 - 31 May, 1958 were examined, and the variations classified. The class to which each variation was assigned is shown in Fig. 16. Where it appeared that a Forbush decrease and a symmetrical decrease were superposed, an estimate of the contribution made by each type of variation was made. These estimates should be satisfactory, as in most cases at least half of the symmetrical event was clearly distinguishable from the Forbush decrease.

For each symmetrical decrease the day of commencement, the day of minimum intensity, and the day of cessation were determined as defined in Fig. 16C. For the 1957/58 period these days were well defined, and should not be in error by more than $\pm$ 1 day. Likewise, the day of cessation of each Forbush decrease was determined, and the duration of the event defined as shown in Fig. 16C.

The duration of each Forbush decrease, and the days of minimum intensity of the symmetrical decreases are indicated in Fig. 16A and B. Two results are apparent.

(1) The symmetrical decreases exhibit a quasi-periodicity. The period is roughly 26 days.

(2) The Forbush decreases had ceased within 10 days of onset.

In connection with the latter statement, Table 8A compares the amplitude and duration of a number of isolated Forbush decreases. The amplitude of the event was taken as the difference between the minimum value of the daily mean intensity and the mean for the day prior to the event. A number of events have not been included in

Figures 16A and 16B - Illustrating the classification of short term cosmic ray variations into Forbush decreases (solid black) and symmetrical decreases (shaded). The classification is based upon the time variations evident in the hourly data. The intervals between adjacent days of minimum intensity (see Fig. 16C), and the durations of the Forbush decreases are given in days.

Figure 16C - Definition of the days of commencement, cessation and minimum intensity of a symmetrical decrease, and of the duration of a Forbush decrease. Daily means are plotted.

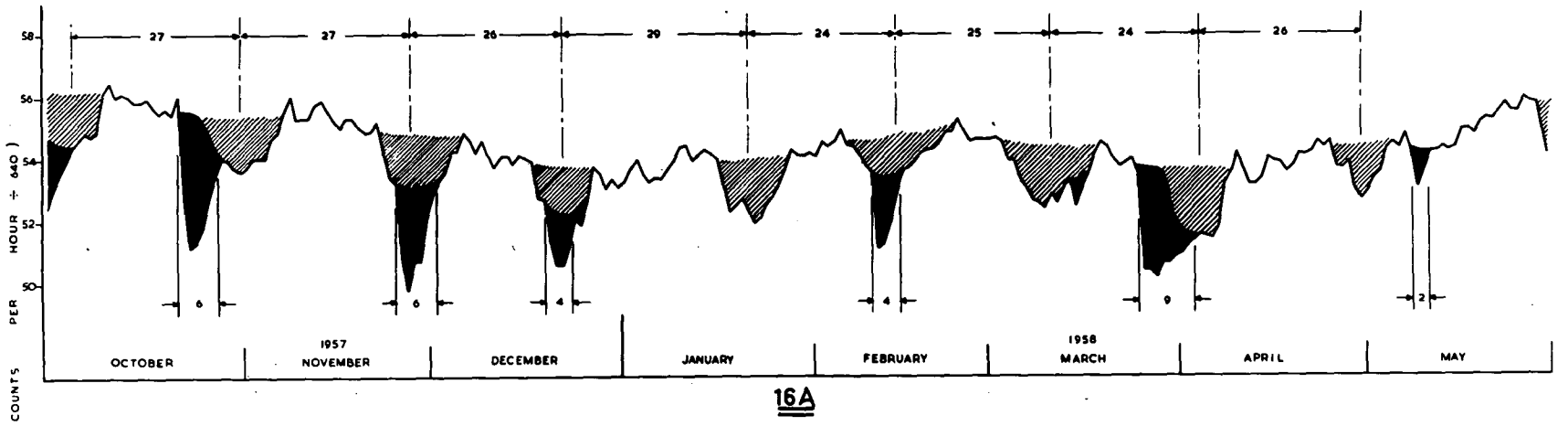
(COUNTS PER HOUR ÷ 640)
58
56
54
52
50
27
27
26
29
24
25
24
26
6
6
4
4
9
2
OCTOBER
1957
NOVEMBER
DECEMBER
JANUARY
FEBRUARY
1958
MARCH
APRIL
MAY

16A

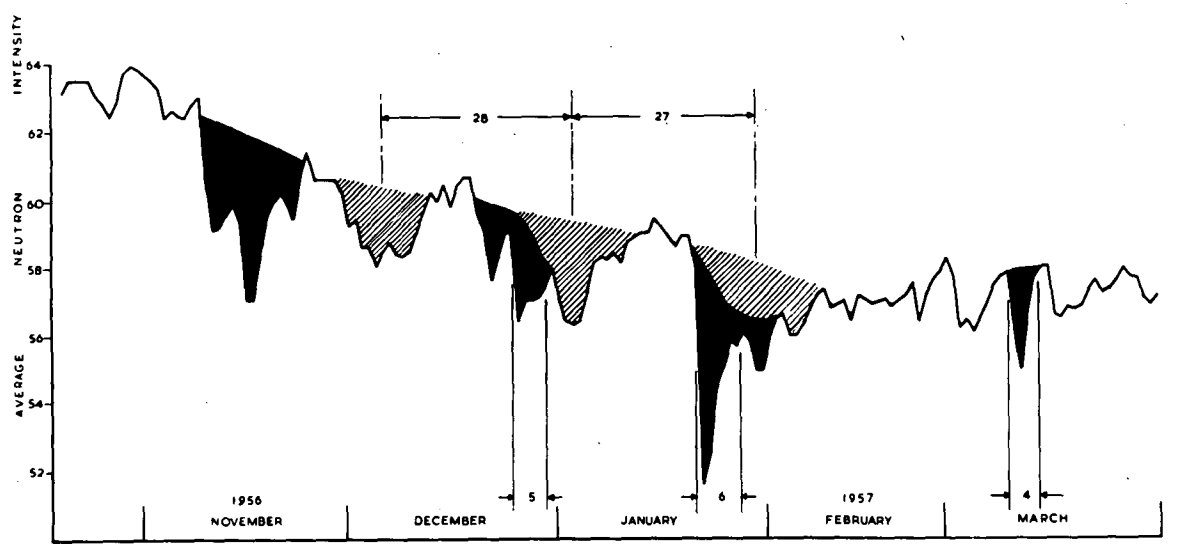
AVERAGE NEUTRON INTENSITY
64
62
60
58
56
54
52
28
27
5
6
4
1956
NOVEMBER
DECEMBER
JANUARY
1957
FEBRUARY
MARCH

16 B

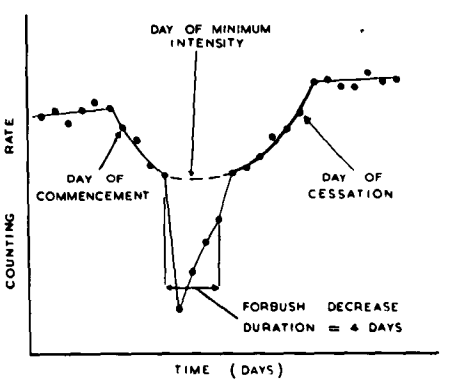
DAY OF MINIMUM INTENSITY
DAY OF COMMENCEMENT
DAY OF CESSATION
FORBUSH DECREASE
DURATION = 4 DAYS
COUNTING RATE
TIME (DAYS)

16C

Table 8A as inspection of the hourly records indicated that two or more Forbush decreases were superposed. For example, while the event commencing on 29 August, 1957 appeared to last 18 days (see Fig. 9A), closer inspection revealed that further Forbush decreases occurred on the 2nd September and the 13th September.

TABLE 8A

Comparison of the amplitude and duration of a number of isolated Forbush decreases.

Date of Commencement	2 Sept '56	25 Dec '56	20 Jan '57	29 Jan '57	10 Mar '57	21 Oct '57	26 Nov '57	19 Dec '57	11 Feb '58	25 Mar '58	9 May '58	8 July '58
Amplitude (%)	5	4	11	2	5	9	7	4	5	6	2	6
Duration (days)	4	5	6	2	4	6	6	4	4	9	2	4

Event duration is plotted against event amplitude in Fig. 17A. It is clear that the two quantities are related, event duration increasing as event amplitude increases.

8.4 Magnetic disturbance accompanying symmetrical decreases

An analysis was carried out to determine whether any features of the symmetrical decreases were correlated with geomagnetic disturbance. Calling the days of commencement of the symmetrical decreases the zero days, and numbering the days before and after the zero days -1, -2, ... and +1, +2, etc, the mean value of ΣKp for each of the days from -5 to +5 was determined. As Forbush decreases are usually accompanied by enhanced magnetic disturbance, only those zero days which were at least three days away from the commencement of a Forbush decrease were included in the analysis. Similar analyses were performed using the days of minimum intensity and the days of cessation as the zero days. In Fig. 17B,C, and D, mean ΣKp is plotted as a function of day number. Table 8B lists the zero days

Figure 17A - The relation between the amplitude and the duration of Forbush decreases. The relation between the amplitude and recovery time of symmetrical decreases is indicated by the point within the circle.

Figures 17B, 17C and 17D - The average manner in which geomagnetic disturbance varies during symmetrical decreases. In Figure 17B the days of commencement of the symmetrical decreases are taken as the zero days, while in 17C the days of minimum intensity, and in 17D the days of cessation are the zero days.

Figure 17E - Bartels diagram of geomagnetic activity for the period 10 Oct 1957 - 9 June 1958. The symbols used are:- white square, C_p = 0.0 to 0.3; small circle, C_p = 0.4 to 0.7; large circle, C_p = 0.8 to 1.0; black square, $C_p > 1.0$. C_p is the daily geomagnetic character figure.

Figure 17F - Bartels diagram of days of decreasing cosmic ray intensity. A decrease identified as part of a symmetrical decrease is shown as a black square, while a Forbush decrease is shown as a white box.

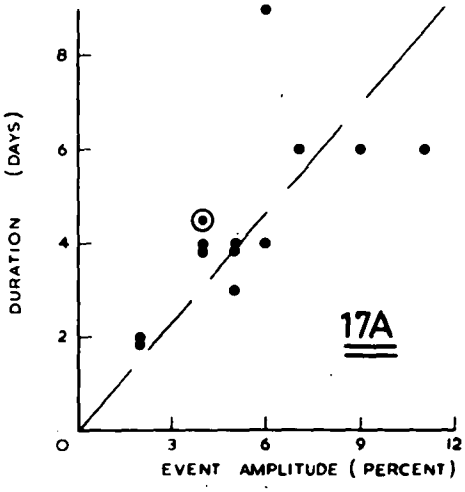
DURATION (DAYS)
EVENT AMPLITUDE (PERCENT)
17A

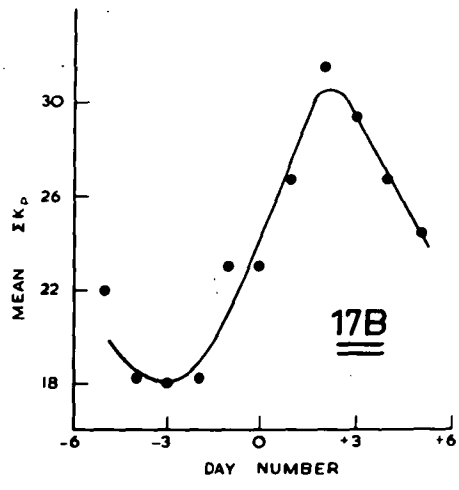
MEAN ΣKp
DAY NUMBER
17B

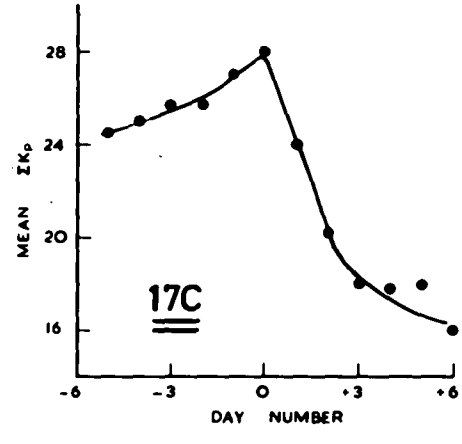
MEAN ΣKp
DAY NUMBER
17C

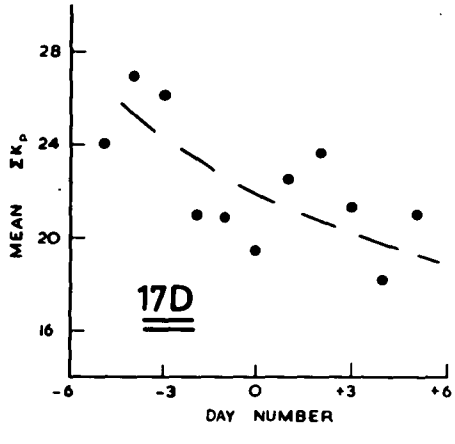
MEAN ΣKp
DAY NUMBER
17D

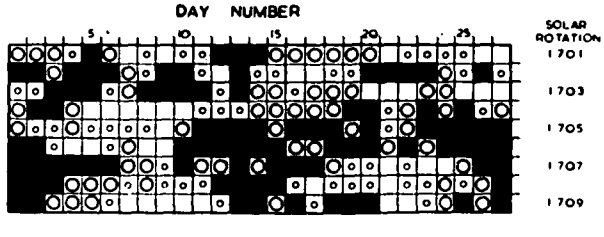
DAY NUMBER
SOLAR ROTATION
1701
1703
1705
1707
1709

17E

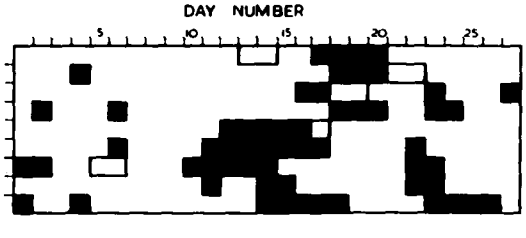
DAY NUMBER

17F

used in these analyses.

TABLE 8B

Zero days used in the derivation of Figs. 17B, 17C and 17D.

Days of Commencement	Days of Minimum Intensity	Days of Cessation
23 Nov, 1957	4 Oct, 1957	8 Oct, 1957
16 Jan, 1958	30 Oct, 1957	6 Nov, 1957
6 Feb, 1958	21 Jan, 1958	27 Jan, 1958
4 Mar, 1958	10 Mar, 1958	21 Feb, 1958
26 Apr, 1958	4 Apr, 1958	18 Mar, 1958
	30 Apr, 1958	8 Apr, 1958
		3 May, 1958

Remembering that there may have been an error of $\pm$ 1 day in assigning the zero days, the following conclusions can be reached about the average behaviour of the events considered.

(1) The commencement of a symmetrical decrease was accompanied by a marked enhancement of magnetic disturbance. This enhancement almost certainly occurred on, or the day before, the cosmic ray intensity commenced to decrease.

(2) The geomagnetic field was still disturbed on the day of minimum cosmic ray intensity, but became much quieter a day or two later. As the symmetrical events took from 4 to 7 days to recover to the pre-event intensity, the majority of the recovery took place after the decrease in geomagnetic disturbance.

(3) There was no marked correlation between geomagnetic disturbance and the cessation of the symmetrical events. A gradual decrease in geomagnetic disturbance which occurred about 3 to 4 days before cessation is consistent with conclusion 2.

To check whether the above conclusions applied to each symmetrical event, the mean ΣKp for days -4, -3 and -2 with respect to each day of commencement was compared with that for days +2, +3 and +4. Likewise, the mean for days -2, -1 and 0 with respect to the day of minimum intensity was compared with that for day +3, +4 and +5. In every one of the eleven comparisons the relation was as found before.

Moderate enhancement of magnetic disturbance often displays a quasi-periodicity of twenty-seven days. The recurrence of symmetrical decreases after about 26 days suggests that they may accompany recurrent geomagnetic storms. To check this, a Bartels diagram of geomagnetic activity (CHAPMAN and BARTELS, 1951, p.407) was prepared (Fig. 17E). A similar diagram was prepared showing those days on which the cosmic ray intensity was decreasing at both Mawson and Hobart (Fig. 17F). Forbush decreases are shown as white boxes, and symmetrical decreases as black boxes. Comparison of Figs. 17E and F indicates that:

(1) There were well defined periodicities in both the magnetic and the cosmic ray data;

(2) For solar rotations 1705-1709, there were recurring magnetic and cosmic ray events starting between days eleven and fourteen;

(3) For rotations 1706-1709, there was a recurring cosmic ray decrease about day 22. The decrease in neutron intensity was quite small ($<$ 2 percent). Close inspection reveals that the magnetic elements were mildly disturbed about this day. A recurrence of intense magnetic disturbance, some 3 to 4 days later, was not accompanied by any marked depression in cosmic ray intensity;

(4) For rotations 1701-1704, there was a marked cosmic ray recurrence starting near day 18. There was no well defined recurrence of magnetic activity about this time, although in all cases the magnetic elements were disturbed.

Thus it can be seen that while the onset of a symmetrical decrease is usually accompanied by an enhancement in magnetic storminess, there is not a one to one correspondence between the two phenomena. Thus a well defined cosmic ray recurrence may be accompanied by a recurrence of either marked or weak geomagnetic disturbance, and well defined magnetic recurrences are not necessarily accompanied by any noticeable cosmic ray effect.

8.5 The duration of the increasing intensity phase of a symmetrical decrease

During each of the symmetrical decreases used in the derivation of Fig. 17C (see Table 8B), the neutron intensity decreased by approximately 4 percent. For each of these events, the time interval between the day of minimum intensity and the day of cessation was obtained. The mean interval was 6 days. Fig. 17C shows that magnetic storminess ceases about one to two days after the day of minimum intensity, thus the symmetrical decrease persists for 4 to 5 days after the cessation of magnetic storminess.

It should be noted that this dependence of recovery time upon event amplitude is in good agreement with the trend found for Forbush decreases (Fig. 17A).

8.6 The two types of magnetic activity

There are apparently two classes of magnetic disturbance. One class has the following characteristics (a) the storms are intense, (b) they are associated with sunspots, (c) they have sudden commencements, (d) they occur a day or two after a solar flare, (e) they show no 27 day recurrence. The storms of the other class (a) are not intense, (b) are not associated with sunspots, (c) the majority start gradually, (d) they are not associated with individual solar flares, (e) they tend to recur after 27 days. It would appear that there is a fundamental difference between the two types of storm.

Extensive examination of the magnetic data obtained over a period of many years has lead to the postulate that intense, non-recurrent magnetic storms are initiated by the arrival of solar matter in the vicinity of the earth. This solar matter is believed to have been ejected by the large solar flares which have been observed 24 to 48 hours before many of the most intense storms (ALLEN, 1944). In recent years, direct evidence that protons impinge on the earth's atmosphere during aurorae has supported this theory (KIEPENHEUER, 1953, p.437).

In the case of the moderate, recurrent storms, it is generally believed that certain regions on the sun (the hypothetical M regions of Bartels) influence the geomagnetic field, the solar-terrestrial link being solar matter. The velocity of this matter is probably 2 to 3 times smaller than that responsible for the intense storms. The M regions apparently avoid sunspots, and the recurrent storms are not correlated with flare activity (ALLEN, 1944).

Thus while both types of storm are attributable to the arrival of solar matter at the earth, there must be two distinct methods by which the matter is ejected from the sun. In the case of intense, non-recurrent storms, ejection by a solar flare seems proven. As yet the ejection mechanism responsible for the recurrent storms has not been positively identified.

8.7 Discussion of the Forbush decrease mechanism

The following facts are known

(a) A Forbush decrease is often accompanied by an intense geomagnetic storm.

(b) Some Forbush decreases occur without there being any great enhancement of magnetic disturbance.

(c) Some intense magnetic storms occur without there being an accompanying Forbush decrease.

(d) In a number of cases, a large solar flare has been observed near the centre of the solar disc some 24 to 48 hours before the Forbush decrease.

(e) The magnetic effect subsides within 1 to 3 days, while the cosmic ray disturbance may still be appreciable 6 days after the event.

(f) Properties (b), (c) and (e), and the observation of Forbush decreases at latitudes well above the cosmic ray "knee", indicate that changes in the geomagnetic cut-off are not the cause of the cosmic ray effect (FONGER, 1953).

It seems certain from (a) and (c) that a solar flare can disturb the magnetic and cosmic ray conditions in the vicinity of the earth. As the magnetic and cosmic ray effects start at roughly the same time, the cloud of solar matter invoked to explain the magnetic storm probably sets up, or embodies the mechanism which depresses the cosmic ray intensity. By assuming that different properties of the cloud are responsible for the two effects, the properties (b) and (c) can be explained.

8.8 The mechanism responsible for symmetrical cosmic ray decreases

Many earlier investigators have reported a 27 day recurrence tendency in cosmic ray intensity. In the light of the recurrence tendency noted above for symmetrical decreases, the tentative conclusion is reached that symmetrical events are identical to the events called 27 day variations in the literature.

Many investigators have studied the correlation between 27 day cosmic ray variations and geomagnetic disturbance. The following summarises some of their results, all of which were obtained by averaging over a large number of events.

(1) SIMPSON (1954). Maximum cosmic ray intensity is most likely to precede maximum geomagnetic disturbance by about two days. Not all intensity decreases are accompanied by magnetic storms.

(2) BROXON (1942). Maximum cosmic ray intensity occurs one day after minimum geomagnetic disturbance. A marked increase in magnetic disturbance occurs one day after cosmic ray maximum. That is, the intensity starts to decrease on the day on which the geomagnetic field becomes disturbed.

Maximum magnetic disturbance precedes minimum cosmic ray intensity by one day. Magnetic disturbance falls off sharply about one day after cosmic ray minimum.

(3) FORBUSH (1954). Maxima of the cosmic ray 27 day variations tend to occur at about the time of minimum geomagnetic disturbance.

(4) KANE (1955). On some occasions, maximum cosmic ray intensity precedes maximum magnetic disturbance by about 3 days. Not every sequence of recurrent magnetic storms is accompanied by cosmic ray maxima.

(5) SIMPSON, BABCOCK and BABCOCK (1955). Maximum cosmic ray intensity is roughly coincident with C.M.P. (central meridian passage) of a long lived "unipolar" magnetic field on the surface of the sun. The cosmic ray intensity falls off sharply about the third day after C.M.P., while geomagnetic disturbance is a maximum four days after C.M.P.

All of these results are in good agreement with the result derived in section 8.4, namely, that the commencement of a symmetrical decrease is accompanied by an enhancement of geomagnetic disturbance, and that magnetic disturbance decreases 1 to 2 days after the minimum of cosmic ray intensity.

It will be noted that the absence of a one to one correspondence between recurrent geomagnetic and cosmic ray sequences is analogous to the absence of a one to one correspondence between

intense geomagnetic storms and Forbush decreases.

The following theory is now postulated. The streams of solar matter which are responsible for the recurrent magnetic storms set up the same type of mechanism in the vicinity of the earth as depresses the cosmic ray intensity during Forbush decreases. The efficiency of the solar streams in producing the cosmic ray and geomagnetic effects varies from stream to stream. In order to explain the persistence of the events after the cessation of magnetic disturbance, it is proposed that the mechanism is geocentric, and that, once set up, it remains in the vicinity of the earth, irrespective of whether or not the earth is still within a solar stream. It is assumed that the mechanism decays with time.

As long as solar matter continues to arrive at the earth the cosmic ray depressive mechanism continues to be built up. However, as the amount of matter arriving decreases, a time is reached when the rate at which the mechanism is decaying exceeds the rate at which it is being built up. Subsequent to this time the cosmic ray intensity increases. Thus minimum cosmic ray intensity occurs shortly before the cessation of magnetic disturbance (this being assumed to cease about the time solar matter ceases to arrive at the earth).

The following comments can be made in support of this theory:

(1) As the increasing intensity phases of both Forbush decreases and 27 day variations are interpreted as being due to the decay of the same type of mechanism, the relation between recovery time and amplitude should be the same for both types of event. This has been shown to be so. (section 8.5).

(2) The evidence (section 6.1) suggests that the spectral changes during Forbush and symmetrical decreases are similar, supporting the view that the mechanisms are similar.

(3) The results of SIMPSON, BABCOCK and BABCOCK (1955) indicate that UM regions may be the hypothetical M regions of Bartels. That is, recurrent geomagnetic storms, and now, the commencement of recurrent cosmic ray decreases may occur about three days after C.M.P. of U.M. regions.

(4) The present proposal is based upon data from a relatively short period. However, it is believed that considerable reliance can be placed in these data because (a) the recurring variations were well defined, (b) only one major cosmic ray recurrence was in progress, (c) high precision recorders were used, and (d) the results are not in conflict with those of other workers.

(5) While there is at present no conclusive evidence in favour of this proposal, the fact that Forbush decreases and 27 day variations can both be satisfactorily explained by a single mechanism is attractive. While a number of assumptions are still necessary (e.g. that some clouds are more effective than others in disturbing either the terrestrial cosmic ray or the geomagnetic conditions), these are common to both phenomena, whereas in the case of two separate mechanisms, two sets of assumptions are necessary.

The type of mechanism the author proposes is not new, elements of it having been suggested by VAN HEERDEN and THAMBYAHPILLAI (1955), NEHER and FORBUSH (1952) and BROWN (1958). Further development of the present theory may allow the fine details (diurnal variations, variation in amplitude of the 27 day recurrence during the solar cycle, etc) to be explained.

CHAPTER 9

THE COMMENCEMENT OF FORBUSH DECREASES

The early observations of Forbush decreases were made using relatively small meson detectors. For most events, the time of onset was consequently masked by statistical fluctuations, and as far as the early workers could tell, the onset occurred simultaneously all over the earth.

An examination of the results from the high counting rate equipment at Mawson, Hobart and Mt. Wellington indicated that on some occasions the times of onset of Forbush decreases differed by many hours, and furthermore, that the intensity variations during the first day were sometimes markedly different at different longitudes. Extending this study, the intensity distribution over the earth during the first few days of a number of Forbush decreases was determined.

It is emphasised that considerable care has been exercised to ensure accurate timing at all stations operated by the Hobart group. The chronometers are frequently checked against W.W.V., the difference being maintained at a value less than ± 2 minutes. Thus the hourly data from different stations are strictly comparable. In what follows, all times are measured in Universal time (U.T.), that is, the time scale appropriate to the meridian of Greenwich.

9.1 Comparison of Forbush decreases at Mawson and Mt. Wellington

In Figs. 18A and B are displayed the data obtained during two Forbush decreases. A number of differences are evident.

21 October, 1957. (Fig. 18A)

(a) Whereas the decrease started before 2300 U.T. at Mawson, it did not commence until after 0000 U.T. at Mt. Wellington and Hobart.

Figure 18A - The pressure corrected data obtained during the onset of the 21 October, 1957, Forbush decrease. Standard deviations are shown.

Figure 18B - The pressure corrected data obtained during the onset of the 26 November, 1957, Forbush decrease. Standard deviations are shown.

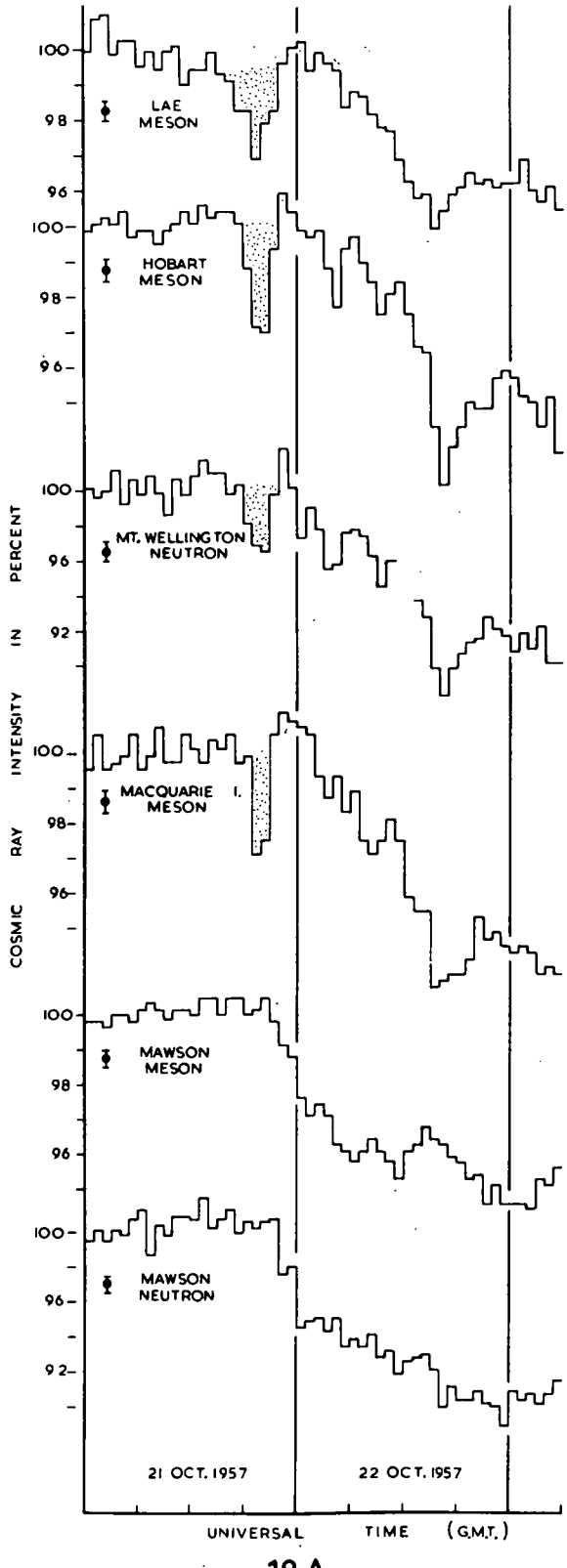
COSMIC RAY INTENSITY IN PERCENT
LAE MESON
HOBART MESON
MT. WELLINGTON NEUTRON
MACQUARIE I. MESON
MAWSON MESON
MAWSON NEUTRON
21 OCT. 1957
22 OCT. 1957
UNIVERSAL TIME (G.M.T.)

18 A

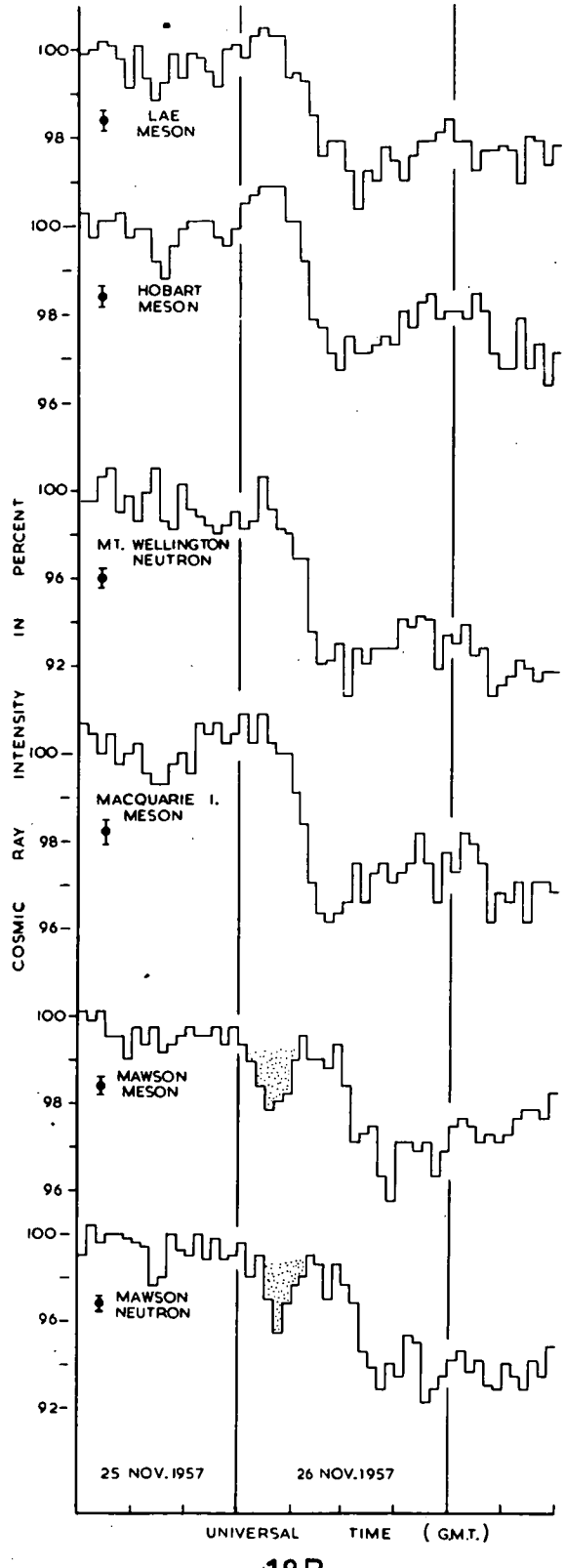
COSMIC RAY INTENSITY IN PERCENT
LAE MESON
HOBART MESON
MT. WELLINGTON NEUTRON
MACQUARIE I. MESON
MAWSON MESON
MAWSON NEUTRON
25 NOV. 1957
26 NOV. 1957
UNIVERSAL TIME (G.M.T.)

18 B

(b) The initial rate of change at Mawson (neutron, 2 percent/hour) was greater than that at Mt. Wellington (neutron, 0.7 percent/hour).

(c) At Mt. Wellington and Hobart, the main decrease was preceded some hours earlier by a sudden intensity depression and subsequent recovery. This feature, while not present in the Mawson records, was clearly defined in the Lae and Macquarie Island data (McCRACKEN and PARSONS, 1958).

26 November, 1957. (Fig. 18B)

(a) Whereas the decrease started before 0900 U.T. at Mt. Wellington and Hobart, it did not commence until after 1300 U.T. at Mawson.

(b) The initial rate of change at Mt. Wellington (neutron, >2 percent/hour) was greater than that at Mawson (neutron, 1.3 percent/hour).

(c) At Mawson, the main decrease was preceded some hours earlier by a short lived depression. This feature was not evident in the Mt. Wellington, Hobart or Lae data.

A similar behaviour was evident for the three other Forbush decreases occurring on the 20 Aug. 1956, 3 Aug. 1957 and 29 Sept. 1957. For brevity, both the Mt. Wellington neutron and the Hobart meson data are referred to as Hobart data. The following generalizations were possible.

(a) The event could start first at either Hobart or Mawson.

(b) On those occasions when there was a marked difference between the Hobart and Mawson data, the Lae and Macquarie Island data showed the same general features as the Hobart data. As Hobart, Lae and Macquarie Island are at approximately the same geomagnetic longitude, this suggests that it is the difference in longitude, and not the difference in latitude which is responsible for the difference

between the Hobart and Mawson variations.

(c) There might be a short lived decrease and subsequent recovery at either station. If so, it would be centred about 2000 U.T. at Hobart (3 cases), and about 0400 U.T. at Mawson (3 cases). If observed at Hobart, it was also observed at about the same time at Lae and Macquarie Island.

9.2 The time and directional dependence of the Forbush mechanism

At any instant, only those primary cosmic rays which come from certain directions may pass through the geomagnetic field and be detected by a recorder on the earth's surface. The major part of the counting rate of a cubical telescope or a neutron monitor is due to radiation arriving from directions within a solid angle small compared to 4π. Thus the counting rate at any time measures the primary intensity from within a relatively small solid angle. The solid angle rotates with the earth, thus the hourly counting rates from such a detector provide a survey of the intensity from various directions in space. This enables the efficiency of the Forbush mechanism in various directions to be determined when the assumption is made that the mechanism is sited outside the geomagnetic field.

Using data from one recorder, the intensity from any one direction is measured once every twenty-four hours. By using data from a number of recorders situated at different longitudes, a more frequent measurement of the intensity in any one direction is obtained. Thus the directional and time dependence of the efficiency of the Forbush mechanism can be surveyed.

For such a survey, two or three days data are required. As the atmospheric structure can change very considerably within this time, meson data may give inconsistent results. Neutron data do not suffer from this disadvantage. For the surveys reported here, the Mawson and Mt. Wellington data have been augmented by data from

Ottawa and Banff*.

Using published data on primary particle trajectories in the earth's magnetic field (BRUNBERG, 1953; BRUNBERG and DATTNER, 1953; JORY, 1956) and conventional geomagnetic co-ordinates, the directions from which particles in the energy range 2-100 Bev can reach the various monitors were determined. Taking into account the specific yield function and the calculated zenith angle dependence of a neutron monitor, the proportion of the counting rate as a function of asymptotic direction was determined for the Mt. Wellington and Mawson monitors (see Chapter 10). For example, it was found that the major part of the Mt. Wellington counting rate is due to radiation arriving from asymptotic directions between the geographic meridians 100° and 20° East of the Mt. Wellington geographic meridian, the direction for which the response is greatest being about 60° East.

TABLE 9A

The geographic longitude of the asymptotic direction of greatest response measured East of the geographic meridian through the observatory. The figures are for neutron monitors. See Chapter 10 for further details.

Observatory	Mt. Wellington	Mawson	Ottawa	Banff
Longitude	60°	05°	45°	35°

The direction of greatest response for each of the other monitors is given in Table 9A. Fig. 19A shows the directions of maximum response of the four instruments at 0000 hours U.T. It is clear that these observatories provide an almost continuous survey of the efficiency of the Forbush mechanism in all directions. A further improvement would be obtained if data from an observatory between Mt. Wellington and Mawson were available. It should be noted that whereas the direction of greatest response at Mt.Wellington

* Supplied by Dr. D. C. Rose of the National Research Council of Canada.

Figure 19A - Showing the directions of greatest response of four neutron monitors at 0000 U.T. The positions of the recorders themselves are also shown relative to the earth-sun line. The convention whereby directions are designated as being west or east of the earth-sun line is illustrated.

Figures 19B, 19C and 19D - Surveys of the directional and temporal dependence of intensity during three Forbush decreases. Direction is measured in terms of longitude east or west of the meridian containing the earth-sun line. Time is measured on the universal time scale. A black square indicates that the recorder whose direction of greatest response was in that direction at that time recorded a depressed intensity, while a circle indicates that the intensity was not significantly depressed. The contour lines were drawn by eye.

The letters along the right hand edges of the surveys indicate from which recorders the adjacent data were obtained. Thus M = Mawson, W = Mt. Wellington, B = Banff, O = Ottawa, C = Climax. The times at which sudden storm commencements occurred are indicated.

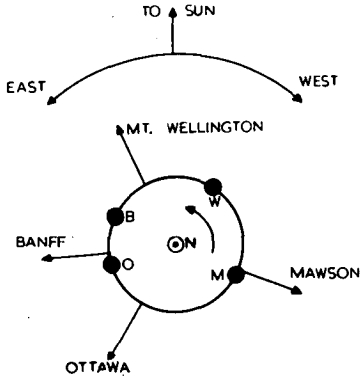

19A

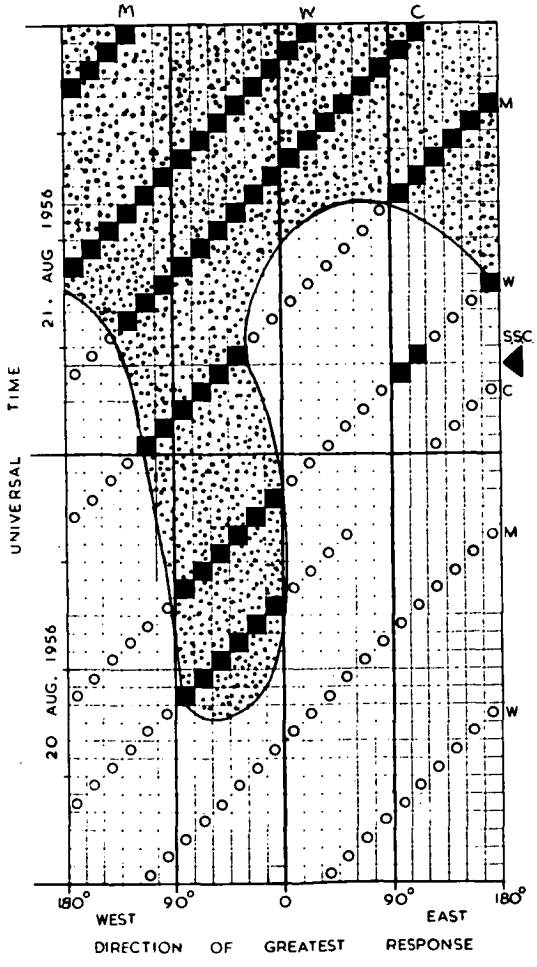

19B

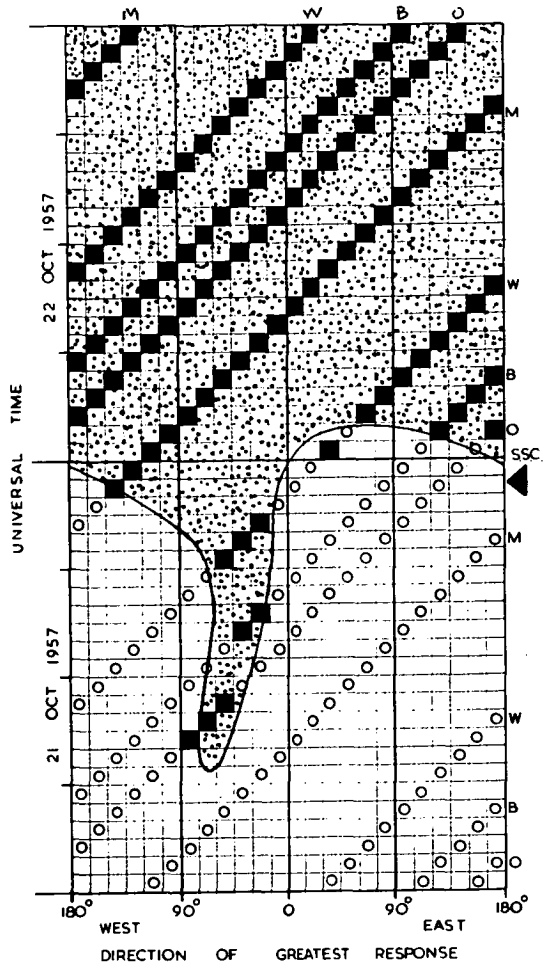

19C

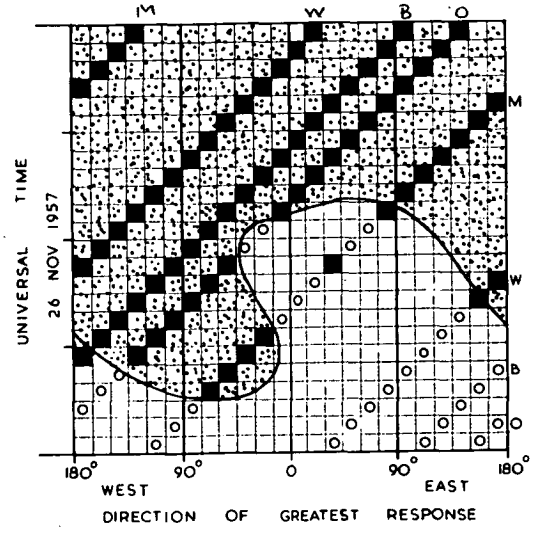

19D

is about 60° East of the Mt. Wellington geographic meridian, the direction of greatest response for the Mawson monitor is only about 5° East of the Mawson geographic meridian. Consequently, a direction of anisotropy in the primary radiation is observed by the two instruments at different local times.

In what follows, asymptotic directions will be specified as being east or west of the geographic meridian containing the earth-sun line. See, Fig. 19A.

Figures 19 B, C and D are surveys of the Forbush decreases which occurred on 20 Aug. 1956, 21 Oct. 1957 and 26 Nov. 1957. They were drawn up as follows. If the intensity at a station were depressed during an hour (depression below pre-event value ≥ 2 standard deviations), the square in the diagram in which the direction of greatest response lay during that hour was filled in with black. If the intensity were within 2 standard deviations of the pre-event level, a small circle was drawn in the square.

Four features are evident from the surveys.

(a) The surveys of the three events show the same general features.

(b) The onset of the decrease did not occur simultaneously in all directions.

(c) The intensity from the directions between the limits 0° - 120° West decreased first.

(d) The intensity from the directions between the limits 0° - 120° East was the last to decrease.

There being a consistent behaviour during the onset of these events, it was deemed worth while making more detailed surveys of the two 1957 events (these being both well defined and widely observed). These surveys are given in Fig. 20A and B. For each hour, the square containing the direction of greatest response of a recorder was marked with a symbol indicating the amplitude of the depression

Figures 20A and 20B - Detailed surveys of two Forbush decreases. The direction of greatest response of a recorder at a given time is marked with a symbol indicating the extent to which the intensity was depressed at that time. The symbols are:- cross = 2 to 4 percent depression; open circle = 4 to 6 percent depression; small solid circle = 6 to 8 percent depression; large solid circle = 8 to 10 percent depression; solid square = 10 to 12 percent depression. Contour lines were drawn by eye.

Figure 20C - Idealised Forbush decrease model, showing the manner in which the depression of the intensity depends upon time and direction. The directions of greatest depression are indicated by dense dotting.

Figure 20D - Surveys of two great Forbush decreases. It should be noted that meson data are used in these surveys (Symbol H). The times at which sudden storm commencements occurred are indicated.

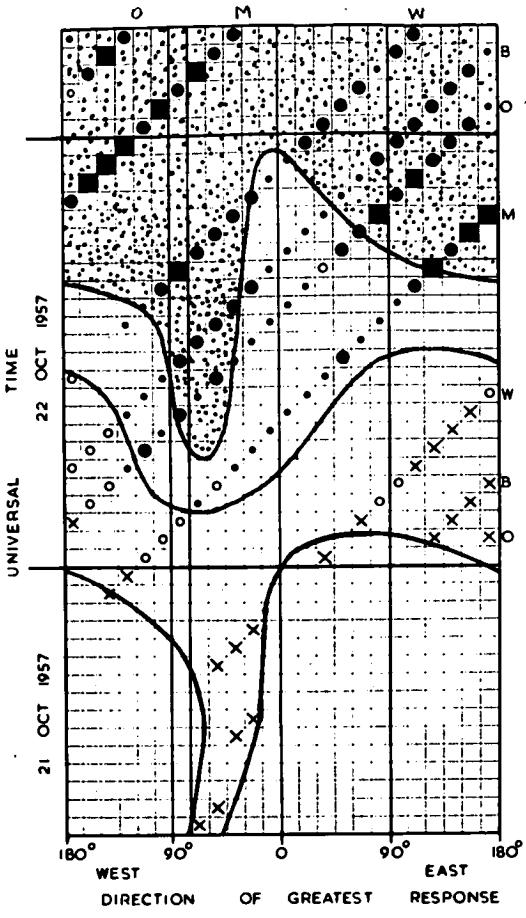

20A

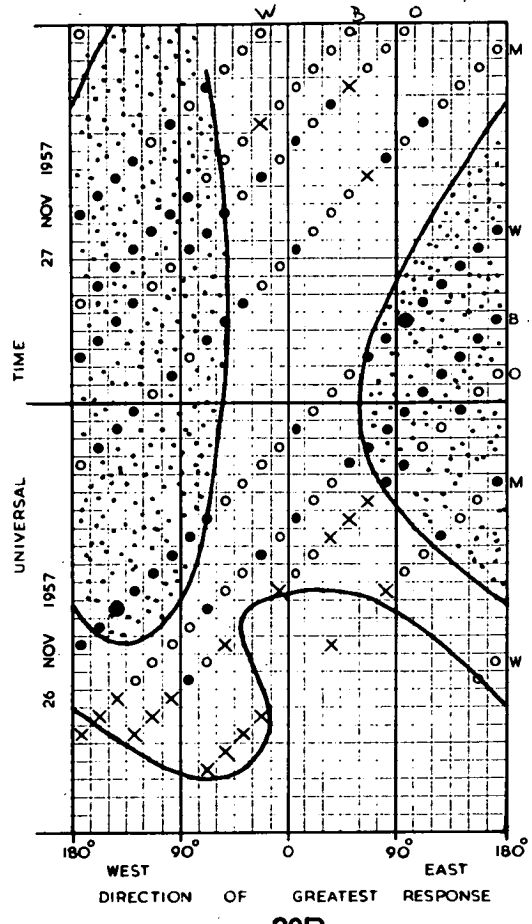

20B

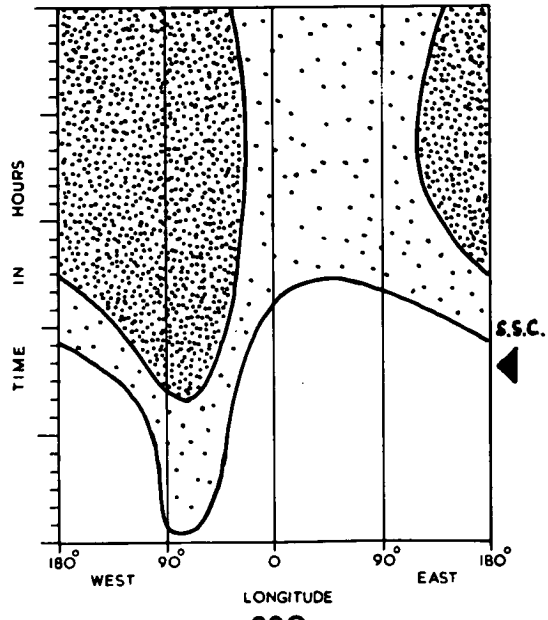

20C

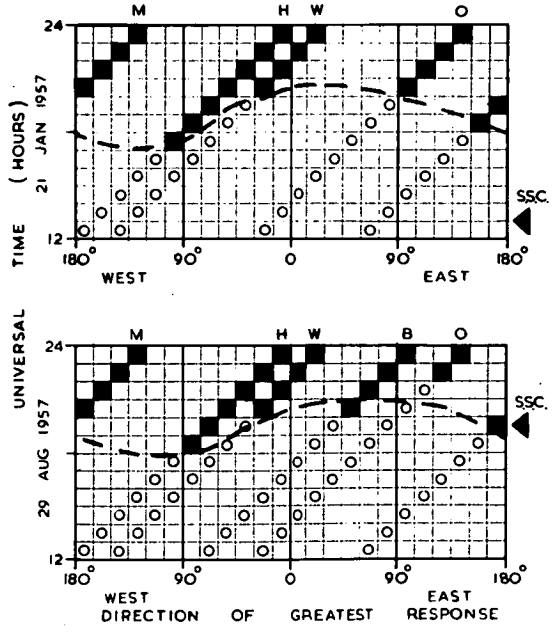

20D

observed during that hour*. A systematic behaviour is evident in the figures, the values of greatest depression avoiding the directions between 30°W and 90°E. Rough "contour lines" have been drawn to emphasise this trend. It is clear that for these two events, the intensity in the directions between 0° - 90°E was the last to be depressed, and that it suffered the least depression during the event. The intensity in the directions between 30°W and 120°W was the first to be depressed, and it suffered the greatest depression during the event.

On the basis of these two events, an idealised plot of depression against time and direction was prepared (Fig. 20C). This idealised model predicts the following features.

(a) Short lived depressions prior to the main Forbush decrease, when observed, will occur at a time characteristic of the observatory. These times are centred about:- Mt. Wellington, 1900-2100 U.T.; Mawson, 0400-0600 U.T.; Ottawa, 1100-1300 U.T.; Banff, 1400-1600 U.T.

(b) Fluctuations after the commencement of the main Forbush decrease will have maxima at a time characteristic of the observatory. These times are:- Mt. Wellington, 2200-0200 U.T.; Mawson, 0800-1200 U.T.; Ottawa, 1300-1700 U.T.; Banff, 1600-2000 U.T.

Table 9B compares these predicted values with those observed for four other well defined events. The agreement is quite good. It is concluded that the idealised model adequately describes the fine details of at least six Forbush decreases.

---

* It has been shown that the neutron variations at mountain altitudes are greater than those at sea level (section 6.2). Consequently the Banff percentage variations were reduced by 20 percent to make them more comparable with the other data.

TABLE 9B

Comparison of the times of occurrence of prominent features of Forbush decreases with those predicted by the idealised model. The tabulated values are Universal times (in hours). Some Climax data are used when Ottawa data not available. Mt. Well = Mt. Wellington.

Feature / Event	Short lived decrease prior to the Forbush decrease			Maximum of intensity fluctuations after the onset of the Forbush decrease		
Date of Commencement	Mt. Well	Mawson	Climax	Mt. Well	Mawson	Ottawa
20 Aug, 56	17-20	01-06 (meson)	12-16	00-05	07-16 (meson)	14-19 (climax)
10 Mar, 57	-	-	-	20-01	05-12	14-17
3 Aug, 57	-	03-10	-	20-04	11-14 not defined	
29 Sept, 57	-	01-06	-	23-04	08-14	09-15
Predicted central values	19-21	04-06	11-13	22-02	08-12	13-17

The 21 Jan 1957 and 29 Sept 1957 events

These two events were notable in that the intensity decrease at all observatories was very sudden, and in excess of 10 percent (neutron). There were slight differences in onset time. (Table 9C). There were no short lived decreases prior to the main event, and the fluctuations subsequent to the decrease were small*.

* This was not strictly true during one event at high southern latitudes. At Mawson and the Japanese antarctic base, Syowa, there was a very marked intensity maximum late on the 22 Jan. 1957. (KODAMA and MIYAZAKI, 1957). A small maximum occurred at Mt. Wellington at the same time. No such increase was observed anywhere else in the world. (Not even at Resolute, a station at a high northern latitude). This is the only example of this type of event occurring during more than two years of marked cosmic ray disturbance, and it is suggested that it is another, unrelated phenomenon.

TABLE 9C

The onset times of two great Forbush decreases measured in Universal Time (in hours).

Event \ Detector	Hobart meson	Mt. Wellington neutron	Mawson	Ottawa neutron
21 Jan. 1957	18	21	19 (meson)	21
29 Aug. 1957	19	21	20 (neutron)	23

Figure 20D is the "survey" for these two events. Both events fit the dotted line, that is, the intensity from about 90° West of the earth-sun line was depressed some hours prior to that from the east of the earth-sun line. This is precisely the type of behaviour noted before, and so it is concluded that both of these events conform to the idealised model.

Six other Forbush decreases between August, 1956, and December, 1957, were studied. None of them were very well defined, and all that can be said is that they are not inconsistent with the idealised model.

It is concluded then, that many, if not all Forbush decreases exhibit the following features

(1) The onset does not occur simultaneously at all points on the earth.

(2) The intensity from directions between about 30° and 120° West of the earth-sun line is the first to be depressed.

(3) The intensity is depressed last from directions between about 0° and 90° East of the earth-sun line.

(4) The maximum intensity depression occurs round about 90° West of the earth-sun line.

9.3 Correlation with geomagnetic disturbance

The fact that the time of onset of a Forbush decrease is different for different directions in space is in distinct contrast to the simultaneity of magnetic storm sudden commencements (S.S.C.), these coinciding to within one minute at widely separated points on the earth's surface. The times of S.S.C. tabulated in the Journal of Geophysical Research were studied in conjunction with the cosmic ray data. The times of S.S.C. are indicated on the "surveys" given in Figs. 19B, 19C and 20D. From the study of fourteen Forbush decreases occurring during 1956-1957, the following generalizations were possible

(a) The S.S.C., if positively identified, occurred before the Forbush mechanism developed in directions to the east of the earth-sun line.

(b) On some occasions the intensity in the directions about 60° West of the earth-sun line was depressed many hours prior to the S.S.C. On other occasions, the intensity in this direction was depressed after the S.S.C.

A typical S.S.C. is represented on the idealised model, Fig. 20C.

9.4 Comparison with the quiet day diurnal variation

The idealised Forbush decrease model predicts intensity maxima at times characteristic of all points on the earth. At Mt. Wellington, this time is between 2200 and 0200 U.T. The average diurnal variation in the meson component at Hobart during 1956 and 1957 was found by my colleague Mr. N. R. Parsons to have a maximum at about 0200 U.T. Analysis of the 1957 neutron data from Mt. Wellington yielded a similar result. This suggests that the mechanism responsible for the quiet day diurnal variation is similar to that responsible for the intensity fluctuations during Forbush decreases.

As it is known that there is a continuous flow of matter from the sun (the so called solar "wind") (VAN DE HULST, 1953), it is plausible that this could set up a mechanism of the same general type as the Forbush mechanism developed by the matter from solar flares.

It is of course well known that the phase of the diurnal variation changes from day to day (FIROR et al, 1954). Examination of 15 months of Mt. Wellington neutron data revealed 23 days on which the diurnal variation was well defined (not counting days immediately after Forbush decreases). On six occasions the diurnal maximum occurred between 0000 and 0400 U.T., on eleven occasions between 0400 and 0800 U.T., and on six occasions between 0800 and 1200 U.T. No diurnal maxima occurred between 1200 and 2400 U.T. During this latter time the direction of greatest response of the neutron monitor changed from 150° West to 30° East, for the majority of which range the idealised Forbush decrease model predicts minimum intensity. Thus the variability of the diurnal variation does not destroy the agreement between the diurnal variation and the idealised Forbush decrease model.

9.5 Review of the literature

No comparisons of the times of commencement of Forbush decreases at different longitudes have been published.

A number of investigators have reported Forbush decreases which commenced prior to a magnetic S.S.C. (CHASSON, 1954; HOGG, 1941; DUPERIER and McCAIG, 1946; SIMPSON, 1954). All events except those reported by CHASSON led the S.S.C. by only a few hours, such a lead being understandable on the basis of the idealised model (Fig. 20C). No short lived depressions of intensity prior to the main Forbush event have been reported (except by McCRACKEN and PARSONS, 1958).

Two events reported by CHASSON are of considerable interest in that the intensity decreases occurred 2 days and 6 days before the sudden storm commencements. The idealised model cannot explain such

great advancements. It would appear doubtful, however, whether the geomagnetic and cosmic ray events were related, as the solar matter which is responsible for magnetic disturbances is believed to take from 1 to 3 days to reach the earth. Thus the cosmic ray intensity decreased before, or very soon after the solar matter left the sun. As Forbush decreases sometimes occur without any accompanying S.S.C. (SIMPSON, 1954), it is suggested that such may have been the case for the events in question.

9.6 Discussion

There is the possibility that the short lived depressions were not related to the main Forbush decrease. This does not seem likely as (a) no short lived depressions were observed by themselves; (b) the direction in which the intensity was depressed during a short lived depression was the same as that in which the depression was greatest during the main event, (c) some of the events showing no short lived depressions did show an early onset in the direction in which short lived depressions always occurred.

The differences in onset times could be explained if the mechanism which affects the terrestrial cosmic ray intensity occupies a large volume, and can act when at a distance from the earth. A cloud of matter approaching the earth would progressively fill up this volume, and the depression would therefore be evident in some directions before others. The cloud of solar matter would arrive at the earth when the volume was about half full. Thus, if the magnetic S.S.C. occurs at the same time as the solar matter arrives at the earth, the S.S.C. would lead the observation of the decrease at some points on the earth, and lag the observation at other points. Such time relations are observed.

Such a hypothesis is worthy of consideration. One problem is why the decrease always commences first in the direction about 60° West of the earth-sun line, suggesting that the cloud advances from

this direction, no matter where the flare occurs on the solar disc. Such might be the case if the path of the solar matter were curved. The probable presence of an ordered solar magnetic field with an intensity of the order of 2×10^{-5} gauss at the earth's orbit (PARKER, 1958) does make an explanation of this kind feasible if the solar cloud were not completely neutral. BEISER (1955) has suggested such a possibility in explaining the time lag between the C.M.P. of a sunspot group and the occurrence of a geomagnetic storm. However, his detailed mechanism cannot apply in the present case, for he proposes that the solar particles travel at a velocity of 10^{10} cm/sec. On the reasonable assumption that the solar matter is ejected in the solar flare which precedes a Forbush decrease, the velocity is in the vicinity of 10^{8} cm/sec, two orders of magnitude smaller than proposed by BEISER. A modification of his theory may be feasible.

On the basis of our present knowledge, the only way in which a cloud can decrease the cosmic ray intensity while at a distance from the earth is for it to be electrically polarised, so that radiation passing through it is decelerated. Ordered or tangled magnetic fields do not have the desired effect, if anything, the albedo from the front surface of the cloud will increase the terrestrial cosmic ray intensity. (MORRISON, 1956; DORMAN, 1957, p.447). There is a further consideration to be made in any "action at a distance" theory. On two occasions the intensity in the direction 60° West was depressed for about 15 hours before the S.S.C. (Figs. 19B, 19C). That is, the intensity was presumably first depressed when the cloud was still 5×10^{12} cm. away. It appears likely that there is a solar magnetic field of about 2×10^{-5} gauss at the earth. (PARKER, 1958). Suppose that a solar cloud has associated with it an electric field as shown in Fig. 21A. The radius of curvature of a 15 Bev proton in a magnetic field of 2×10^{-5} gauss is 2.5×10^{12} cm., so for any energies less than this the cone of radiation decelerated in the solar cloud will not reach the earth (Fig. 21A). Above about 15 Bev the decelerated radiation will arrive at the earth at an angle to the

Figure 21A - Showing that an ordered solar magnetic field and a decelerating electric field within a cloud of solar matter can result in a direction of reduced intensity while the cloud is still remote from the earth.

Figure 21B - The situation after the cloud envelopes the earth.

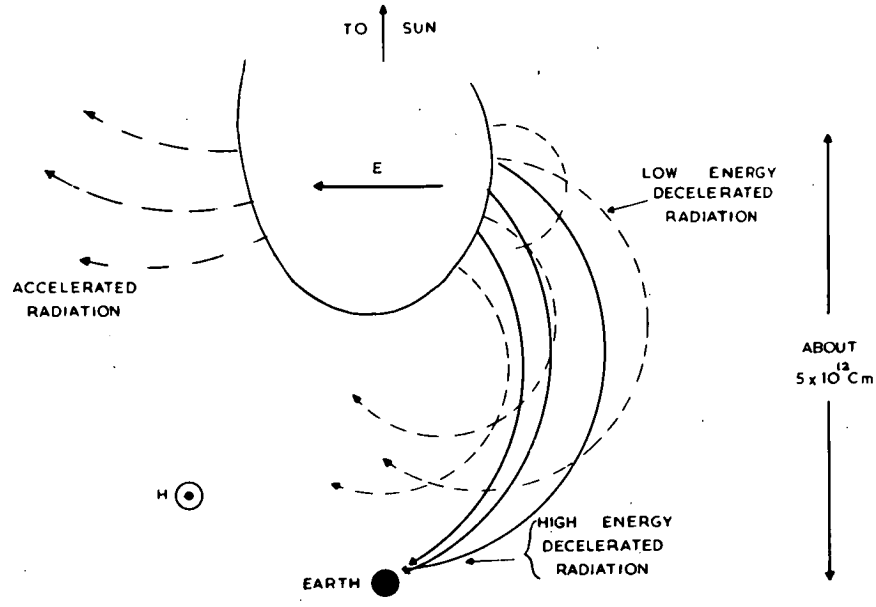
TO SUN
E
LOW ENERGY
DECELERATED
RADIATION
ACCELERATED
RADIATION
ABOUT
5 x 10^12 Cm
H
HIGH ENERGY
DECELERATED
RADIATION
EARTH

21A

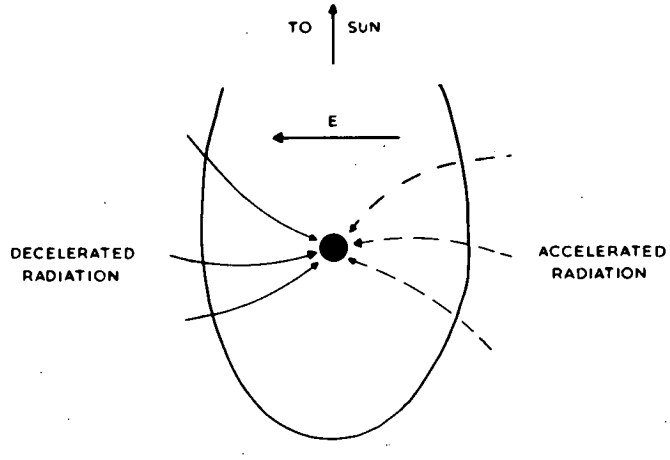
TO SUN
E
DECELERATED
RADIATION
ACCELERATED
RADIATION

21B

earth-sun line, and this could explain the observation of the preliminary depressions in directions West of the earth-sun line. (Fig. 21A). From the data presented by McCRACKEN and PARSONS (1958), (see Fig. 18A), it can be seen that the short lived decrease on the 21 Oct. 1957 had an amplitude in the meson component of 3 percent at both high and low latitudes. This supports the idea that the effect was confined to relatively high energies ($>$ 15 Bev). However, the idealised model presented in Fig. 21A encounters serious difficulties when the cloud envelopes the earth (Fig. 21B), for it then predicts that the intensity to the west of the earth-sun line should be greater than that from the east. This is contrary to observation.

Although the evidence presented in this chapter points to a mechanism capable of acting at a considerable distance, there are still very cogent reasons for proposing that the solar matter sets up a second, stationary mechanism close to the earth. If instead it is proposed that the only mechanism affecting the cosmic ray intensity is sited in the moving stream of solar matter, it is necessary that the stream continue to flow past the earth for as many as six days, whereas it is known that the magnetic storm accompanying a Forbush decrease usually subsides in a matter of from 1 to 3 days. It is proposed then that there are two separate mechanisms, one responsible for the highly directional onset phenomena, the other responsible for the main Forbush event.

It is emphasised that the aim of much of this thesis is to arrive at a satisfactory phenomenological description of terrestrial cosmic ray phenomena. Such a description should facilitate the development of a satisfactory theory as to the physical nature of the mechanisms controlling the cosmic ray intensity. The method of analysis presented in this chapter reveals a systematic behaviour during Forbush decreases, and leads to a tentative phenomenological model of this type of event. A critical test of the model will be possible when all the cosmic ray data accumulated during the International Geophysical Year are available.

CHAPTER 10

THE COUNTING RATES OF NEUTRON MONITORS AND MESON TELESCOPES AS FUNCTIONS OF ASYMPTOTIC LONGITUDE

In the previous chapter, evidence was presented that suggested that at least some of the mechanisms affecting the terrestrial cosmic radiation are sited at a considerable distance from the earth. In this chapter, the time variations produced by a directional anisotropy of the primary radiation outside the geomagnetic field are investigated. The predicted variations show considerable similarity to those actually observed.

10.1 The zenith angle dependence due to atmospheric absorption

Consider a small volume ∂v of the lead of a neutron monitor. The rate of production of stars in ∂v depends only upon the intensity of high energy neutrons passing through ∂v. Consider a beam of high energy neutrons incident upon the monitor at an angle of θ to the zenith, the intensity being independent of θ. As θ increases, the amount of material through which the neutrons pass before entering ∂v increases as $(\cos\theta)^{-1}$. As the high energy neutrons have a m.f.p. of 340 gm cm^{-2} in lead (TREIMAN and FONGER, 1952) the intensity of high energy neutrons passing through ∂v will fall off with increasing θ. Thus the counting rate of the monitor will fall off slowly.

If it is assumed that either (1) a neutron monitor will record the same counting rate irrespective of θ, or (2) the counting rate falls off as $\cos\theta$ (i.e., the counting rate is proportional to the area of the monitor projected in the plane perpendicular to the direction of incidence), the zenith angle dependence of counting rate can be easily derived. In practice, neither (1) nor (2) is correct, (1) probably being closer to the truth than (2). To make

the problem tractable, the zenith angle dependence will be calculated for the two cases (1) and (2), these providing upper and lower limits of the actual dependence.

Approximation 1

Let $I(x,\theta,\phi)$ be the neutron intensity in direction θ,ϕ at atmospheric depth x. The counting rate $dR(x,\theta,\phi)$ due to neutrons from within the solid angle dw in the direction θ,ϕ is given by

$$dR(x,\theta,\phi) = I(x,\theta,\phi)\,dw \qquad \text{(neglecting a multiplicative constant)}$$

Making the usual assumptions for the Gross transformation (JANOSSY, 1950, p.139, see note on page 45 of this thesis), and integrating, the total counting rate $R(x)$ at depth x is given by

$$R(x) = 2\pi \int_0^{\pi/2} I\left(\frac{x}{\cos\theta}, 0, 0\right) \sin\theta \; d\theta$$

and by substituting $\frac{x}{\cos\theta} = y$, and differentiating with respect to x, this yields the Gross transformation

$$2\pi\, I(x,0,0) = R(x) - x\,\frac{d\,R(x)}{dx}$$

In the lower atmosphere,

$$R(x) \approx R_o \exp\left(-\frac{x}{\lambda}\right) ; \quad R_o = \text{const}; \; \lambda = \text{const.}$$

so $$I(x,0,0) \approx \frac{R_o}{2\pi} \exp\left(-\frac{x}{\lambda}\right)\left\{1 + \frac{x}{\lambda}\right\}$$

Thus $$I(x,\theta,\phi) \approx \frac{R_o}{2\pi} \exp\left(-\frac{x}{\lambda\cos\theta}\right)\left\{1 + \frac{x}{\lambda\cos\theta}\right\}$$

Approximation 2

$$dR(x,\theta,\phi) = I(x,\theta,\phi) \cos\theta \quad dw$$

Making the same assumptions as in approximation 1, and integrating

$$R(x) = 2\pi \int_0^{\frac{\pi}{2}} I\left(\frac{x}{\cos\theta}, 0,0\right) \cos\theta \cdot \sin\theta \quad d\theta$$

and after taking the same steps as in approximation 1,

$$2\pi \; I(x,0,0) = 2R(x) - x \frac{d\,R(x)}{dx}$$

inserting $R(x) \approx R_o \exp\left(-\frac{x}{\lambda}\right)$

then $$I(x,\theta,\phi) \approx \frac{Ro}{2\pi} \exp\left(-\frac{x}{\lambda \cos\theta}\right) \left\{ 2 + \frac{x}{\lambda \cos\theta} \right\}$$

Taking $\lambda = 145$ gm cm^{-2}, $x = 1000$ gm cm^{-2}, $I(x,\theta,\phi)$ was calculated for both approximations. These functions were then integrated to give the total counting rate due to all neutrons arriving at the monitor making an angle of less than θ to the vertical. These functions are plotted in Fig. 22A. It is clear that over 95 percent of the counting rate is due to neutrons arriving at an angle of less than 45° to the vertical.

10.2 The effect of the geomagnetic field

Outside the geomagnetic field, let the primary differential rigidity spectrum be written $J(N)$. At the top of the atmosphere, the flux of particles of rigidity between N and $N + dN$ from within the solid angle $dw(\theta,\phi)$ in the direction (θ,ϕ) is $J(N).dN.dw(\theta,\phi)$ if (θ,ϕ) is an allowed direction, otherwise it is zero (Liouville's Theorem).

Figure 22A - The proportion of the counting rate of a neutron monitor which is due to neutrons arriving at zenith angles which are less than any given figure.

Figure 22B - The dependence of neutron counting rate upon asymptotic geographic longitude. Longitude is measured relative to the meridian through the observatory, being taken as positive towards the east.

Figure 22C - The calculated curves relating counting rate to asymptotic direction, and counting rate to time. Left hand and bottom scales The proportion of the total counting rate which comes from asymptotic geographic directions east of any given meridian. Longitude is measured relative to the meridian through the observatory. Right hand and top scales The time variations predicted when the intensity to the east of a given hour circle on the celestial sphere is assumed to be depressed by k percent at all rigidities. Time is measured relative to the time at which the meridian of the observatory coincides with the given hour circle.

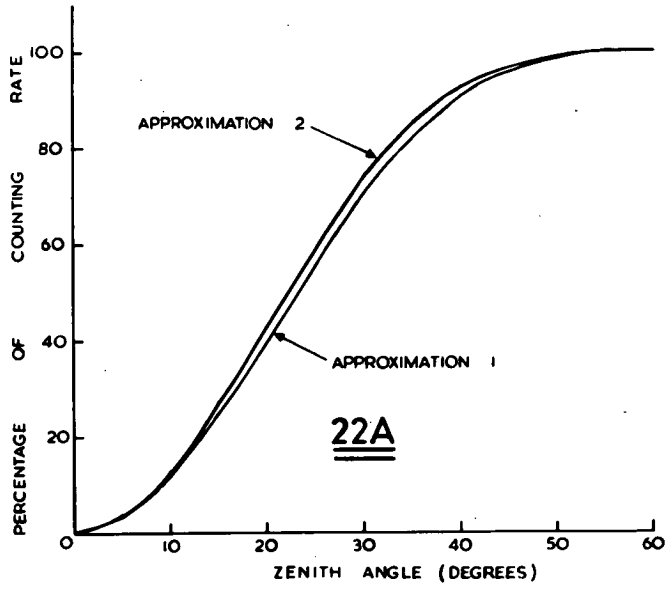
PERCENTAGE OF COUNTING RATE
APPROXIMATION 2
APPROXIMATION 1
ZENITH ANGLE (DEGREES)

22A

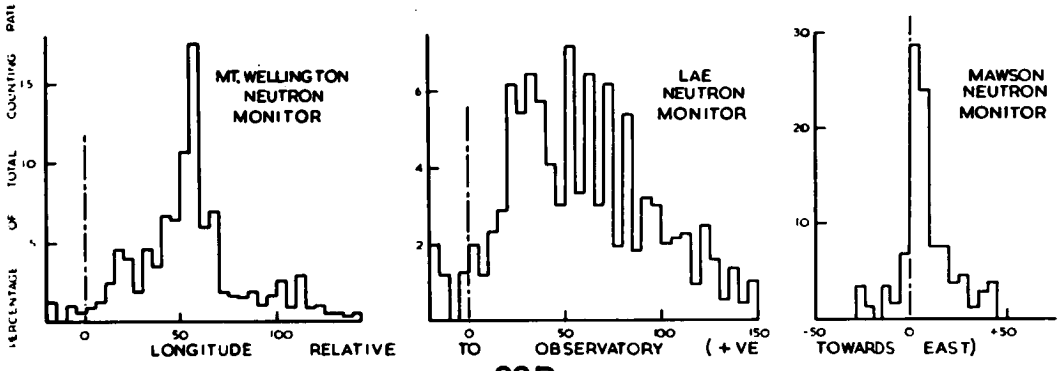
MT. WELLINGTON NEUTRON MONITOR
LAE NEUTRON MONITOR
MAWSON NEUTRON MONITOR
LONGITUDE RELATIVE TO OBSERVATORY (+VE TOWARDS EAST)

22B

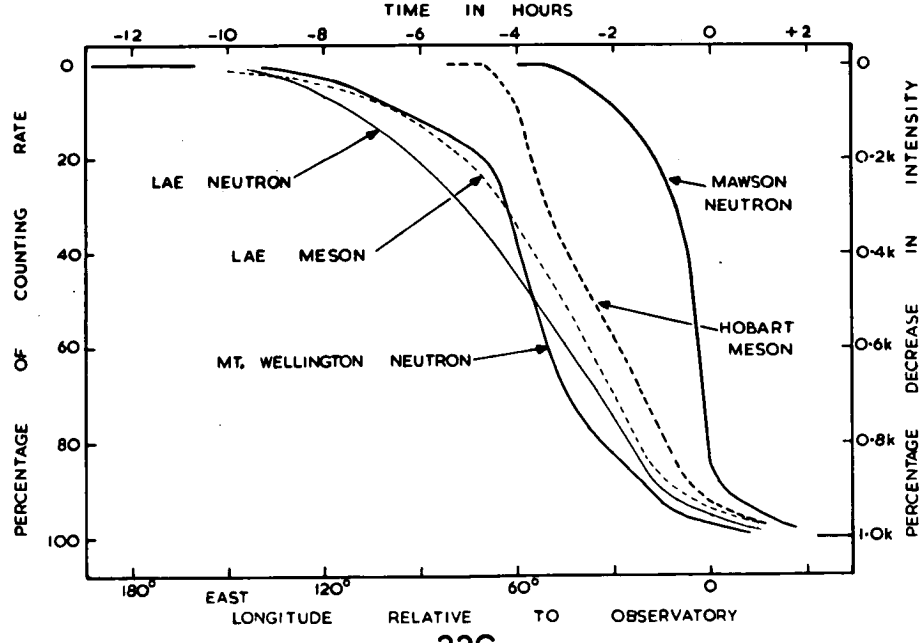
TIME IN HOURS
PERCENTAGE OF COUNTING RATE
PERCENTAGE DECREASE IN INTENSITY
LAE NEUTRON
LAE MESON
MT. WELLINGTON NEUTRON
MAWSON NEUTRON
HOBART MESON
EAST LONGITUDE RELATIVE TO OBSERVATORY

22C

At ground level, the counting rate due to this flux of particles from an allowed direction (θ,ϕ) is given by

$$dC(N,\theta,\phi) = J(N).T(N,\theta,\phi).dN \;.\; dw(\theta,\phi)$$

where $T(N,\theta,\phi)$ is a characteristic of the atmosphere. As a first approximation, assume that $T(N,\theta,\phi) = S(N).Z(\theta,\phi)$.

Then

$$dC(N,\theta,\phi) = J(N).S(N).dN.Z(\theta,\phi) \;.\; dw(\theta,\phi)$$

and the total counting rate

$$C = \int_0^\infty J(N).S(N).\left\{\int Z(\theta,\phi)\,dw(\theta,\phi)\right\}_N dN \cdots\cdots 10(1)$$

where $\left\{\int Z(\theta,\phi)\;dw(\theta,\phi)\right\}_N$ is the integral over all directions which are allowed for rigidity N.

Except for rigidities close to the cut-off, all the directions within the cone defined by a zenith angle of 45° are allowed. That is

$$C \approx \int_{\text{cut-off}}^\infty J(N).S(N).dN \int_{\theta=0^\circ}^{\theta=45^\circ} Z(\theta,\phi)\;\; dw(\theta,\phi) \cdots 10(2)$$

The justification for restricting zenith angles to $\theta < 45^\circ$ is the result in section 10.1, that only a small fraction of the counting rate is due to radiation arriving at $\theta > 45^\circ$. In section 10.1, the zenith angle dependence of the total counting rate was estimated, and from 10(2) it is seen that this is the distribution of

$$\int_0^{\theta_0} Z(\theta,\phi)\;dw(\theta,\phi) \quad \text{with} \quad \theta_0.$$

It was desired to calculate the counting rate due to radiation coming from asymptotic directions between any given limits. To do this, it was required to know for what solid angle $dw(\theta,\phi)$ at the top of the atmosphere and rigidity N the radiation from within these limits could reach the detector. A large number of cosmic ray orbits have been calculated for a pure dipole field. From some of the published data (BRUNBERG, 1953; BRUNBERG and DATTNER, 1953, JORY, 1956; LUST, 1957) the asymptotic directions of approach resulting in arrival at the top of the atmosphere with zenith angles of 0°, 16° and 32° in the N, S, E and W were determined. If a direction (θ_o, ϕ_o) at the top of the atmosphere were accessible from asymptotic directions falling within any given limits, it was assumed that the whole of the solid angle between the limits of $\theta = \theta_o \pm 8^\circ$; $\phi = \phi_o \pm 45^\circ$ was likewise accessible.

From Fig. 22A,

$$4 \int_{\theta=0}^{\theta=8^\circ} Z(\theta,\phi).dw(\theta,\phi) \approx \int_{\theta=8^\circ}^{\theta=24^\circ} Z(\theta,\phi).dw(\theta,\phi) \approx \int_{\theta=24^\circ}^{\theta=40^\circ} Z(\theta,\phi).dw(\theta,\phi)$$

and so $\int_{\theta_o-8^\circ}^{\theta_o+8^\circ} Z(\theta,\phi).dw(\theta,\phi)$ for $\theta_o = 16^\circ$ and 32°, and ϕ within the limits of $\phi_o \pm 45^\circ$ is approximately equal to $\int_{\theta=0}^{\theta=8^\circ} Z(\theta,\phi).dw(\theta,\phi)$. Thus if a direction (θ_o, ϕ_o) were accessible for N, then $\left\{\int Z(\theta,\phi).dw(\theta,\phi)\right\}_N$ between the limits of $\theta_o \pm 8^\circ$, $\phi_o \pm 45^\circ$ in 10(1) was set equal to one, while if not accessible, it was set equal to zero.

From the equation 10(2), it is seen that S(N) is

proportional to the specific yield function°(section 4.4). Using the specific yield function employed in section 7.2, and the proton spectrum found by KAPLON et al (1952), the integral 10(1) was calculated for all asymptotic directions within a geographic longitude range of 5^{o}. Repeating this for other non-overlapping ranges of 5^{o}, the dependence of counting rate upon asymptotic geographic longitude was found. These functions are plotted in Fig. 22B for the Mt. Wellington, Mawson and the Lae neutron monitors. Similar computations were performed for the meson telescopes at Hobart and Lae.

The proportion of the total counting rate due to radiation arriving from directions east of any given meridian was calculated. These functions are plotted in Fig. 22C. It can be seen that the Lae detectors and the Mt. Wellington neutron monitor "look" further to the east than does the Hobart meson telescope. Further, it is clear that the Mawson detectors respond to radiation whose asymptotic directions are closer to the geographic meridian through the observatory than in the cases of the Hobart, Mt. Wellington or Lae detectors. This results in the time lag between the observation of a direction of anisotropy at the latter stations and Mawson being greater than that expected from the rate of axial rotation of the earth. This increased time lag is actually observed in practice, the Mt. Wellington-Mawson time lag being observed to be about 7 to 8 hours, while the meridians through the observatories are only 83^{o} ($5\frac{1}{2}$ hours) apart.

Consider the case where the intensity to the east of a given hour circle on the celestial sphere is decreased by k percent at all rigidities. As the earth rotates, the counting rates of the various instruments vary as shown in Fig. 22C. The following general features are predicted:-

(1) The decrease is observed by the Hobart meson detector some hours after being first observed by the other detectors at the same longitude.

(2) At Mt. Wellington, the neutron intensity decreases

slowly at first, and then, at the same time as the Hobart meson intensity commences to decrease, it decreases suddenly.

(3) The decrease at Lae is gradual.

(4) The decrease occurs at Mawson at a time closer to the time at which the geographic meridian of the observatory crosses the given hour circle than in the cases of the other observatories.

In Fig. 23A, data obtained during an event which occurred on the 3 Sept. 1957 are compared with the theoretical curves. The general features (1) to (3) predicted in the preceding paragraph are evident.

In Fig. 23B are plotted the data obtained at the time of the short lived decrease on the 21 Oct. 1957. It has already been suggested that this event was due to a direction of reduced intensity in the general direction of 60° West of the earth-sun line (Chapter 9). Assuming that the intensity between the hour circles 60° and 30° West of the hour circle through the sun was depressed by k percent at all rigidities, the theoretical intensity against time curves in Fig. 23B were calculated. Once again the general features predicted earlier are evident. Although the depression was assumed to be the same at all rigidities, the events predicted for the different recorders have different amplitudes. This is a consequence of the fact that some of the detectors respond to radiation from a wider range of longitudes than do the others. The short lived decrease is predicted to have the following amplitudes:- Mt. Wellington neutron, 0.54k percent; Hobart meson, 0.50k percent; Lae meson 0.38k percent. Clearly the comparison of the amplitudes of this type of transient variation does not immediately provide a measure of the rigidity dependence of the variation.

It is concluded that the general features of at least some of the time variations which reach completion within a few hours at Lae and Hobart can be explained in terms of a direction of anisotropy

Figure 23A and 23B - Comparing observed intensity fluctuations with those predicted on the basis of a direction of anisotropy in the primary radiation. The standard deviations of the experimental data are given. It is assumed that for some directions, the intensity at all rigidities is depressed by k percent, the value of k giving the best fit to the experimental data being used in each comparison.

Figure 23A Intensity depressed in directions to the east of the meridian 120° East of the earth-sun line.

Figure 23B Intensity depressed in all directions between the limits of 60° West and 30° West of the earth-sun line.

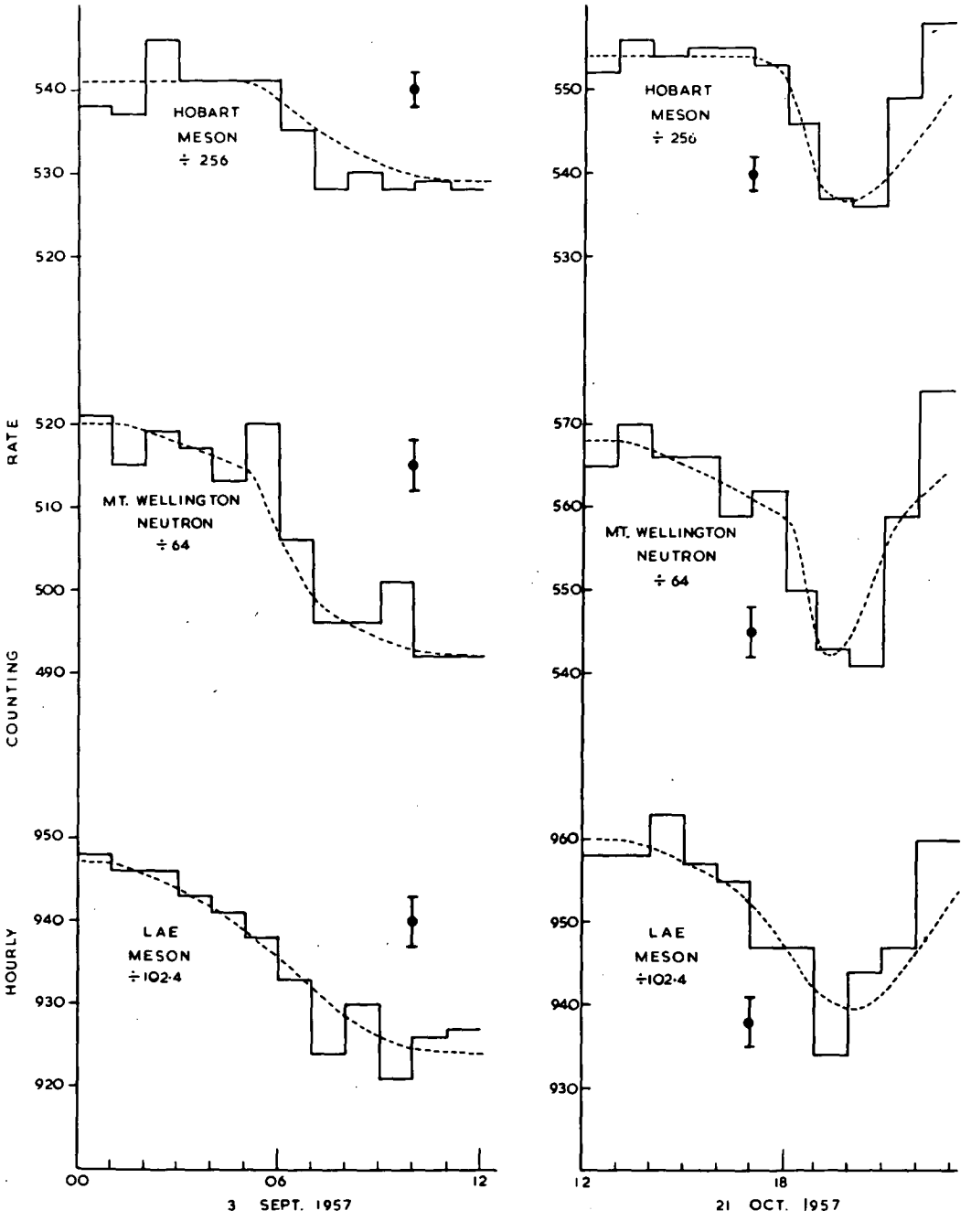
HOBART
MESON
÷ 256
MT. WELLINGTON
NEUTRON
÷ 64
LAE
MESON
÷102·4
COUNTING RATE
HOURLY
540
530
520
510
500
490
950
940
930
920
00
06
12
3 SEPT. 1957
HOBART
MESON
÷ 256
MT. WELLINGTON
NEUTRON
÷ 64
LAE
MESON
÷102·4
550
540
530
570
560
550
540
960
950
940
930
12
18
21 OCT. 1957
UNIVERSAL TIME

23A

23B

outside the geomagnetic field. Detailed examination of the rigidity dependence of the spectral changes, or of the directional dependence of the spectral changes is not worth while, as the standard deviations of the counting rates do not permit identification of anything except general features.

The fact that the Lae meson telescope is "looking" about one hour further to the east than the Hobart meson telescope (Fig.22C) explains in part the observed fact that the Lae diurnal variation leads that at Hobart by one to two hours. Such differences between high and low latitude diurnal variations have been observed before. (ELLIOT, 1952).

REFERENCES

ALLEN, C. W., 1944, Mon. Not. R. Astr. Soc., 104, 13.

BARTELS, J., 1957, Planetary Magnetic Three Hour Range Indices(Gottingen).

BEISER, A., 1955, J. Geophys. Res., 60, 161.

BROWN, R. R., 1958, Nuovo Cimento, 9, 197.

BROXON, J. W., 1942, Phys. Rev., 62, 508.

BRUNBERG, E. A., 1953, Tellus, 5, 135.

BRUNBERG, E. A. and DATTNER, A., 1953, Tellus 5, 269.

CHAPMAN, S. and BARTELS, J., 1951, Geomagnetism. (Oxford University Press).

CHASSON, R. L., 1954, Phys. Rev. 96, 1116.

COMPTON, A. H., WOLLAN, E. O., and BENNETT, R. D., 1934, Rev. Sci. Inst., 5, 415.

CRAMER, H., 1951, Mathematical Methods of Statistics. (Princeton).

DORMAN, L. I., 1957, Cosmic Ray Variations. (State Publishing House for Technical and Theoretical Literature, Moscow). Translation by United States Technical Documents Liaison Office).

DUPERIER, A., and McCAIG, M., 1946, Nature, 157, 477.

ELLIOT, H., 1952, Progress in Cosmic Ray Physics, Vol. 1. (Interscience Publishers, New York).

FENTON, A. G., McCRACKEN, K. G., PARSONS, N. R., and TROST, P. A., 1956, Nature, 177, 1173.

FENTON, A. G., FENTON, K. B. and ROSE, D. C., 1958, Can. J. Phys., 36, 824

FIROR, J. W., FONGER, W. H., and SIMPSON, J. A., 1954, Phys. Rev. 94, 1031.

FONGER, W. H., 1953, Phys. Rev., 91, 351.

FORBUSH, S. E., 1938, Phys. Rev., 54, 975.

FORBUSH, S. E., 1954, J. Geophys. Res., 59, 525.

FORD, P. W., 1958, Rev. Sci. Inst., 29, 728.

GEIGER, K. W., and ROSE, D. C., 1954, Can. J. Phys. 32, 498.

GEORGE, E. P., 1952, Progress in Cosmic Ray Physics, Vol. 1. (Interscience Publishers, New York.).

HOGG, A. R., 1941, Terr. Mag. and Atmos. Elect., 46, 51.

JANOSSY, L., 1950, Cosmic Rays, (Oxford University Press).

JORY, F. S., 1956, Phys. Rev., 103, 1068.

KANE, R. P., 1955, Phys. Rev., 98, 130.

KAPLON, M. F., PETERS, B., REYNOLDS, H. L., and RITSON, D. O., 1952, Phys. Rev. 85, 295.

KIEPENHEUER, K. O., 1953, The Sun, (University of Chicago Press).

KODAMA, M and MIYAZAKI, Y., 1957, Rep. Ionosphere Res. Japan, 11, 99.

KUPFERBERG, K. M., 1948, Phys. Rev., 73, 804.

LOCKWOOD, J. A., and CALAWA, A. R., 1957, J. Atmos. Terr. Phys., 11, 23.

LOCKWOOD, J. A., and YINGST, H. E., 1956, Phys. Rev., 104, 1718.

LUST, R., 1957, Phys. Rev., 105, 1827.

LUST, R., and SIMPSON, J.A., Phys. Rev., 108, 1563.

MEYER, P., and SIMPSON, J. A., 1954, Phys. Rev., 96, 1085.

MEYER, P., and SIMPSON, J. A., 1955, Phys. Rev. 99, 1517.

MEYER, P., and SIMPSON, J. A., 1957, Phys. Rev., 106, 568.

McCRACKEN, K. G., and PARSONS, N. R., 1958, Phys. Rev. (in press).

MONTGOMERY, D. J. X., 1949, Cosmic Ray Physics (Princeton).

MORRISON, P., 1956, Phys. Rev., 101, 1397.

NAGASHIMA, K., 1953, J. Geomag. Geoelect., 5, 141.

NEHER, H. V., 1957, Phys. Rev., 107, 588.

NEHER, H. V., and FORBUSH, S. E., 1952, Phys. Rev., 87, 889.

PARKER, E. N., 1956, Phys. Rev., 103, 1518.

PARKER. E. N., 1958, Phys. Rev., 110, 1445.

PARSONS, N. R., 1957, Aust. Nat. Antarctic Res. Expedition Interim Rep. No. 17.

RATHGEBER, H. D., 1950, Aust. J. Phys., 3, 183.

ROOS, C. F., 1937, Metron, 13, 3.

ROSE, D. C., FENTON, K. B., KATZMAN, J., and SIMPSON, J. A., 1956, Can. J. Phys. 34, 968.

ROSSI, B., 1952, High Energy Particles. (Prentice Hall).

SARABHAI, V., and NERURKAR, N. W., 1956, Annual Review of Nuclear Science, 6, 1.

SIMPSON, J. A., 1954, Phys. Rev., 94, 426.

SIMPSON, J. A., 1956, Annals of the International Geophysical Year, p.349, (Permagon Press).

SIMPSON, J. A., BABCOCK, H. W., and BABCOCK, H. D., 1955, Phys. Rev., 98, 1402.

SIMPSON, J. A., and FAGOT, W. C., 1953, Phys. Rev., 90, 1068.

SIMPSON, J. A., FONGER, W., and TREIMAN, S. B., 1952a, Cosmic Radiation Studies (University of Chicago), Appendix A.

SIMPSON, J. A., FONGER, W., and TREIMAN, S. B., 1953, Phys. Rev., 90, 934.

SIMPSON, J. A., FONGER, W., and WILCOX, L., 1952, Phys. Rev., 85, 366.

SINGER, S. F., 1958, Progress in Elementary Particle and Cosmic Ray Physics, Vol. 4 (North-Holland Publishing Company, Amsterdam).

SITKUS, A., 1946, Z. Naturforsch., 1, 204.

STOREY, J. R., FENTON, A. G., and McCRACKEN, K. G., 1958, Nature, 181, 1155.

TAYLOR, R. B., 1958, Honours Thesis, (University of Tasmania).

TREFALL, H., 1955, Proc. Phys. Soc. Lond., A68, 953.

TREIMAN, S. B., 1952, Phys. Rev., 86, 917.

TREIMAN, S. B., and FONGER, W., 1952, Phys. Rev., 85, 364.

VAN DE HULST, H. C., 1953, The Sun, (University of Chicago Press).

VAN HEERDEN, I. J., and THAMBYAHPILLAI, T., 1955, Phil. Mag. 46, 1238.

VENKATESAN, D., Private Communication.

WADDINGTON, C. J., 1956, Nuovo Cimento, 3, 930.

YOSHIDA, S., and KAMIYA, Y., 1953, J. Geomag. Geoelect. 5, 136.